A FUNCTIONAL ORTHOLOG OF THE *ARABIDOPSIS PARVUS/ATGATL1* GENE AFFECTS GROWTH AND DEVELOPMENT IN THE MOSS *PHYSCOMITRELLA PATENS*

by

YIWEN YANG

(Under the Direction of Michael G. Hahn)

## ABSTRACT

The *Arabidopsis* gene, *PARVUS/AtGATL1*, belongs to the *Ga*lacturonosyl-*t*ransferase-*L*ike (*GATL*) gene family, which is part of CAZy Family GT8. Five *GATL* sequences of the moss *Physcomitrella patens* (*PpGATL-A,B,C,D,E*) have been identified through phylogenetic analyses. The five *PpGATLs* form a sister group that lies basal to all of the vascular plant GATLs. Homozygous *parvus/gatl1* mutants in *Arabidopsis thaliana* are semi-sterile and exhibit a dwarf growth phenotype with collapsed xylem. Cell walls of *parvus/gatl1* show significant reductions in xylose content compared with wild-type cell walls. Constitutive expression of *PpGATL-A* in the *Arabidopsis parvus* mutant rescues the defects conferred by the *parvus* mutation, including changes in plant growth and tissue morphology, collapsed xylem, decreased xylose content based on cell wall monosaccharide composition and the altered overall cell wall structure as indicated by glycome profiling. These findings suggest that *PpGATL-A* is a functional ortholog of *PARVUS/GATL1* and at least one basic function of GATL1 is conserved in highly divergent land plants. Sub-cellular

localization experiments showed that PpGATL-A is a Golgi-localized protein, as is the *Arabidopsis* AtGATL1. Promoter::*β*-glucuronidase expression studies show that *PpGATL-A* is expressed at the base of leaves in the apical region of leafy gametophores. The role of *PpGATL-A* in the development of *Physcomitrella* was investigated by targeted gene knock-out experiments. The *ppgatl-a* knockout mutants produce significantly reduced numbers of leafy gametophores compared to wild type plants. The mutation of *PpGATL-A* gene blocked the developmental stage transition from protenema to leafy gametophores, resulting in a protonema-rich mutant phenotype. Analysis of the *ppgatl-a* knockout phenotype indicates that *PpGATL-A* is required for leafy gametophore development in *Physcomitrella*.

INDEX WORDS: *Physcomitrella patens*, plant cell walls, xylan, pectin, PARVUS/GATL1, protonema, leafy gametophores, homologous recombination, targeted gene knockout

# A FUNCTIONAL ORTHOLOG OF THE *ARABIDOPSIS PARVUS/ATGATL1* GENE AFFECTS GROWTH AND DEVELOPMENT IN THE MOSS *PHYSCOMITRELLA PATENS*

by

YIWEN YANG

B.S., Nanjing University, China, 2008

A Dissertation Submitted to the Graduate Faculty of The University of Georgia in Partial Fulfillment of the Requirements for the Degree

DOCTOR OF PHILOSOPHY

ATHENS, GEORGIA

2014

# A FUNCTIONAL ORTHOLOG OF THE *ARABIDOPSIS PARVUS/ATGATL1* GENE AFFECTS GROWTH AND DEVELOPMENT IN THE MOSS *PHYSCOMITRELLA PATENS*

by

YIWEN YANG

Major Professor: Michael G. Hahn
Committee: Alan Darvill
Debra Mohnen
Jim Leebens-Mack
Kelly Dawe

Electronic Version Approved:

Julie Coffield
Interim Dean of the Graduate School
The University of Georgia
December 2014

# DEDICATION

I dedicate this work to my family, for their continuous love, support, and encouragement.

ACKNOWLEDGEMENTS

I would first like to thank my major professor, Dr. Michael Hahn, for giving me the opportunity to learn and work on this project. I deeply appreciate his guidance, friendship, inspiration and encouragement that he has given me throughout my graduate studies. I also want to express my gratitude to the rest of my committee members, Dr. Alan Darvill, Dr. Debra Mohnen, Dr. Kelly Dawe and Dr. Jim Leebens-Mack for their valuable advice and support in my research. I would like to thank Dr.Wolfgang Lukowitz for offering me the opportunity to rotate in his lab when I applied to the PhD program in Plant Biology Department and teaching me molecular cloning.

I would also like to thank the many people who generously provided me with assistance and materials to do my research: Dr. Utku Avci for help with the immunolabeling experiments and confocal microscopy; Dr. Sivakumar Pattathil for his help with glycome profiling; Stefan Eberhard for teaching me *Physcomitrella* subculture; Katrina Saffold, Dr. Li Tan and Dr. Zhirui Wang, for their help with the GC-MS; Dr. Alison Roberts at University of Rhode Island for sharing the pBSNRG vector and help with targeted gene knockout experiments in *Physcomitrell*a; Dr. Mitsuyasu Hasebe from the National Institute for Basic Biology for providing the pCAMK1 and pTN85 plasmid. I am also very thankful to Drs.Yingzhen Kong, Li Tan, Fangfang Fu, Breeanna Urbanowicz, Maria Pena, Melani Atmodjo, Ameya Kulkarni and Zhangying Hao, for

their support and for the knowledge and experience they shared with me whenever I had questions.

My gratitude also goes to the great administrative staff at the CCRC and the Plant Biology Department, especially Sheilah Dixon-Huckabee, Karen Howard, Carol Connelly, Saeid Roshanzamir, Melissa Archer, Lynn Berryman, and Susan Watkins, who have always been very friendly and helpful.

Lastly, I appreciate the love and support from my parents, my grandparents and my husband over the years.

TABLE OF CONTENTS

Page

# CHAPTER 1

# INTRODUCTION AND LITERATURE REVIEW

## Plant Cell Wall

The polysaccharide-rich cell wall surrounding growing plant cells is a complex yet dynamic structure. Normal plant growth and development depend on the structure and function of the cell wall. There are two general types of walls that differ in both composition and function. The primary wall is the first wall laid down around plant cells and synthesized during cell expansion in growing cells, while secondary walls are deposited in certain cell types when the cell has ceased to grow (Liepman et al. 2010). Primary plant cell walls contain roughly 90% polysaccharides, including cellulose, hemicelluloses and pectin; and ~10% proteins (McNeil et al. 1984). Secondary cell walls also contain cellulose and hemicelluloses, but contain reduced amounts of pectin and protein. Secondary cell walls normally contain phenolic compounds such as lignin, providing additional rigidity and compressive strength (Whetten and Sederoff 1995). Cellulose is the most abundant component of the primary cell wall, serving as a scaffold for the binding of other wall polymers. Hemicelluloses are thought to bind to cellulose microfibrils via hydrogen bonds, providing a strong cross-linked matrix that resists tension. Pectins consist of a family of structurally-related, negatively charged polysaccharides that are thought to be covalently cross-linked to form a gel-like network which resists compression and controls wall permeability. This pectic network is coextensive with the cellulose-hemicellulose network, easing the slippage of microfibrils during cell growth yet also holding them in place once the growth stops (Cosgrove 2005). Figure 1.1 shows a simplified model for the structure of the primary cell wall indicating the interactions of the three classes of polysaccharides.

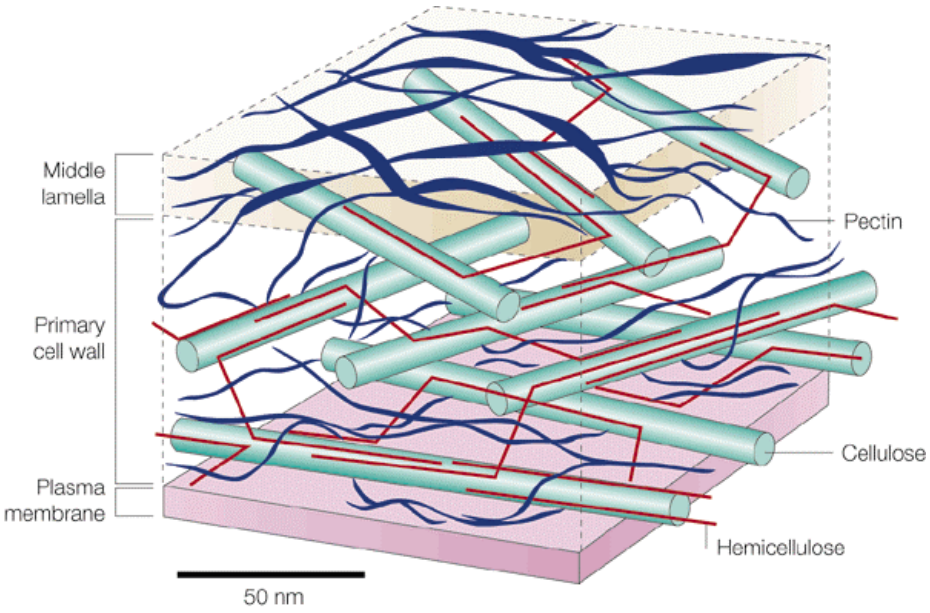


Figure 1.1.Structure of primary plant cell wall. Taken from Smith, (2001); adapted from McCann & Roberts (1991).

The plant cell wall maintains and determines the shapes of plant cells, provides a physical barrier for the defense against pathogens and environmental stresses, and plays fundamental roles in plant growth and development (Underwood 2012). Furthermore, cell walls have great economic importance for carbohydrate-based products such as paper, wood, dietary fiber, etc. As a major source of plant biomass, plant cell walls have recently gained importance as a resource that can be engineered for biofuel production (Pauly and Keegstra 2010; Burton and Fincher 2014). The complex yet highly organized structure of plant cell walls requires a significant dedication of the plant's genomic resources: over 2000 genes in *Arabidopsis* (~15% of the *Arabidopsis* genome) have been estimated to participate in plant cell wall biogenesis, assembly, and modification (Carpita et al. 2001). Identification of key proteins/genes involved in cell wall polysaccharide biosynthesis may enable researchers to produce modified cell walls for applications in agriculture, pharmaceutical and nutraceutical industries.

## Xylan Biosynthesis

### Xylan structure

Xylans are the major hemicellulosic polysaccharides in grasses and trees and the third most abundant polymer on earth after cellulose and chitin (Faik et al. 2014). Xylans consist of a β-1,4-linked xylose (Xyl) backbone that may be substituted to varying degrees with side chains, including glucuronic acid, 4-O-methylglucuronic acid and/or arabinose (Ebringerová and Heinze 2000).

The backbone of dicot xylans are usually substituted with α-D-glucosyluronic acid (Glc*p*A) or 4-*O*-methyl α-D-glucosyluronic acid (MeGlc*p*A) at the *O*-2 of xylose and are known as glucuronoxylans (GX) (Figure 1.2A). Grass xylans are frequently substituted with α-L-arabinofuranose residues at *O*-2 or *O*-3, and sometimes can also be substituted with Glc*p*A and MeGlc*p*A at *O*-2; these xylans are known as arabinoxylans (AX) and glucuronoarabinoxylans (GAX), respectively (Figure 1.2 D). Another common feature of grass xylans is *O*-5 substitution of some arabinofuranosyl residues with ferulic acid esters (Figure 1.2 C), which can be crossed-linked with lignin (Grabber 2005).

A glycosyl sequence with the structure [4-β-D-Xyl*p*-1,4-β-D-Xyl*p*-1,3-α-L-Rha*p*-1,2-α-D-Gal*p*A-1,4-D-Xyl] (Sequence **1**; Figure 1.2 B) was found at the reducing end of xylans in several dicots, including birch and Arabidopsis, and the gymnosperm, spruce (Picea) (Johansson and Samuelson 1977; Andersson et al. 1983; Pena et al. 2007). This structure has not been detected in seedless plants including *Physcomitrella patens*, *Selaginella kraussiana*, and *Equisetum hyemale* or grasses (e.g., *Panicum virgatum, Brachypodium, Oryza, Miscanthus* and foxtail millet) (Kulkarni et al. 2012b). This pattern suggests that Sequence **1** existed in the last common ancestor of all extant seed plants. The absence of Sequence **1** in a few xylan-deficient *Arabidopsis* mutants suggests a role for Sequence **1** in the initiation or termination of xylan backbone elongation (Pena et al. 2007; York and O'Neill 2008).

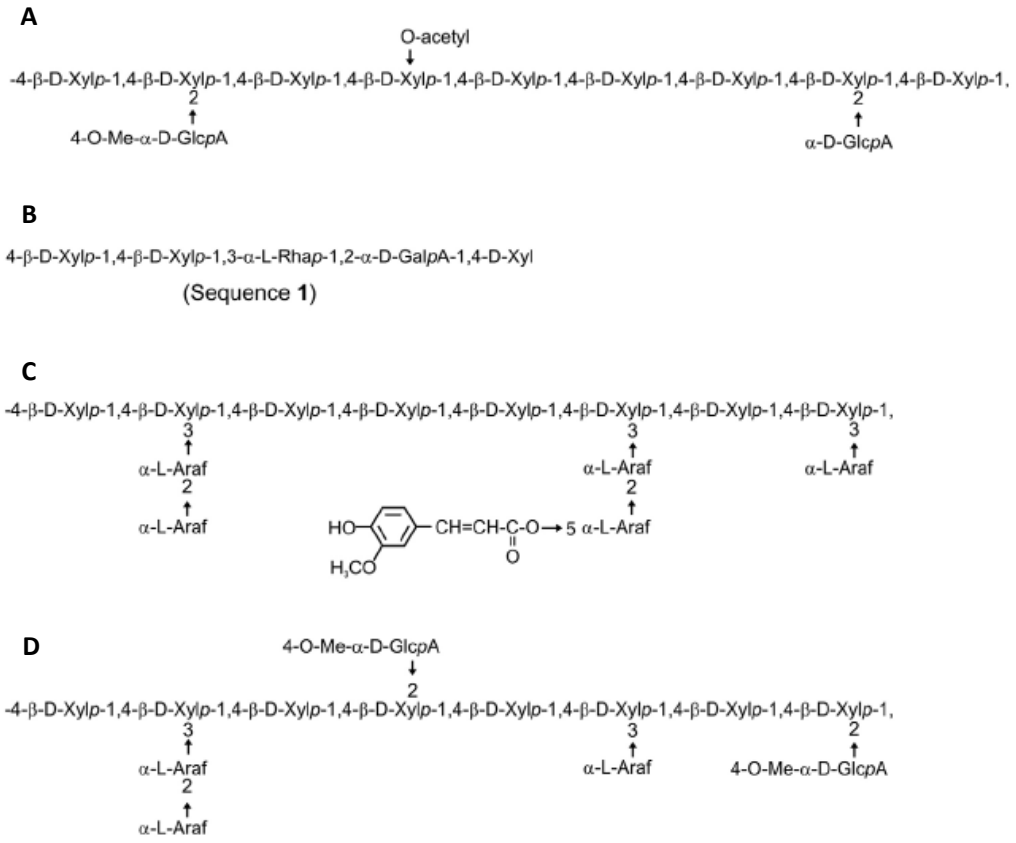


Figure 1.2. Xylan structures in land plants. Adapted from York and O'Neill, (2008).

(A) Glucuronoxylan (GX) typically found in dicots and gymnosperms. The xylosyl residues are substituted with D-GlcA and 4-*O*-methyl-GlcA and can be acetylated to varying degrees at *O*-3 or *O*-2 of xylose residues.

(B) The reducing-end glycosyl sequence **1** found in Arabidopsis, birch and spruce xylan.

(C) Feruloylated arabinoxylans produced by grasses.

(D) Glucuronoarabinoxylan (GAX) predominantly found in grasses

Xylan biosynthetic genes and enzymes

A number of biosynthetic enzymes involved in xylan synthesis have been identified, most of which are from glycosyltransferase (GT) families. Table 1.1 below summarizes the proven and putative proteins involved in xylan biosynthesis.

Table 1.1 Summary of proven and putative xylan biosynthesis enzymes.

| CAZy family | GT names | Activity | Comment | References |
|---|---|---|---|---|
| GT43 | IRX9 | β(1→4)-XylT | IRX-10L is a β-(1,4)-xylosyltransferase involved in xylan backbone synthesis. *IRX9-L*, *IRX10-L*, *IRX14-L* and *IRX15-L* are homologs of *IRX9*, *IRX10*, *IRX14* and *IRX15* which exhibit partial functional redundancy. | Brown et al., 2007; Lee et al., 2007; Pena et al., 2007; Lee et al., 2010; Wu et al., 2010; Lee et al., 2012; Jensen et al.,2014 |
| | IRX14 | | | |
| | IRX-9L | | | |
| | IRX-14L | | | |
| GT47 | IRX10/GUT2 | | | Brown et al., 2009; Wu et al., 2009; Urbanowicz et al., 2014; Jensen et al., 2014 |
| | IRX-10L/GUT1 | | | |
| NOT GT | IRX15 | | | Brown et al., 2011; Jensen et al., 2011 |
| | IRX-15L | | | |
| GT47 | IRX7/FRA8 | β(1→3)-XylT | Possibly involved in the synthesis of xylan reducing end Sequence1; Catalytic activities have not been determined | Shao et al., 2004; Brown et al., 2007; Lee et al., 2007; Pena et al., 2007; Kong et al., 2009; Lee et al., 2009; Hao et al., 2014 |
| | F8H | | | |
| GT8 | IRX8/GAUT12 | α(1→4)-GalAT? | | |
| | PARVUS/GATL1 | α-XylT? | | |
| GT8 | GUX1 | α(1→2)-GluAT<br>α(1→2)-meGluAT | Overexpressed GUX1-4 proteins in tobacco leaf cells or BY2 cells exhibited xylan GlcAT activity | Mortimer et al., 2010; Lee et al., 2012; Rennie et al., 2012 |
| | GUX2 | | | |
| | GUX3 | | | |
| | GUX4 | | | |
| GT61 | XAT1 | α(1→3)-Ara*f*T | *XAT1*-RNAi resulted in large reduction of α(1→3)-Ara*f* | Anders et al., 2012 |
| | XAT2 | | | |
| | XAX1 | β(1→2)-XylT | Xylp-(1→2)-α-Araf substitution | Chiniquy et al., 2012 |
| Not GT | GXMT1 | methyltransferase | *O*-methyl-transferase that catalyzes 4-*O*-methylation of the glucuronic acid substituents of xylan | Urbanowicz et al., 2012 |
| | ESK1/TBL29 | *O*-acetyltransferase | ESK1/TBL29 is a xylan *O*-acetyltransferase. Catalytic activities for RWA1-4 have not been determined. | Lee et al., 2011; Manabe et al., 2011; Manabe et al., 2013; Xiong et al., 2013; Urbanowicz et al., 2014 |
| | RWA1 | | | |
| | RWA2 | | | |
| | RWA3 | | | |
| | RWA4 | | | |

Backbone synthesis

Genetic studies in *Arabidopsis* have identified multiple genes that are involved in xylan backbone synthesis, including *IRX9*, *IRX10*, *IRX14* and their redundant homologs, *IRX9-L*, *IRX10-L* and *IRX14-L* (Brown et al. 2007; Brown et al. 2009; Wu et al. 2009; Wu et al. 2010).

The *Arabidopsis* double mutants *irx9 irx9-l*, *irx10 irx10-l*, and *irx14 irx14-l*, exhibit a more severe dwarf mutant phenotype with reduced fertility and xylan content than most of the single mutants, which exhibit either a mild or no mutant phenotype (Wu et al. 2009; Wu et al. 2010). Microsomes isolated from transgenic tobacco BY2 cells that co-express *IRX9* and *IRX14* exhibit increased xylosyltransferase activity compare to microsomes with the expression of *IRX9* or *IRX14* alone (Lee et al. 2012b). *Arabidopsis* IRX10 protein heterologously expressed in *Pichia pastoris* showed a low level of xylan xylosyltransfersase activity compared to its homolog from the moss *Physcomitrella patens*, which displayed robust xylosyltransferase activity and formed β-1,4 xylosidic linkage (Jensen et al. 2014). *Arabidopsis* IRX10-L protein expressed in human embroyonic kidney (HEK) 293 cells exhibits xylosyltransferase activity by catalyzing the transfer of xylosyl residues from UDP-Xyl to 2-aminobenzamide β-(1,4)-xylohexaose ($Xyl_6$-2AB) (Urbanowicz et al. 2014). However, IRX9 and IRX14 evaluated under the same assay conditions did not catalyze the transfer of xylosyl residues to $Xyl_6$-2AB either alone or in combination (Urbanowicz et al. 2014). These results suggest that IRX10 and IRX10-L are xylosyltransferases, and that IRX9 and IRX14 are involved in some as yet undefined capacity with xylan synthesis. *Arabidopsis* IRX10-L and *Physcomitrella* IRX10 are xylan β-(1,4)-xylosyltransferases involved in the elongation of the xylan backbone. IRX9 and/or IRX14 may function in xylan chain initiation or play structural roles by forming a xylan synthase complex (Urbanowicz et al. 2014). IRX15 and IRX15-L proteins have also been shown to have a role in xylan synthesis (Brown et al. 2011; Jensen et al. 2011). These two proteins contain a Domain of Unknown Function (DUF)579, and they do not belong to GT families classified by

CAZy. The *Arabidopsis* double mutant *irx15 irx-15l* has irregular xylem vessels with ~35% reduction of xylose content, and a lower degree of xylan polymerization. The biochemical function of these genes in xylan biosynthesis remains unclear.

Reducing end Sequence **1** synthesis

As mentioned above, xylans in several dicots and gymnosperms have a unique reducing end sequence termed Sequence **1** (Figure 1.2 B). This glycosyl sequence is present in all of the single and double mutants of *irx9 irx9-l, irx10 irx10-l, irx14 irx14-l* and *irx15 irx15-l* (Brown et al. 2007; Pena et al. 2007; Brown et al. 2009; Wu et al. 2009; Wu et al. 2010; Brown et al. 2011). In contrast, Sequence **1** is absent in a number of other xylan-deficient mutants, including *irx7/fra8, gaut12/irx8* and *parvus/gatl1*, while these mutants retain *in vitro* xylan synthase activity (Brown et al. 2007; Lee et al. 2007; Pena et al. 2007). IRX7/FRA8 and GAUT12/IRX8 have been suggested to be a Rha-specific Xyl transferase and a α-(1→4)-GalA transferase, respectively, to form the linkages of Xyl-Rha and GalA-Xyl in Sequence **1**,while PARVUS/GATL1 has been suggested to be an α-Xyl transferase that transfers the reducing-end Xyl to an unknown primer in the endoplasmic reticulum (Scheller and Ulvskov 2010). It was hypothesized that Sequence **1** is involved in controlling xylan backbone elongation either as a primer or as a terminator (York and O'Neill 2008). Acting as a primer for the initiation of chain synthesis, Sequence **1** is proposed to be synthesized, and the xylan chain is elongated by sequential addition of xylosyl residues to the non-reducing end of Sequence **1**. If Sequence **1** acts as a terminator, the xylan backbone is elongated by the addition of the xylosyl residues to the reducing end, and this process is

terminated by transfer of the nascent polymer to Sequence **1** once the desired backbone chain length is achieved (York and O'Neill 2008).

Side chain synthesis

Backbones of xylans are usually substituted with glucosyluronic acid (Glc*p*A), 4-*O*-methyl-glucosyluronic acid (MeGlc*p*A) or arabinose. Thus, glucuronosyltransferases and arabinofuranosyltransferases are important for xylan side chain synthesis. Four members from the CAZy GT8 family, GUX1 to GUX4 (GlucUronic acid substitution of Xylan), have been reported to be xylan glucuronosyltransferases required for the addition of GlcA and MeGlcA side chains to the xylan backbone in *Arabidopsis* (Mortimer et al. 2010; Lee et al. 2012a; Rennie et al. 2012). The *gux1* gux2 double mutant lacks almost all detectable GlcA substitution and shows a loss of GlcAT activity. The double mutant also has weaker stems compared to wild type plants (Mortimer et al. 2010). The *gux1 gux2 gux3* triple mutant shows a complete loss of GlcA and MeGlcA side chains of xylan with reduced plant growth and secondary wall thickening, as well as collapsed xylem vessels (Lee et al. 2012a). The GUX1, GUX2 and GUX3 proteins, when expressed in tobacco BY2 cells, exhibit xylan GlcAT activity by catalyzing the addition of GlcA from UDP-GlcA onto xylooligomer acceptors (Lee et al. 2012a). Transiently overexpressed GUX1, GUX2 and GUX4 proteins in *Nicotiana benthamiana* leaf cells showed increased GlcAT activity over background levels (Rennie et al. 2012). Recent analyses have shown that GUX1 and GUX2 decorate different domains of the xylan backbone with different patterns of [Me]GlcA spacing: GUX1 substitutes the xylan backbone with [Me]GlcA at evenly spaced xylosyl residues,

mostly at intervals of 8 to 10 residues; while GUX2 substitutes the backbone more tightly with the most frequent spacing of 5, 6 or 7 residues (Bromley et al. 2013). Grass xylans are frequently substituted with α-(1,2)- and α-(1,3)-arabinofuranose residues. Two genes, *XAT1* and *XAT2* from the CAZy GT61 family that are highly expressed in wheat endosperm play an important role in arabinoxylan biosynthesis (Anders et al. 2012). The *XAT1* RNAi construct in which the XAT1 transcript was suppressed by 6- to 30- fold resulted in a large reduction of α-(1,3)- arabinosyl substitution of xylan (Anders et al. 2012). Heterologous expression of wheat *XAT2* in the *Arabidopsis gux1 gux2* mutant plants led to arabinosylation of xylan, providing evidence for gain-of-function of α-(1,3)-arabinosyltransferase activity (Anders et al. 2012).

An Arabidopsis protein AtGXMT1 which was previously classified as domain of unknown function (DUF) 579 has been functionally characterized to be a methyltransferase that catalyzes the 4-*O*-methylation of glucuronic acid substituents of xylan (Urbanowicz et al. 2012). *O*-Acetyl groups are abundant substituents of the backbone of dicot xylans, yet little is known about the process of xylan acetylation, which is thought to be catalyzed by *O*-acetyltransferases (Gille and Pauly 2012). Genetic studies identified four *Arabidopsis* genes *REDUCED WALL ACETYLATION* (*RWA1-4*) that function redundantly in cell wall acetylation (Lee et al. 2011; Manabe et al. 2011; Manabe et al. 2013). Mutants lacking one or more RWA proteins exhibit a reduction in the amount of acetylation of several cell wall polysaccharides including xylan, xyloglucan, mannan and pectin. The *Arabidopsis* quadruple mutant *rwa1 rwa2 rwa3 rwa4* also displays a severe dwarf growth phenotype with reduced secondary wall thickness and stem mechanical strength (Lee et al. 2011; Manabe et al. 2011; Manabe et al. 2013). *TRICHOME*

*BIREFRINGENCE-LIKE29/ESKIMO1 (TBL29/ESK1)* has been suggested to be a xylan or mannan *O*-acetyltransferase as the mutation of this gene resulted in an overall ~60% reduction of xylan *O*-acetylation and ~ 26% reduction of mannan acetylation (Xiong et al. 2013). A recent study has demonstrated that TBL29/ESK1 is a xylan *O*-acetyl transferase rather than a mannan *O*-acetyltransferase (Urbanowicz et al. 2014). TBL29/ESK1 expressed in HEK293 cells exhibits *O*-acetyltransferase activity by catalyzing the transfer of *O*-acetyl groups from acetyl-coenzyme A (acetyl-CoA) to $Xyl_6$-2AB residues, but not to $Man_5$-2AB (Urbanowicz et al. 2014).

**Pectin Biosynthesis**

Pectin structure and function

Pectins are structurally complex plant cell wall polysaccharides that contain 1,4-linked galacturonic acid (GalA) residues. GalA comprises roughly 70% of total cell wall pectin and is a major component of the three major types of pectic polysaccharides: homogalacturonan (HG), rhamnogalacturonan I (RG-I) and the substituted galacturonan, rhamnogalacturonan II (RG-II). Pectin also includes two additional substituted galacturonans: apiogalacturonan (AGA) and xylogalacturonan (XGA), which are less abundant, yet are still present in some plant cell walls. Pectin is abundant in primary walls, comprising about 35% of the polysaccharides in the primary walls of dicot and non-graminaceous monocots, 2-10% of the walls of grasses, and up to 5% of the secondary walls in woody tissues (Mohnen 2008). Pectin is also a major component of the middle lamella, which holds the primary walls of two adjacent plant cells together. Pectins have multiple roles in plants including promoting cell-cell adhesion (Ogawa et al. 2009), providing

structural support in primary walls (Hongo et al. 2012), influencing secondary wall formation in woody tissues (Siedlecka et al. 2008; Roach et al. 2011; Hao et al. 2014), acting as a hydration polymer to support seed growth (Willats et al. 2001), and providing a reservoir of oligosaccharide signaling molecules (Ridley et al. 2001). Pectin, along with hemicelluloses and cellulose, is also an important component of biomass for bioenergy and renewable biopolymers (Mohnen 2008).

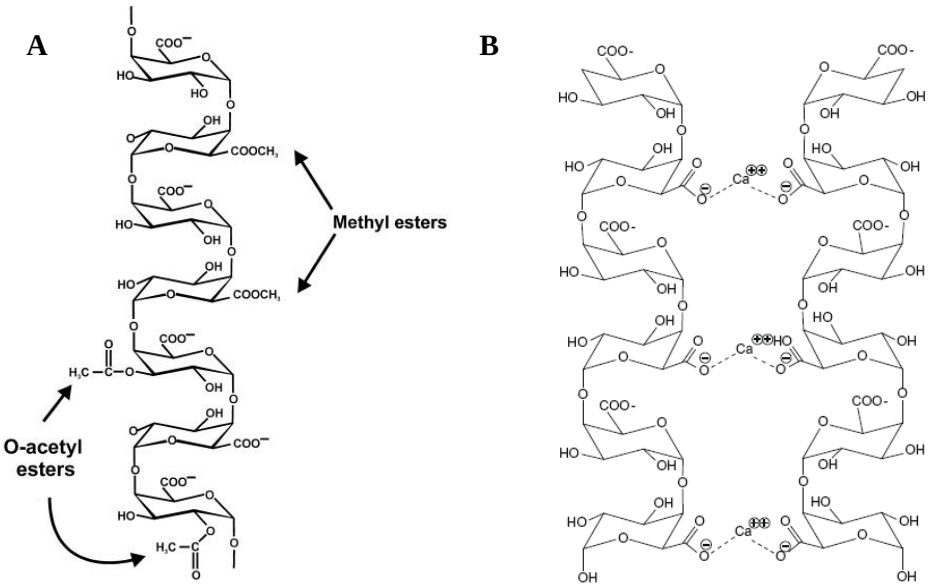


Figure 1.3. Representative structure of homogalacturonan.

(A) HG structure and modification.

(B) The "egg-box" model of calcium cross-linking of non-esterified HG. Adapted from Caffall and Mohnen (2009).

The most abundant pectic polysaccharide is HG, a linear homopolymer of α-1,4-linked GalA that comprises ~65% of pectin (Figure 1.3A). HG is partially methyl-esterified at the *O*-6

position and may also be partially *O*-acetylated at *O*-2 and *O*-3 (Mohnen 2008). Non-esterified carboxyl groups of HG are negatively charged and may interact with $Ca^{2+}$ to form a stable HG-calcium complex (Figure 1.3B). This structure is referred to as an "egg-box" and may form the pectic gel, which is involved in control of cell wall porosity and holds adjacent cells together (Willats et al. 2001).

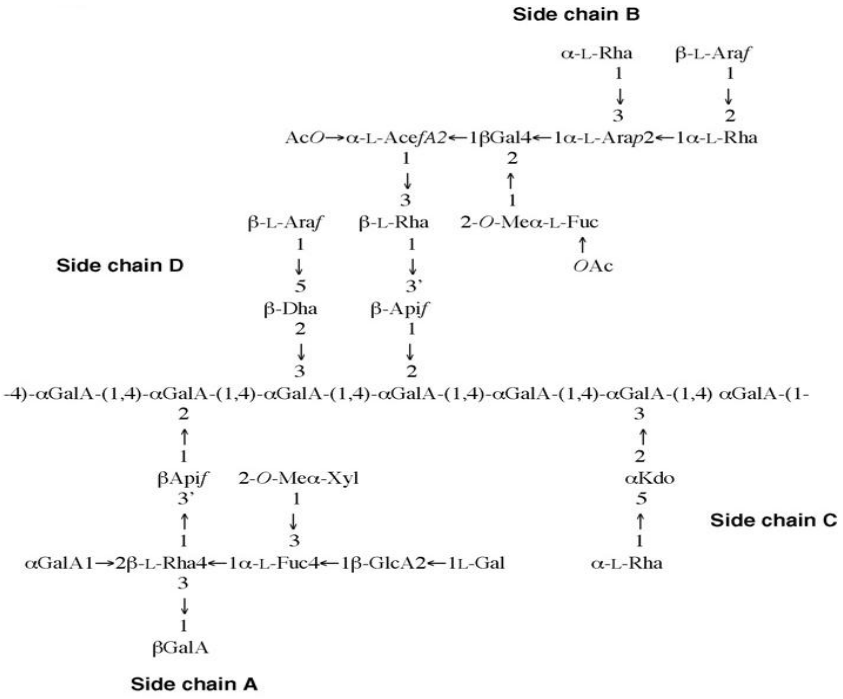


Figure 1.4. Structure of RG-II with its four side chains A-D. Adapted from Mohnen, (2008).

RG-II is a branched galacturonan consisting of a short HG backbone (7-9 GalA residues) substituted with side chains A-D (Figure 1.4). The four side branches consist of at least 12 different glycosyl residues in over 20 different glycosidic linkages. RG-II makes up ~10% of

pectin, and is the most structurally complex pectin. Yet it is highly conserved across plant species (O'Neill et al. 2004). RG-II exists in plants walls primarily as a dimer that is covalently cross-linked by a borate diester between the apiosyl residues of side chain A (Ishii et al. 2001; O'Neill et al. 2004). The borate cross-linked RG-II dimer is required for plant growth and development. The *Arabidopsis* mutant, *mur1*, with reduced RG-II cross-linking exhibits a dwarf phenotype with brittle stems, which can be rescued by spraying exogenous aqueous borate (O'Neill et al. 2001).

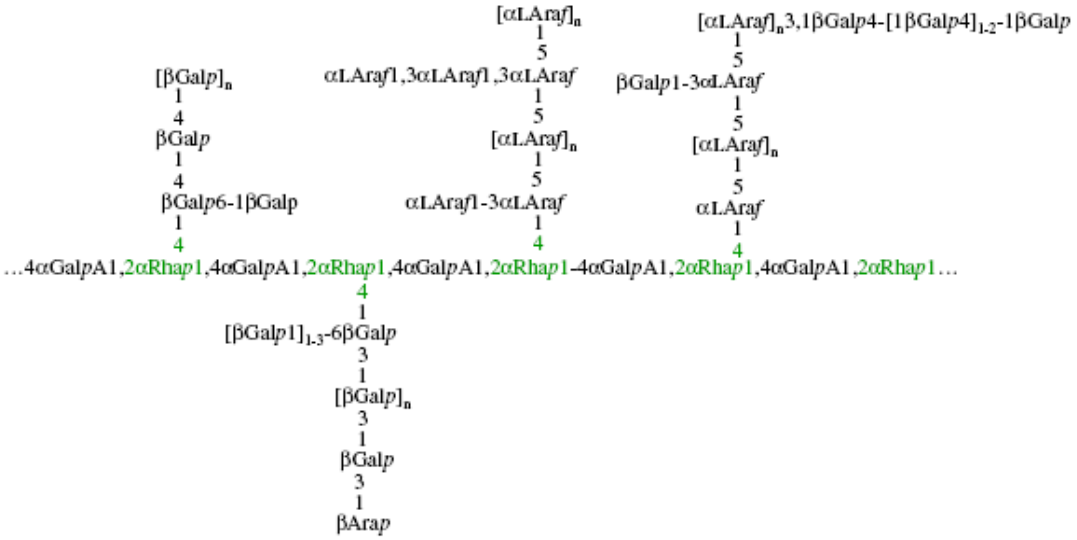


Figure 1.5. Structure of RG-I backbone and representative side chains. Adapted from Caffall and Mohnen, (2009).

RG-I constitutes 20-35% of pectin and contains a disaccharide repeat backbone of [4)-α-D-GalA-(1,2)-α-L-Rha-(1,]$_n$, in which 20-80% of the rhamnosyl residues are substituted at *O*-4 with side chains of arabinan, galactan, and/or arabinogalactan (Figure 1.5) (Willats et al.

2001). The composition and length of RG-I side chains vary between cell types and in different plant species, as shown by immunolabelling studies (Freshour et al. 1996; Guillemin et al. 2005). As shown in Figure 1.5, the main types of side chains include α-1,5-linked L-arabinan with some arabinose or arabinan branching at *O*-2 and *O*-3; β-1,4-linked D-galactan with some arabinan branching at *O*-3; and β-1,3-linked D-galactan with β-6-linked galactan or arabinogalactan branching (Caffall and Mohnen 2009).

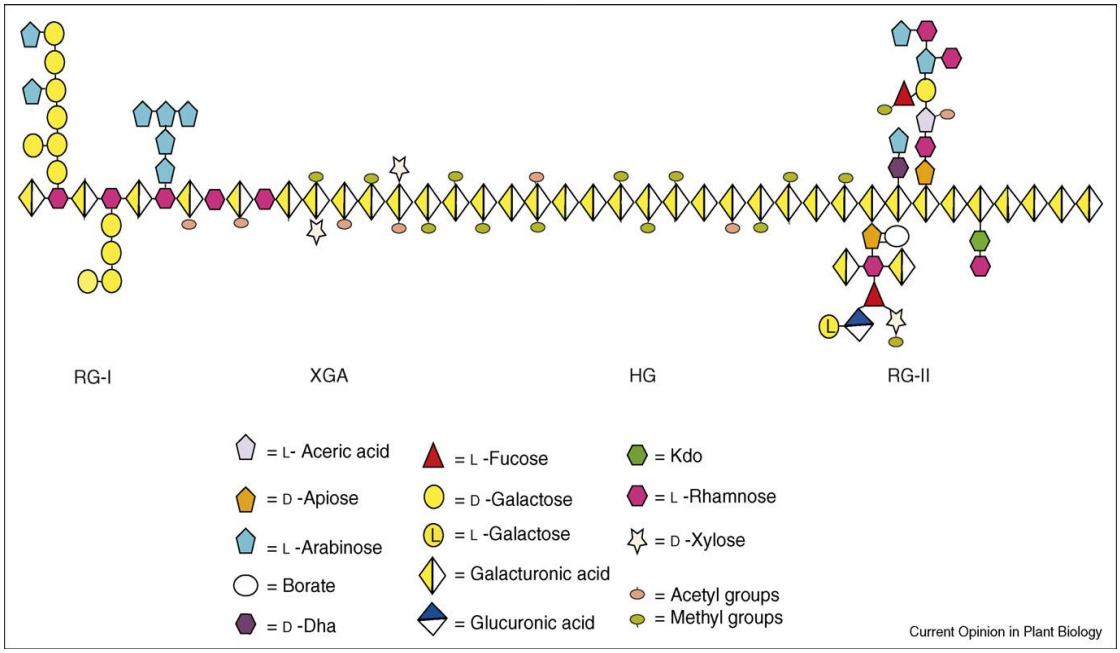


Figure 1.6. Schematic structure of pectin shows the connections between four different types of pectic polysaccharides HG, RG-I, RG-II, and XGA through their backbones. The HG and RG-I domains should be increased by ~12.5 fold and ~2.5-fold, respectively, to approximate the estimated actual amounts of these polymers in the wall. Adapted from Mohnen (2008).

In the wall, pectic polysaccharides form a gel-like matrix network via both non-covalent and covalent interactions, which is coextensive with the load-bearing cellulose-hemicellulose network. The backbone of pectic polysaccharides are believed to be covalently linked to each other (Figure 1.6), as harsh chemical treatment or endopolygalacturonase (EPG) digestion is required to isolate HG, RG-I and RG-II from each other and release them from the wall (Caffall and Mohnen 2009). The covalent linkages via the backbones between HG and RG-II, HG and XGA, and HG and RG-I have been demonstrated (Ishii and Matsunaga 2001; Nakamura et al. 2002; Coenen et al. 2007). Pectic polysaccharides may also be cross-linked to other wall components, such as xylan (Nakamura et al. 2002), xyloglucan (Popper and Fry 2005), phenolic compounds (Laine et al. 2004) and wall proteins (Caffall and Mohnen 2009; Tan et al. 2013), which add to the structural and functional complexity of pectic polysaccharides.

Pectin biosynthetic genes and enzymes

Pectins are the most complex plant cell wall polysaccharides and at least 67 different transferases are estimated to be involved in pectin biosynthesis, including glycosyltransferases (GTs), methyltransferases (MTs), and acetyltransferases (Mohnen 2008). A number of putative pectin biosynthetic glycosyltransferases have been identified from biochemical and genetic studies. These genes include: *ARAD1*, which is believed to be involved in the synthesis of arabinan side chains of RG-I as an α-arabinosyltransferase (Harholt et al. 2006); *NpGUT1* encoding a putative glucuronosyltransferase in RG-II side chain A biosynthesis in tobacco (Iwai et al. 2002); *QUASIMODO1* (*QUA1/GAUT8*) encoding a putative galacturonosyltransferase, the mutation of which results in a dwarf phenotype with reduced cell to cell adhesion and a 25%

reduction in the amount of GalA in leaves (Bouton et al. 2002; Orfila et al. 2005)；*QUASIMODO2* encoding a putative methyltransferase that affects cell adhesion and HG synthesis (Krupkova et al. 2007; Mouille et al. 2007); *QUASIMODO3* encoding a putative methyltransferase involved in controlling pectin methylation and cell wall biosynthesis in *Arabidopsis* suspension cell cultures (Miao et al. 2011); and CGR3, encoding a putative methyltransferase involved in HG methylesterification (Held et al. 2011). Characterization of mutants of *GAUT12/IRX8* and *PARVUS/AtGATL1* suggest a possible role of these two genes in the synthesis of a sub-fraction of pectin (Persson et al. 2007; Hao et al. 2014) and/or as a putative α-1,4-GalAT that participates in the synthesis of the GalA-containing tetrasaccharide sequence located at the reducing end of some xylans (Pena et al. 2007). However, confirmation of enzyme activity of these putative transferases is still required.

So far, enzymatic activity has been demonstrated biochemically for only seven transferases involved in pectin biosynthesis including: GAUT1 from CAZy (Cantarel et al. 2009) family GT8 is involved in HG synthesis as a (1,4)-α-D-galacturonosyltransferase (Sterling et al. 2006); four genes from GT77, *RGXT1*, *RGXT2*, *RGXT3* and *RGXT4/MGP4*, that encode (1,3)-α-D-xylosyltransferases involved in the synthesis of side chain A of RG-II (Egelund et al. 2006; Egelund et al. 2008; Liu et al. 2011); XGD from GT47 that participates in the synthesis of XGA as β-(1,3)-xylosyltransferase (Jensen et al. 2008); *GALS1* from GT92 that encodes a β-(1,4)-galactosyltransferase involved in the synthesis of β-(1,4)-galactan side chains of RG-I (Liwanag et al. 2012).

*Arabidopsis GAUT1*-related gene family

GAUT1 is the first identified galacturonosyltransferase (GalAT) that was functionally determined to be involved in pectin synthesis. It specifically catalyzes the transfer of GalA from UDP-GalA onto a growing stretch of HG (Sterling et al. 2006). Blast analysis of the *GAUT1* coding sequence against the Arabidopsis genome identified 24 additional genes with high sequence similarity to *GAUT1*. These genes include 14 additional *GAUT* genes (*GAUT2-GAUT15*) in *Arabidopsis* with 36-68% amino acid sequence identity and 56-84% sequence similarity to *GAUT1*. The remaining 10 genes have reduced sequence identity and similarity to *GAUT1* (23-29% identity and 42-53% similarity), and are named the *GAUT1-Like* (*GATL)* genes (Sterling et al. 2006). The 15 *GAUT* genes encode proteins predicted to be 61 to 78 KD, and most GAUT proteins are predicted to be type II transmembrane proteins with variable N-terminal sequences. In contrast, the 10 *GATL* genes encode 39-44 KD proteins with N-terminal signal peptides but no apparent transmembrane domain (Sterling et al. 2006; Kong et al. 2011). All 25 *Arabidopsis* genes were suggested to represent putative GalATs and have been grouped into a GAUT1-related gene superfamily (Figure 1.7). All the GAUT proteins and their orthologs share the GAUT family motif (H-x(2)-[ILV]-x-[ST]-D-N-[IV]-[IL]-A-[ASTV]-S-V-V-[AIV]-x-S-x-[AIV]-x(2)-[AS]-x(2)-[PS]-x(3)-V-[FL]-H-[ILV]-[ILV]-T-[DN]-x(2)-[NST]-x(2)-[AGP]-[IM]-x(3)-F); while the GATL motif [IV]-F-[AGS]-G-x-[IV]-x-[AP] -[IV]-[DENS]-H -[QR]-W-N-Q-H-G-L-G-G-D-N-[FILV]-x-[GS]-x-C-R is shared by the 10 *Arabidopsis* GATLs and their orthologs (Sterling et al. 2006). The conserved DxD motif identified in diverse GT families is also shared between GAUTs and GATLs (Sterling et al. 2006; Yin et al. 2010) .

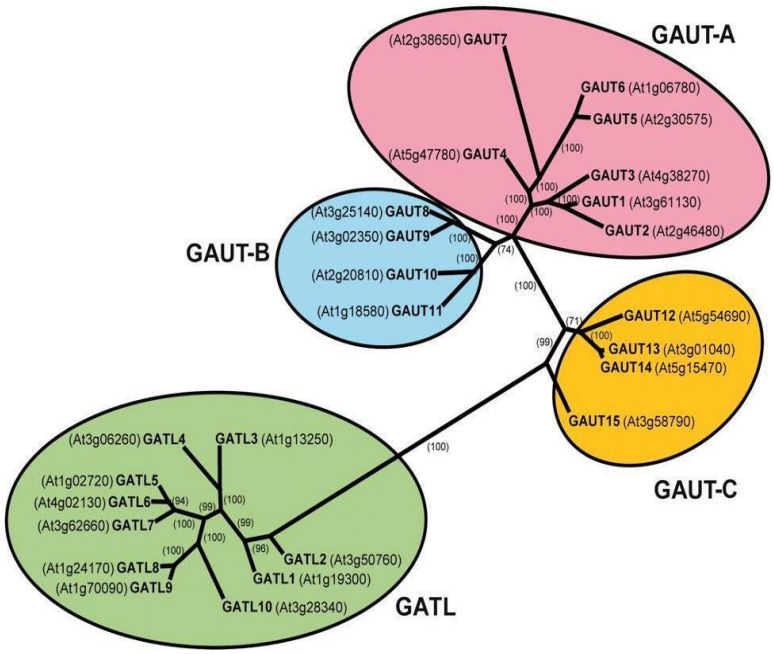


Figure 1.7. The GAUT1-related gene family in *Arabidopsis*. The phylogenetic tree is constructed using Bayesian analysis (Sterling et al. 2006).

Detailed phylogenetic analysis of 378 plant GT8 proteins from 15 genomes categorized the GAUTs, GATLs and a lower plant specific GAUT and GATL-related (GATR) subfamily into plant cell wall synthesis-related proteins (class I) in the GT8 family, which are distinct from the galactinol synthase (GolS) and plant glycogenin-like starch initiation protein (PGSIP) clades (class II) and from the bacterial GT8 proteins (class III) (Yin et al. 2010). Orthologs of *Arabidopsis* GAUT and GATL family members have been identified in all 9 land plant species analyzed at the time of the phylogenetic study, including the moss *Physcomitrella patens* and the spike moss *Selaginella moellendorffii*, yet are not present in any of the 6 green algae species examined (Yin et al. 2010). One green algal protein from *Ostreococcus lucimarinus* was placed

ancestral to the GAUT and GATR clades, and a *Synechococcus* cyanobacterial protein was identified to be a putative progenitor for all GAUTs and GATLs. These results suggest that the GAUT, GATL and GATR clades may have an early evolutionary divergence from the other plant GT8 members that have other distinct functions.

Function of GAUT proteins

*GAUT* genes are expressed in all tissues in *Arabidopsis* examined to date using RT-PCR, with the exception of *GAUT2*, which was suggested to be a pseudogene (Caffall et al. 2009). Proteomic analysis of the trypsin-digested, HG:GalAT-enriched solubilized protein fraction from *Arabidopsis* suspension culture cells revealed two putative glycosyltransferases, GAUT1 (At3g61130) and GAUT7 (At2g38650). However, only GAUT1 has been functionally demonstrated as a HG:GalAT when transiently expressed in human embryonic kidney (HEK) cells (Sterling et al. 2006). Although no GalAT activity was detected for heterologously expressed GAUT7, GAUT7 functions to anchor GAUT1 in the Golgi, and the immunoprecipitated GAUT1:GAUT7 complex shows HG:GalAT activity, confirming that GAUT7 is part of a GAUT1:GAUT7 complex and is involved in HG biosynthesis (Atmodjo et al. 2011).

Analysis of cell walls isolated from 26 *Arabidopsis* homozygous transfer DNA (T-DNA) mutants lines representing 13 *GAUT* genes demonstrated that eight *gaut* mutants (*atgaut6, atgaut8, atgaut9, atgaut10, atgaut11, atgaut12, atgaut13* and *atgaut14*) have significant changes in mol% levels of GalA, Xyl, Rha, Gal or Ara compared to wide-type plants (Caffall et al. 2009). These results suggest that these GAUTs are involved in pectin and/or xylan biosynthesis.

Homozygous mutant lines for *GAUT1* and *GAUT4* have not been recovered, suggesting that these two genes may encode proteins that are essential for plant growth and development (Caffall et al. 2009). Despite the changes in cell wall compositions, only a few mutants exhibit easily distinguishable growth phenotypes from wide-type. Plants carry a mutation in the *QUA1/GAUT8* (Bouton et al. 2002; Orfila et al. 2005) and *IRX8/GAUT12* (Persson et al. 2007; Pena et al. 2007; Hao et al. 2014) genes show growth defects such as dwarfism and reduced fertility. *atgaut8* (*qua1-1*) mutants show defects in cell-cell adhesion and have reduced GalA and Xyl content in the cell wall, and *qua1-1* mutant stem microsomal membrane protein preparations show a ~30% reduction in HG:GalAT activity and a 40% reduction in β-1,4-xylan synthase activity (Orfila et al. 2005), suggesting that GAUT8 is involved in pectin and/or xylan synthesis. *atgaut12*/*irx8* mutants exhibit a collapsed xylem phenotype as observed by histochemical analyses (Brown et al. 2005). Glycosyl residue- and linkage-composition analyses of *atgaut12/irx8* mutant walls indicate reduced levels of GalA and reduced secondary wall xylan content (Persson et al. 2007). Chemical studies of *atgaut12* walls revealed the absence of the pentasaccharide sequence [4-β-D-Xyl-1,4-β-D-Xyl-1,3-α-L-Rha- 1,2-α-D-GalA-1,4-D-Xyl] that is present at the reducing end of the glucuronoxylan chains (Pena et al. 2007). The mutation of *GAUT12/IRX8* also causes anther indehiscence and leads to reduced amounts and altered extractability of G lignin in *Arabidopsis* (Hao et al. 2014). However, immunoabsorbed GAUT12 does not have GAUT1-like HG:GalAT activity as demonstrated by enzymatic activity assays (Hao et al. 2014). These results suggest that GAUT12 may participate in xylan synthesis by adding GalA residues onto the xylan reducing end sequence, or may be

involved in the synthesis of a specific sub-domain of HG required for xylan and lignin deposition in secondary walls (Pena et al. 2007; Persson et al. 2007; Tan et al. 2013; Hao et al. 2014). Cell walls of *atgaut6, atgaut9, atgaut10,* and *atgaut11* mutants have significant reductions in GalA, suggesting a role for these genes in pectin synthesis in *Arabidopsis*. *atgaut11* mutants also show a seed mucilage phenotype as observed by ruthenium red staining, suggesting a possible role in RG-I synthesis (Caffall et al. 2009). Cell walls of *atgaut13* and *atgaut14* mutants have increased GalA and Gal content and reduced Xyl and Rha content compared to wild type walls, suggesting a role for the proteins encoded by these genes in RG-I or xylan synthesis. However, demonstration of the enzymatic activity is required to elucidate the biochemical function of these GAUT proteins.

Function of GATL proteins

GATL proteins are smaller than GAUTs and lack a trans-membrane domain that is found in almost all GAUTs. Nonetheless, GATL proteins contain N-terminal signal peptides that direct them to the secretory pathway (Kong et al. 2009; Kong et al. 2011). RT-PCR studies show that most of the *GATL*s are expressed at various levels throughout the *Arabidopsis* plant, with the exception of *GATL4* which is expressed only in flowers (Kong et al. 2011). Each of the GATL proteins shows a unique expression pattern along with some overlaps, as indicated by promoter::*β-glucuronidase* expression studies (Kong et al. 2011). Subcellular localization studies demonstrate that AtGATL1 is localized to both endoplasmic reticulum (ER) and Golgi, and several other AtGATL proteins (AtGATL2, AtGATL3, AtGATL7, and AtGATL9) are localized in the Golgi (Kong et al. 2009; Kong et al. 2011).

Mutational studies have provided evidence for the involvement of GATL proteins in the synthesis of xylans and/or pectins. The *parvus/gatl1* mutants grown under low humidity conditions exhibit severely dwarfed growth phenotype and have reduced anther dehiscence leading to semi-sterility (Lao et al. 2003). Early glycosyl composition analyses of the *parvus/gatl1* mutant shows slight increases in Rha, Ara and Gal residues and decreased xylose content compared to WT. Glycosyl linkage composition analysis shows that the ratio of 2- to 2,4-linked Rha residues is 2:1 in mutant leaves while the ratio is 1:1 in wild-type leaves, indicating reduced levels of RG-I branching in the *parvus/gatl1* mutant (Lao et al. 2003). Later studies demonstrated that the *parvus/gatl1* mutant plants display a collapsed xylem phenotype with a significant decrease in xylose content of the cell walls and a drastic reduction of the secondary walls thickness in xylem tissues (Brown et al. 2007; Lee et al. 2007; Kong et al. 2009). Furthermore, the tetrasaccharide sequence [4-β-D-Xyl-1,3-α-L-Rha-1,2-α-D-GalA-1,4-D-Xyl] present at the reducing end of xylan in wild-type plants is absent in the *parvus/gatl1* mutant (Pena et al. 2007). These results implicate GATL1 in xylan and possibly pectin synthesis. Plants carrying T-DNA insertions in three *AtGATL* genes, *ATGATL3*, *ATGATL6* and *ATGATL9* show 23.7%, 16.4% and 20.5% reduction in GalA content, respectively, suggesting that these *GATLs* may encode putative GalATs involved in pectin synthesis (Kong et al. 2011). *atgatl9* mutant plants also exhibit defects in cell adhesion (Kong *et al*., unpublished results); this phenotype has been previously observed in *qua1/gaut8* mutant plants (Bouton et al. 2002). Mutations in *AtGATL5* result in a significant decrease in the synthesis of seed mucilage, and monosaccharide composition analyses revealed a 34% and 40% reduction in Rha and GalA content in *atgatl5-1*

mucilage (Kong et al. 2013). The *Arabidopsis atgatl5 atgatl6* double mutants have an almost complete absence of seed mucilage; however, the *atgatl6* single mutant shows little if any defect in mucilage synthesis (Kong *et al*., unpublished results). These results suggest a role for these two genes in pectin, specifically RG-I biosynthesis. *Arabidopsis* plants carrying single mutations in the other *GATL* genes do not show easily identifiable morphological defects or cell wall abnormalities, indicating that some functional redundancies may exist in the *GATL* gene family.

**The moss, *Physcomitrella patens,* as an experimental system for plant cell wall studies**

The absence of functional characterization of most of the GATL proteins leaves open the question of their roles in cell wall synthesis. Recent sequencing of the spike moss, *Selaginella moellendorffi*, and the availability of the genome sequence of the moss, *Physcomitrella patens*, gives new insight into the evolution of the *GATL* gene family (Figure 1.8). The phylogram (Kong et al. 2011) shows a basal clade, GATL-g, that includes five GATLs from *Physcomitrella* and one from *Selaginella*, and six clades of angiosperm GATLs. From lower plants to higher plants, there is a sharp increase in the number of GATLs, suggesting that GATLs have important roles in plants as they colonized the terrestrial environment. The five *Physcomitrella GATL* homologs and the one *Selaginella GATL* homolog are basal to all other angiosperms *GATL*s included thus far in phylogenetic analyses, raising the possibility that they might also share one or more similar functions with the *AtGATLs.* *Physcomitrella* contains only primary cell walls, and its cell wall composition is comparable with that of vascular plants, making it an advantageous

system for investigating cell wall biosynthesis and evolution. Other advantages of *Physcomitrella* as a model system for plant cell wall studies include the ease of culture and experimental manipulation (Cove 2005), the feasibility of gene targeting and the reduced gene redundancy in multigene families (Rensing et al. 2002). The gene identifier information for the five *PpGATL*s is given in Table 1.2 below.

Table 1.2. *PpGATLs* gene identifier information

| *PpGATLs* | JGI model name in Figure 1.4 | Protein IDs |
|---|---|---|
| *PpGATL-A* | Pp-estExt_Genewise1.C_1290049 | XP 001770768.1 |
| *PpGATL-B* | Pp-estExt_Genewise1.C_2810001 | XP 001780550.1 |
| *PpGATL-C* | Pp-fgenesh1_pg.scaffold_4000222 | XP 001752454.1 |
| *PpGATL-D* | Pp-e_gw1.43.57.1 | XP 001760568.1 |
| *PpGATL-E* | Pp-fgenesh1_pg.scaffold_229000012 | XP 001777911.1 |

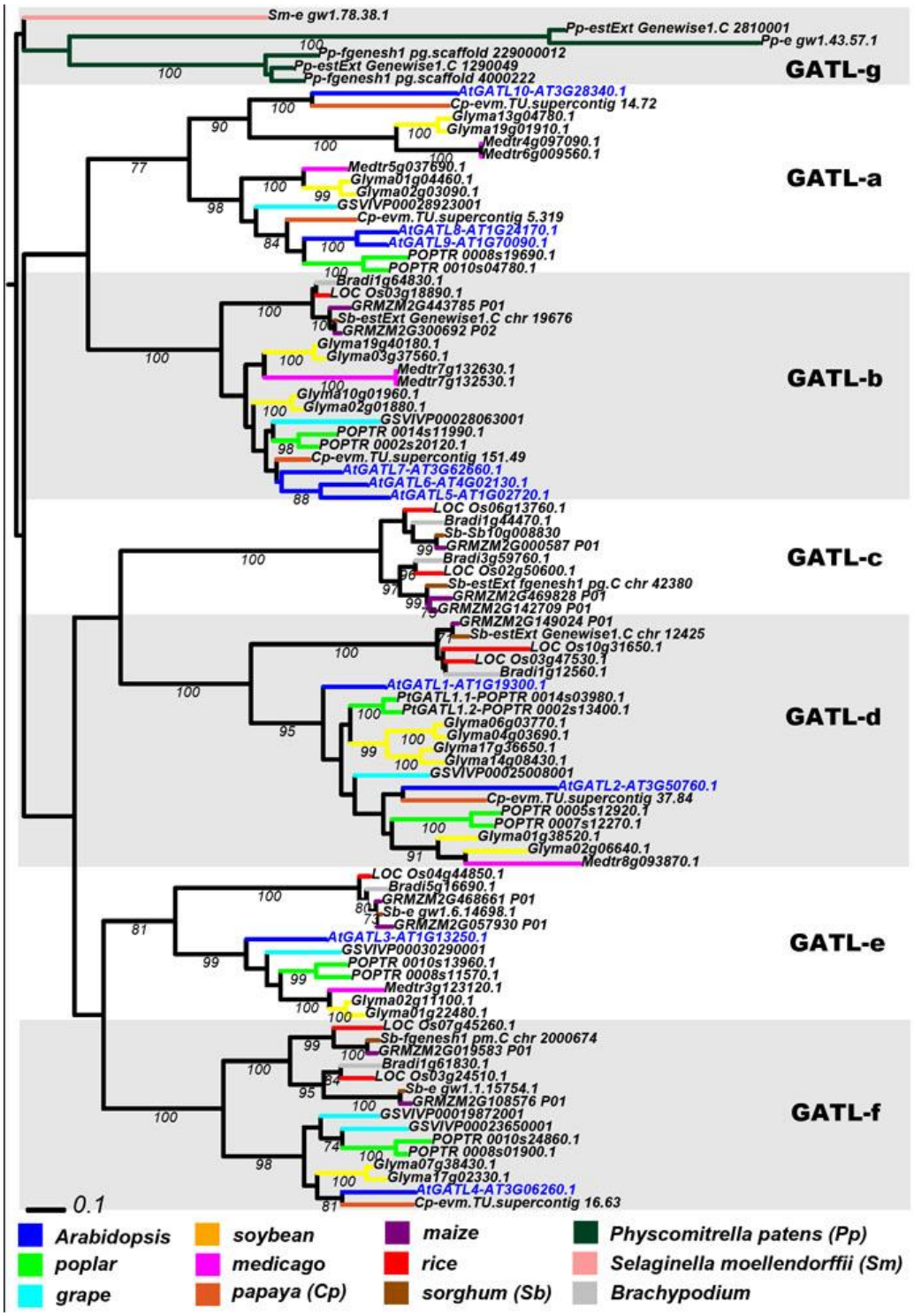


Figure 1.8. Phylogenetic tree of 95 GATL proteins from 12 plant species whose genomes have been sequenced. The GATL-g clade was selected as the outgroup to root the phylogeny (Kong et al. 2011).

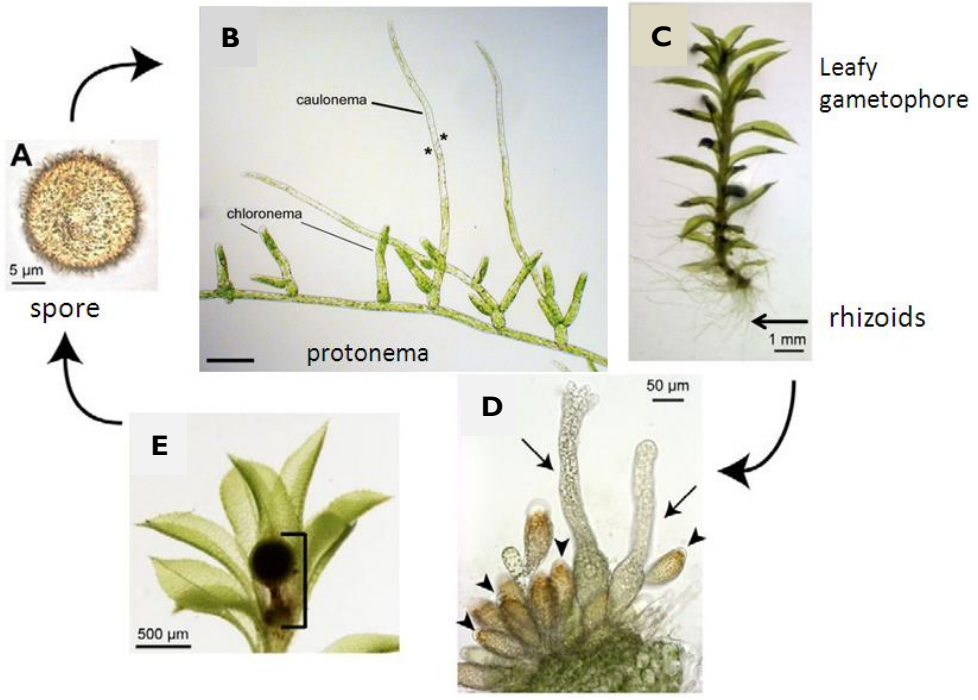


Figure 1.9. *Physcomitrella patens* life cycle. Adapted from Menand et al. (2007) and Prigge and Bezanilla (2010).

(A) A haploid spore arising from the diploid sporophyte through meiosis.

(B) Chloronemal and caulonemal cells. Asterisks indicate the oblique cross wall of caulonemal cells. Scale bar = 100 µm.

(C) Leafy gametophores with rhizoids at the base indicated by the arrow.

(D) Female organ (archegonia, arrows), and male organ (antheridia, arrowheads) form at the apex of the gametophores.

(E) Sporophyte (marked with a bracket) develops at the apex of the gametophore.

## The life cycle of *Physcomitrella*

The moss *Physcomitrella patens* is a member of the bryophyte family (liverworts, mosses and hornworts). The life cycle of *Physcomitrella* (Figure 1.9) comprises an alternation of two generations that is typical of all mosses and vascular plants: a haploid gametophyte and a diploid sporophyte. The haploid gametophyte generation is the predominant phase of the *Physcomitrella* life cycle. Haploid spores produced by a diploid sporophyte develop into filamentous protonema. The protonema are differentiated into two types of cells: chloronemal cells with many fully developed chloroplasts, and the fast growing caulonemal cells that contain fewer less-developed plastids and have oblique cell walls (Prigge and Bezanilla 2010). Both types of cells expand by tip growth through the elongation and division of the apical and sub-apical cells to form side branches (Menand et al. 2007). As the plant continues to grow and becomes mature, some side branch initial cells can differentiate into buds, which ultimately develop into leafy shoots termed adult gametophores. Gametophores comprise of stems, leaves, axillary hairs and rhizoids, and both male (antheridia) and female (archegonia) sexual organs can form at the top of a single gametophore, which ultimately give rise to the diploid sporophyte.

## Experimental methods and tools to study *Physcomitrella*

### Gene targeting in *Physcomitrella*

Unlike all other land plants tested so far, the moss *Physcomitrella patens* exhibits a very high rate of homologous recombination in its nuclear DNA. Foreign DNA harboring a homologous sequence can be stably integrated into the corresponding genomic locus at frequencies up to

100% (Schaefer and Zryd 1997; Schaefer 2001; Kamisugi et al. 2005; Cove 2005), whereas in flowering plants, the observed rate for homologous recombination events barely reaches $10^{-4}$ (Mengiste and Paszkowski 1999; Britt and May 2003). This unique feature of *Physcomitrella* enables gene targeting studies to be performed to replace the coding sequence of a selected gene with suitable gene disruption constructs (Figure 1.10 A). A number of *Physcomitrella* genes have been successfully disrupted by targeted gene knockout resulting in a mutant phenotype that reveals the biological function of the disrupted gene (Strepp et al. 1998; Girod et al. 1999; Imaizumi et al. 2002; Olsson et al. 2003; Mittmann et al. 2004; Lee et al. 2005a; Thelander et al. 2007; Martin et al. 2009; Wu et al. 2011; Buda et al. 2013). In addition to targeted knockout lines, targeted knock-in lines can also be generated by transformation with replacement vectors carrying transcriptional and/or translational fusions of moss genomic sequence with reporter genes such as β-glucuronidase (GUS) or green fluorescent protein (GFP) for spatial and temporal gene expression studies (Figure 1.10 B).

RNAi in *Physcomitrella*

For genes belonging to a large gene family, whose members may possess redundant functions, multiple knockouts may need to be generated in order to observe a mutant phenotype, which is time consuming and labor intensive. Knockout strategies are not applicable if the gene(s) under investigation have essential functions, and the disruption of such genes leads to lethal knockouts which cannot be recovered. In the above two cases, gene function can be analyzed by gene silencing via RNA interference (RNAi) instead of targeted gene knockout (Bezanilla et al. 2003). Bezanilla *et al*. developed a rapid RNAi system incorporating a nuclear

localized GFP:GUS fusion reporter protein as a marker for active gene silencing in transient assays. RNAi induced phenotypes can be observed in transgenic lines as early as 24 hours and as long as approximately 4 weeks after transformation (Bezanilla et al. 2005). By incorporation of conserved regions of sequence from different members of a gene family into a single RNAi construct, this approach allows the simultaneous silencing of all family members (Vidali et al. 2007; Vidali et al. 2009). Gene knockdown by artificial microRNAs in *Physcomitrella* has also been successfully performed, which can produce stable transgenic plants for studies of later growth stages (leafy gametophores and sporophytes, etc.) (Khraiwesh et al. 2008).

*Physcomitrella* transformation methods

The most commonly used technique for transformation of *Physcomitrella* is the polyethylene glycol (PEG)-mediated transformation of protoplasts (Schaefer et al. 1991). Protoplasts are isolated using the enzyme mixture Driselase for cell wall digestion of 6-day-old protonemal tissue (Grimsley et al. 1977). Freshly isolated protoplasts are counted and the density is estimated using a haemocytometer (Figure 1.11); intact protoplasts are round with their chloroplasts pressed against the plasma membrane. PEG functions to stabilize the protoplasts and to enclose the DNA to enable it pass through the cell membrane. After transformation, the protoplasts can develop a new cell wall and regenerate into protonemal tissue in the presence of an osmotically controlled medium. Transformed plants that survive after two rounds of antibiotic selection are considered to be stable transformants (Cove et al. 2009). The PEG-mediated transformation is highly efficient and can be easily performed in any standard laboratory with a sterile hood (Liu and Vidali 2011). However, it requires a lot of DNA (routinely 20 μg per transformation) and a

large amount of plant tissue and protoplast manipulation under scrupulously sterile conditions (Šmídková et al. 2010).

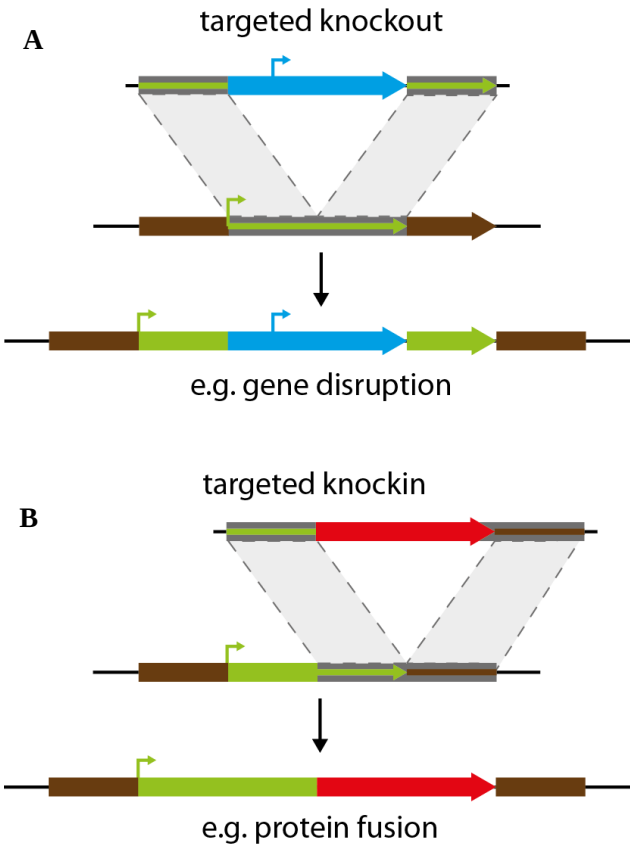


Figure 1.10. Targeted knockout and knock-in strategies in *Physcomitrella*. Adapted from Strotbek *et al.* (2013).

(A) knockout of the coding sequence of a gene.

(B) knock-in of a reporter gene to form a fusion protein with a targeted gene.

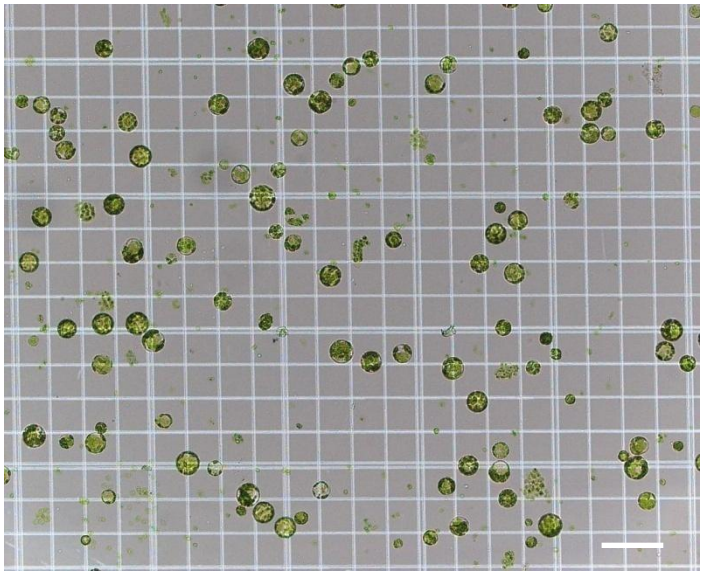

Figure 1.11. View of freshly isolated protoplasts in haemocytometer. Intact protoplasts are round and green with the presence of chloroplasts. Scale bar = 100μm.

An alternative method widely used for transformation of plant cells is particle bombardment which directly delivers DNA biolistically into plant tissues (Klein et al. 1988). This technique is also applicable for the transformation of *Physcomitrella* by shooting the DNA onto protonemal tissue (Sawahel et al. 1992; Cho et al. 1999). Compared to PEG-mediated transformation, the biolistic transformation requires less DNA and can result in higher transformation efficiencies (Cho et al. 1999; Šmídková et al. 2010). However, this technique requires specialized devices such as gene guns, which are not readily available to many laboratories (Liu and Vidali 2011).

*Agrobacterium*-mediated transformation is another widely used method for the genetic transformation of seed plants (Valvekens et al. 1988; Tsai et al. 1994; Hiei et al. 1994; Clough and Bent 1998). *Agroabacterium tumefaciens* can transfer foreign DNA into plant cells by infecting the plant through its Ti plasmid, resulting in the random integration of the DNA into the plant

genome (Deblaere et al. 1985). *Physcomitrella* was considered to be not amenable to *Agrobacterium* infection previously. Yet recently new virulent strains of *A. tumefaciens* have been used successfully for the transformation of *Physcomitrella* (Cove 2005). *Agrobacterium*-mediated transformation may generate stable transformed plants at higher rates than the above two described methods. However, so far, there are no published data available on the generation of stable T-DNA integration mutants in *Physcomitrella*.

*Physcomitrella* cell wall

The simple morphology, the availability of a sequenced and assembled genome, and the ease of conducting targeted gene knockout makes *Physcomitrella* an attractive system for genetic and physiological studies. It is also an ideal model for comparative studies of the evolution of plant gene function by virtue of its basal position in land plant phylogeny (Rensing et al. 2008). *Physcomitrella* offers a well-established genetic system for the study of plant cell wall biosynthesis genes with the potential to provide insight into evolutionary aspects of plant cell walls.

*Physcomitrella* cell wall composition and structure

Evolution of plants over millions of years has resulted in increasing diversity and complexity in cell wall components, structures and functions. Considerable similarities, yet subtle differences exist between angiosperm and bryophyte cell walls. Similar to vascular plants primary walls, *Physcomitrella* cell walls contain almost all non-lignin cell wall components including cellulose, hemicelluloses, pectins and arabinogalactan proteins (AGPs), but in different

proportions (Lee et al. 2005a; Liepman et al. 2007; Fu et al. 2007; Moller et al. 2007; Pena et al. 2008). The side chain composition and structure of these cell wall components also differ between vascular plants and *Physcomitrella*. For example, detailed structural analysis of xyloglucans revealed that *Physcomitrella* synthesize XXGGG- type xyloglucans, with side chains containing a GalA and a branched xylosyl residue, which appears to be a unique structure of moss xyloglucans (Pena et al. 2008). Xylans are major polysaccharides in secondary cell walls in vascular plants, and cell walls of vascular plants have significantly more xylans than bryophytes as shown by immunolabeling and chemical analyses (Popper and Fry 2003; Carafa et al. 2005). The cell walls of *Physcomitrella* contain glucuronoxylans with a 1,4-linked β-D-xylan backbone and α-D-glucosyluronic acid side chains that are structurally similar to glucuronoxylans produced by vascular plants (Kulkarni et al. 2012b). However, in contrast to vascular plants, neither 4-*O*-methyl-α-D-glucosyluronic acid side chains nor the conserved reducing end oligosaccharide sequence characteristic of seed plant xylans have been detected in *Physcomitrella* xylan (Johansson and Samuelson 1977; Ebringerová and Heinze 2000; Kulkarni et al. 2012b).

Phylogenetic analysis of *Physcomitrella* genes potentially involved in cell wall biosynthesis

The genomes of *Physcomitrella* and vascular plants encode the same families of cell wall glycosyltransferases, which may have diversified and specialized independently in each lineage. The *Physcomitrella* genome includes ten Cellulose Synthase genes (*PpCESA1* - *PpCESA10*), among which three are pseudogenes (*PpCESA1*, *PpCESA2*, and *PpCESA9*) (Roberts and Bushoven 2007; Yin et al. 2009; Wise et al. 2011). *PpCESA5* is required for leafy gametophore

morphogenesis as demonstrated by targeted mutagenesis studies (Goss et al. 2012). *PpCESA6* and *PpCESA7* single knockouts have no morphological phenotype, while the *ppcesa6 ppcesa7* double knockout mutant line has shorter leafy gametophores, indicating that these two genes may play a similar role in cellulose biosynthesis with redundant functions (Wise et al. 2011). The generation and characterization of additional *Physcomitrella PpCESA* knockout mutants will be required to fully understand CESA diversification and functional specialization in *Physcomitrella*.

The *Physcomitrella* genome contains putative homologs of the *Arabidopsis* xyloglucan xylosyltransferases XXT1 and XXT2, which catalyze the transfer of Xyl from UDP-Xyl to the glucan backbone of xyloglucan (Cavalier and Keegstra 2006). Homologs of the galactosyl transferases MUR3 and GT18 have also been identified in the *Physcomitrella* genome; the proteins encoded by these genes may be involved in the biosynthesis of xyloglucan side chains (Pena et al. 2008). Members from the *CSLA* gene family have been show previously to encode glucomannan synthase enzymes that make the $\beta$-1,4-linked backbones of mannans (Dhugga et al. 2004; Liepman et al. 2005; Suzuki et al. 2006). Three *CSLA* genes have been identified in the *Physcomitrella* genome and at least two of them catalyze $\beta$-1,4-mannan and glucomannan synthase reactions as shown by heterologous expression in insect cells, indicating the conserved enzymatic function of CSLA proteins across major land plant lineages (Liepman et al. 2007).

Xylan has been detected in *Physcomitrella* leaf cells and axillary hairs by immunolabeling (Kulkarni et al. 2012b). The *Physcomitrella* genome contains homologs of all of the *Arabidopsis* glycosyltransferases that are possibly involved in xylan backbone biosynthesis, including IRX9, IRX10 and IRX14 (Hornblad et al. 2013). The *Physcomitrella* IRX10 protein

(PpGT47A) can partially rescue morphological abnormalities in the Arabidopsis *irx10 irx10-l* double mutant (increased inflorescence stems and rosette diameters), yet the *Physcomitrella ppgt47a* knockout lines do not display any identifiable defects (Hornblad et al. 2013). Therefore, the PpGT47A shares some function with the homologous *Arabidopsis* proteins. However, it is not essential for normal growth and development in *Physcomitrella*. The *Physcomitrella* genome also contains homologs of *IRX8/GAUT12* (Yin et al. 2010), *IRX7/FRA8(Kulkarni et al. 2012b),* and *GUX1* and *GUX2* (Harholt et al. 2012). Since xylan shows only a very limited presence in *Physcomitrella* by immunological and biochemical analyses (Moller et al. 2007; Kulkarni et al. 2012b), additional targeted knockout studies will be required to fully understand the functional diversity of these genes from an evolutionary view.

Desterified pectin and RG-I have been detected by immunolabeling in leaves and shoot-axes of *Physcomitrella* (Kulkarni et al. 2012b), and have been previously detected in *Phycomitrella* cell walls by comprehensive microarray polymer profiling (CoMPP) and sugar linkage analysis (Moller et al. 2007). A recent phylogenetic analysis of pectin-related gene families in *Physcomitrella* showed that the *Physcomitrella* genome contains at least one member in 12 out of 16 gene families associated with pectin biosynthesis; although the total number of pectin-related gene family members in *Physcomitrella* is much lower compared to that in *Arabidopsis* (McCarthy et al. 2014). No *Physcomitrella* homologs have been detected for xylogalacturonan xylosyltransferase, rhamnogalacturonan I arabinosyltransferase, pectin methylesterase inhibitor, or polygalacturonase inhibitor protein families (McCarthy et al. 2014). The *Physcomitrella* genome encodes 9 members of the GAUTs and 5 members of the GATLs (Yin et al. 2010).

However, to date, no complementation studies of *Arabidopsis* pectin mutants with homologous *Physcomitrella* genes have been reported, and no targeted knockout studies of pectin-related genes in *Phycomitrella* have been carried out. The demonstration that *PpGATL-A* can complement the *Arabidopsis parvus/gatl1* mutation described in this thesis (Chapter 2) is the first report of conserved functionality of a pectin-related gene across large phylogenetic distance in the plant kingdom. Furthermore, the isolation and characterization of *ppgatl-a* described in this dissertation (Chapter 3) is the very first study to generate galacturonosyltransferase-related gene knockout mutants in *Physcomitrella.*

**Overview of Dissertation**

The overall goal of this dissertation was to use the moss *Physcomitrella patens* to investigate the function of the five putative *PpGATL* glycosyltransferases and to identify their role(s) in plant cell wall biosynthesis.

Chapter 2 describes the cloning and characterization of a moss glycosyltransferase gene, *PpGATL-A*, which is a functional ortholog to *PARVUS/AtGATL1* in *Arabidopsis*. Expression studies by quantitative real time PCR demonstrate that all five *PpGATLs* genes are expressed in *Physcomitrella* tissues at different levels. Subcellular localization studies show that PpGATL-A is a Golgi localized protein. Overexpression of *PpGATL-A* in the *Arabidopsis parvus* mutant rescues the defects conferred by the *parvus* mutation, including changes in plant growth and tissue morphology, collapsed xylem, and decreased xylose content based on cell wall monosaccharide composition.

Chapter 3 describes the generation of a *ppgatl-a* targeted knockout mutant in *Physcomitrella*, and characterization of the knockout mutant lines shows that *PpGATL-A* is required for leafy gametophore development. Promoter::β-*glucuronidase* expression studies show that *PpGATL-A* is expressed at the base of leaves in the apical region of the *Physcomitrella* leafy gametophores, while *PpGATL-C* and *PpGATL-E* exhibit overlapping and distinct expression patterns compared to *PpGATL-A*. Monosaccharide composition analysis and glycome profiling of cell walls fractions of the *ppgatl-a* mutants reveal changes in cell wall monosaccharide composition as well as the alteration of epitope extractability patterns, which resemble characteristics of wild type protonema cell walls.

Chapter 4 is a summary chapter which discusses data presented in previous chapters and summarizes major conclusions. Future research work is also proposed at the end of this chapter.

# CHAPTER 2

## A MOSS GLYCOSYLTRANSFERASE GENE IS A FUNCTIONAL ORTHOLOG TO *PARVUS/ATGATL1* IN *ARABIDOPSIS THALIANA*

Yiwen Yang, Utku Avci, Sivakumar Pattathil and Michael G. Hahn. To be submitted to Molecular Plant or Plant Physiology.

**Abstract**

The *Arabidopsis* gene, *PARVUS/AtGATL1*, belongs to the *Galacturonosyl-transferase-Like* (*GATL*) gene family, which is part of CAZy Family GT8. *PARVUS/AtGATL1* has been associated previously with secondary wall xylan synthesis and possibly pectin synthesis in *Arabidopsis*. Homozygous *parvus/gatl1* mutants are semi-sterile and exhibit a dwarf growth phenotype with collapsed xylem. Cell walls of *parvus/gatl1* show significant reductions in xylose content compared with wild-type cell walls. However, the phenotype of the *parvus/AtGATL1* mutant is complex, with many character traits affected, including both primary wall and secondary wall defects, which complicates the characterization of *AtGATL1* gene function. The availability of the genome sequence for the moss, *Physcomitrella patens*, provides a basis for investigating the evolution of the *GATL* gene family and its function(s) in cell wall biosynthesis. *Physcomitrella* contains only primary cell walls, and its cell wall composition is comparable with that of vascular plants, making it an advantageous system for investigating cell wall biosynthesis and evolution. Phylogenetic analyses of Family GT8 glycosyltransferase sequences from the *Physcomitrella* genome have identified five orthologs (*PpGATL-A,B,C,D,E*) to *AtGATLs* that all lie basal to vascular plant GATLs. Expression studies by Quantitative RT-PCR demonstrate that all five *PpGATLs* genes are expressed in *Physcomitrella* tissues at different levels. Subcellular localization studies show that PpGATL-A is a Golgi localized protein. Overexpression of *PpGATL-A* in the *Arabidopsis parvus* mutant rescues the defects conferred by the *parvus* mutation, including changes in plant growth and tissue morphology, collapsed xylem, the decreased xylose content based on cell wall monosaccharide composition,

and the altered overall cell wall structure as indicated by altered epitope extractability patterns. These findings suggest that *PpGATL-A* is a functional ortholog of *PARVUS/GATL1* and at least one basic function of GATLs is conserved in highly divergent land plants.

**Introduction**

The plant cell wall is a complicated polysaccharide-rich network, composed of a variety of polymers, primarily cellulose, hemicelluloses and pectins. Evolution of plants over millions of years has resulted in increasing diversity and complexity in cell wall components, structures and functions. Current understanding of cell wall evolutionary changes is very limited since our knowledge of cell wall biosynthesis and function are mainly derived from studies on a few angiosperms species. Recently, however, there has been growing interest in the cell walls of non-angiosperms such as algae, bryophytes and lycophytes (Matsunaga et al. 2004; Carafa et al. 2005; Van Sandt et al. 2006; Van Sandt et al. 2007; Pena et al. 2008; Kulkarni et al. 2012b). Studies have shown that members of the charophycean green algae and land plants, which shared a common ancestor 725 to 1,200 million years ago (Becker and Marin 2009), have many cell wall components in common, including polysaccharides, glycoproteins and lignin (Popper and Tuohy 2010; Popper et al. 2011; Sorensen et al. 2011). However, algal cell walls also exhibit enormous cell wall compositional variation and structural diversity compared to land plant cell walls, and some key changes appear to have accompanied major evolutionary events such as the colonization of terrestrial habitats and vascularization as indicated by phylogenetic analyses (Popper et al. 2011).

The increasing use of the moss *Physcomitrella patens* as a model for investigating vascular plant cell wall structure and biosynthesis also demands more complete knowledge of bryophyte walls (Lee et al. 2005b). Recent analyses using a diversity of approaches based on enzymatic digestion, glycosyl residue and glycosyl linkage analysis, and immunolocalization of polysaccharide epitopes indicate that considerable similarities with subtle differences exist between the cell wall components of angiosperms and bryophytes (Popper and Fry 2003; Lee et al. 2005a; Moller et al. 2007; Pena et al. 2008; Kulkarni et al. 2012b). The cell walls of *Physcomitrella* and vascular plants are composed of the same types of polysaccharides, though in different proportions. Cellulose, hemicelluloses (including xylan, xyloglucan and mannan), and pectins [including homogalacturonan (HG) and rhamnogalacturonan I(RG-I)], have been detected in *Physcomitrella* cell walls by biochemical methods and immunological and/or affinity approaches using glycan-directed monoclonal antibodies and carbohydrate binding modules (Moller et al. 2007; Pena et al. 2008; Kulkarni et al. 2012b).

To date, little is known about the evolutionary relationship between the genes involved in the biosynthesis of cell wall components among different plant lineages. However, it could be expected that some cell wall-related genes (e.g., glycosyltransferases) are conserved between non-vascular and vascular plants, as these plants have at least some cell wall characteristics in common (e.g., polysaccharides). Such conserved gene functions could arise from conservation of function via a shared common ancestor and/or convergent evolution (Popper and Tuohy 2010).

Pectins are the most complex plant cell wall polysaccharides structurally and at least 67 different GTs are required for pectin biosynthesis (Mohnen 2008; Atmodjo et al. 2013). A

number of putative pectin biosynthetic glycosyltransferases (GTs) have been identified from biochemical and genetic studies; however, the enzymatic activity has been biochemically demonstrated for only seven of them. These include four genes from CAZy (Cantarel et al. 2009) family GT77, *RGXT1, RGXT2, RGXT3* and *RGXT4/MGP4*, which appear to encode (1,3)-α-D-xylosyltransferases involved in the synthesis of side chain A of rhamnogalacturonan II (RG-II) (Egelund et al. 2006; Egelund et al. 2008; Liu et al. 2011); the *GAUT1* gene from family GT8, which encodes a (1,4)-α-D-galacturonosyltransferase involved in HG synthesis (Sterling et al. 2006); XGD from family GT47, which participates in the synthesis of xylogalacturonan (XGA) as a β-(1,3)-xylosyltransferase (Jensen et al. 2008); and *GALS1* from family GT92, which encodes a β-(1,4)-galactosyltransferase involved in the synthesis of β-(1,4)-galactan side chains of RG-I (Liwanag et al. 2012).

GAUT1 is the first identified galacturonosyltransferase (GalAT) that has been functionally determined to be involved in pectin synthesis. Comparison of *GAUT1* gene sequence against all genes in the *Arabidopsis* genome identified 24 additional genes with high sequence similarity to *GAUT1*. All 25 Arabidopsis genes were suggested to represent putative GalATs and have been grouped into a GAUT1-related gene superfamily, including 15 *GAUT* genes and 10 *GATL* (GAUT-Like) genes. Analysis of cell walls isolated from *Arabidopsis* homologous transfer DNA (T-DNA) mutants demonstrated that mutants in 8 members of the *GAUT* family (*atgaut6, atgaut8, atgaut9, atgaut10, atgaut11, atgaut12, atgaut13* and *atgaut14*) and 3 members of the *GATL* family (*atgatl3, atgatl6* and *atgatl9*) resulted in significantly changes in GalA content (Caffall et al. 2009; Kong et al. 2011). *atgatl5* mutants show defects in seed mucilage synthesis

and cell adhension, and GalA and Rha contents in *atgatl5* mucilage are significantly reduced compared to wild type mucilage (Kong et al. 2013). These results suggest that the corresponding genes may encode putative GalATs involved in pectin synthesis. Plants carry homozygous mutations in the *QUA1/GAUT8* (Bouton et al. 2002; Orfila et al. 2005), *IRX8/GAUT12* (Persson et al. 2007; Pena et al. 2007; Hao et al. 2014) and *PARVUS/GLZ1/GATL1* (Brown et al. 2007; Lee et al. 2007) genes are affected in both pectin and xylan biosynthesis. Mutant plants of these genes show growth defects such as dwarfism and reduced fertility. *gaut8*/*qua1* mutants also show defects in cell-cell adhesion and have reduced GalA and Xyl content in cell wall, and studies of *qua1* stem microsomes reveal a reduction in both GalAT and xylan synthase activity (Orfila et al. 2005). *gaut12*/*irx8* and *parvus/gatl1* mutants exhibit a collapsed xylem phenotype with a significant decrease in xylan content of the cell walls as indicated by biochemical and histochemical analyses (Brown et al. 2005; Brown et al. 2007; Lee et al. 2007; Persson et al. 2007; Kong et al. 2009). Chemical studies of *gaut12* and *parvus/gatl1* walls also reveal the absence of the xylan reducing end glycosyl sequence [4-β-D-Xyl-1,3-α-L-Rha-1,2-α-D-GalA-1,4-D-Xyl] (Pena et al. 2007), and several studies have suggested that PARVUS/GATL1 is involved in the synthesis of this tetrasaccharide sequence, which has been detected in xylans from many higher plants including *Arabidopsis*, birch, aspen and spruce (Shimizu et al. 1976; Johansson and Samuelson 1977; Andersson et al. 1983; Pena et al. 2007), but is absent in other plants, particularly the monocot grasses (Kulkarni et al. 2012a). These results indicate that *GAUT8*/*QUA1*, *GAUT12*/*IRX8*and *PARVUS/GATL1*genes are possibly involved in pectin and/or xylan polysaccharide biosynthesis.

*Populus* homologs of *PARVUS/AtGATL1* are able to rescue the plant growth defects and structural defects caused by the *parvus* mutation in *Arabidopsis*, indicating the functional conservation of the PARVUS/GATL1 protein between herbaceous and woody plants (Lee et al. 2009; Kong et al. 2009). The *Physcomitrella* genome encodes five genes that are homologous to *Arabidopsis GATL*s; these genes form a phylogenetic clade that is basal to the clade containing GATL1 (Yin et al. 2010; Kong et al. 2011). The five *Physcomitrella* GATL homologs share a common ancestor with all vascular plant GATLs, raising the possibility that one or more of the *Physcomitrella* proteins might also share similar functionality with the AtGATLs. Xylan has been detected by immunofluorescence in leaf cells and axillary hairs in *Physcomitrella* (Kulkarni et al. 2012). However, the absence of the distinctive reducing-end sequence in *Physcomitrella* xylan and the absence of secondary walls in this moss leaves open the question of the roles of *Physcomitrella* GATLs in cell wall biosynthesis (Kulkarni et al. 2012b).

In this study, *Physcomitrella* has been used to investigate the origin and functional role(s) of *GATL* gene family members. We examined the expression patterns of *PpGATL* genes, the subcellular localization of the corresponding proteins, and their ability to complement the *Arabidopsis parvus* mutant, which carries a mutation in the *AtGATL1* gene. The reason to choose *PARVUS*/*ATGATL1* is because homozygous *parvus/gatl1* mutants exhibit growth defects that are easily distinguishable from WT plants, including dwarfism, dark-green leaves, reduced size of all organs and reduced fertility (Lao *et al*., 2003; Shao *et al*., 2004; Lee *et al*., 2007). We report here that overexpression of *PpGATL-A* in the *Arabidopsis parvus* mutant rescues all plant growth defects, the decreased xylose content in the cell walls, and altered overall wall structure to

restore wild-type characteristics for these traits. Results obtained suggest that *PpGATL-A* is a functional ortholog of *PARVUS/GATL1* and at least one GATL protein function has been conserved in these two highly divergent land plants.

**Results**

Gene Structure and Expression Profiles of five *PpGATLs*

Five GATL orthologs named *PpGATL-A* to *PpGATL-E* have been identified in *Physcomitrella*: they form a sister group to seed plant GATLs (Yin et al. 2010; Kong et al. 2011). *PpGATL-A*, *-B* and *–C* each encode proteins of 280 amino acids, and *PpGATL-D* and *PpGATL-E* encode proteins of 275 and 279 amino acids, respectively. Based on multiple sequences alignments of the amino acid sequences of the encoded proteins, the five PpGATLs cluster into two groups (PpGATL-A, PpGATL-C and Pp-GATL-E, PpGATL-B and PpGATL-D) (Figure 2.1). PpGATL-A, PpGATL-C and PpGATL-E share 63%, 62% and 61% identity with PARVUS/AtGATL1, while PpGATL-B and PpGATL-D have 53% and 48% identity respectively with PARVUS/AtGATL1 (Figure 2.2).

The expression profiles of the five *PpGATL* genes were analyzed by quantitative real-time PCR using primers that were specific to each gene. Protonema and leafy gametophore tissues were harvested 6 days and 4 weeks after inoculation, respectively. EFα1 (Eukaryotic translation elongation factor alpha 1) was used as a consitutively expressed internal control to normalize all samples. As indicated in Figure 2.3, all the five *PpGATL* genes are expressed in protonema and leafy gametophores, yet the transcript levels of *PpGATL-B* and *PpGATL-D* are much lower than

those of the other three genes. Subsequent studies focused on three *PpGATLs* that have relatively higher expression levels, i.e., *PpGATL-A, PpGATL-C* and *PpGATL-E.*

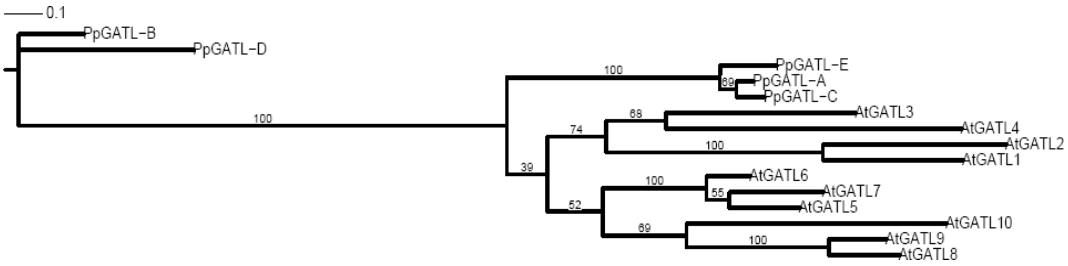


Figure 2.1. Molecular phylogenetic tree of full-length GATLs amino acid sequences from *Physcomitrella* and *Arabidopsis*. The protein sequences from *Arabidopsis* and *Physcomitrella* were aligned using MUSCLE (Edgar, R.C., 2004), and a maximum likelihood phylogenetic tree was constructed using PhyML 3.0 (Guindon S et al., 2010) based on the multiple sequence alignment.

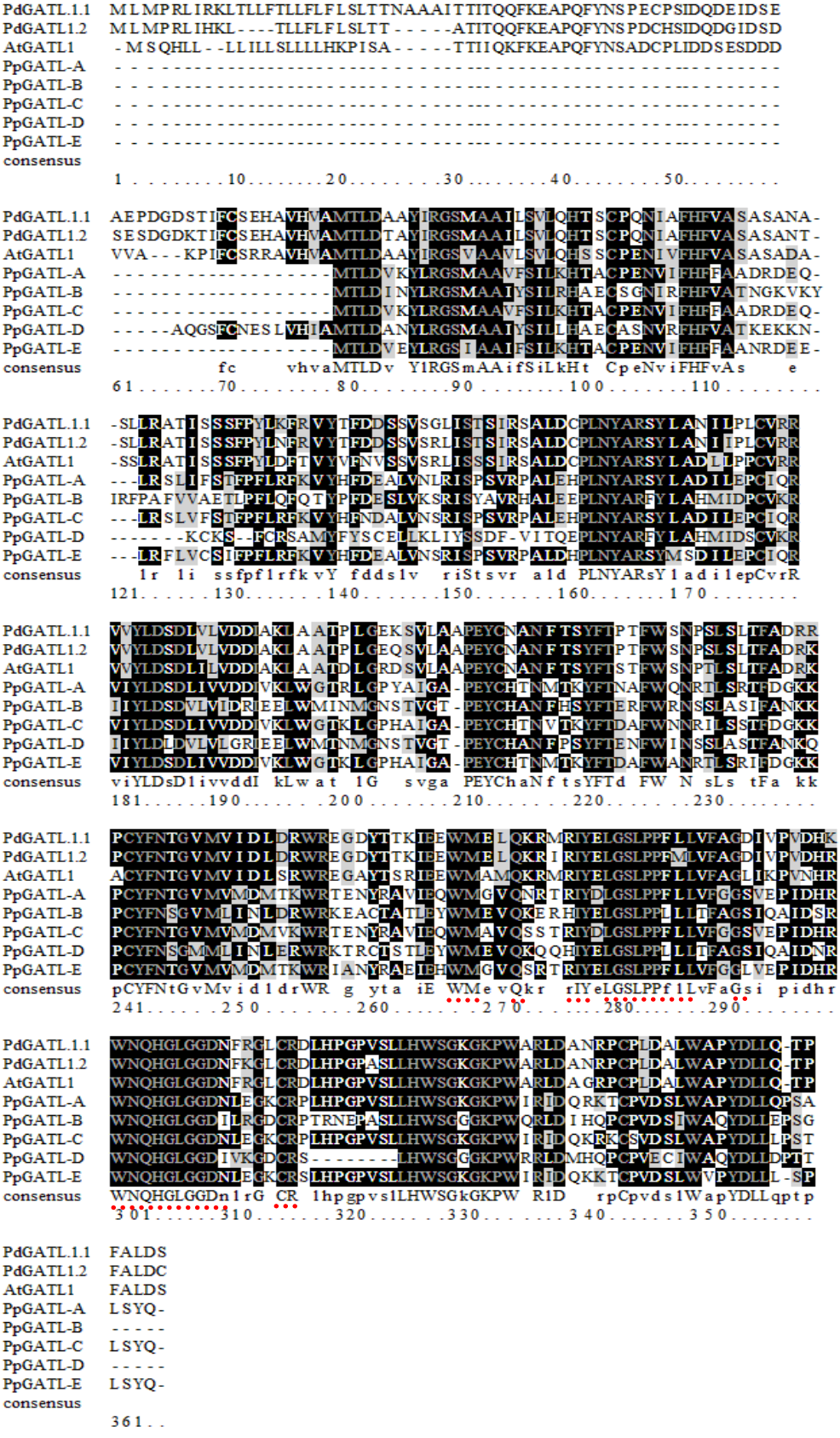
PdGATL.1.1
PdGATL1.2
AtGATL1
PpGATL-A
PpGATL-B
PpGATL-C
PpGATL-D
PpGATL-E
consensus

Figure 2.2. Multiple sequence alignment of PdGATL1.1, PdGATL1.2, PARVUS/AtGATL1 and PpGATL-A to PpGATL-E. The GATL-related protein sequences from *Arabidopsis thaliana*(At) , *Populus deltoides* (Pd) and *Physcomitrella patens* (Pp) were aligned using MUSCLE (Edgar, R.C., 2004). Identical and similar amino acid residues are shades with black and grey, respectively. The conserved amino acid residues within the amino acid motifs diagnostic for the GATL family are marked with red dots.

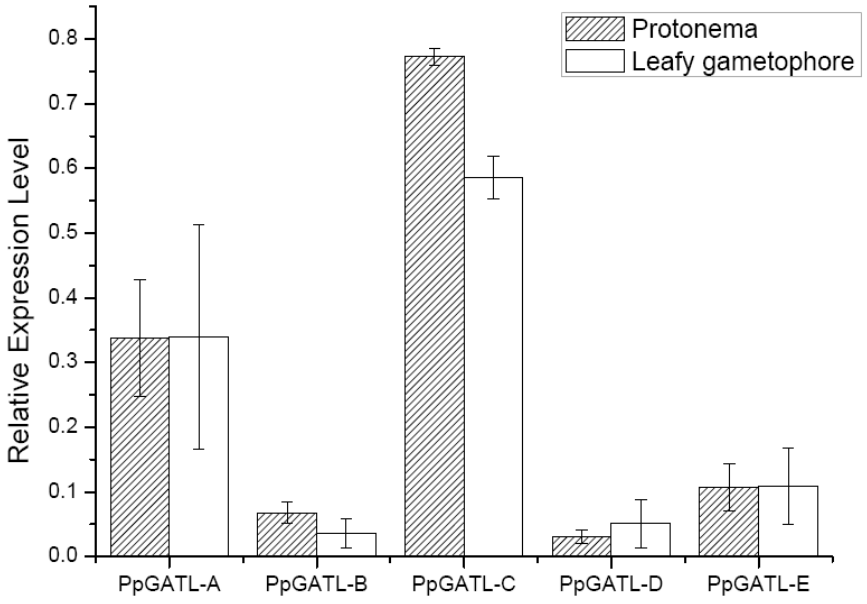


Figure 2.3. Quantitative Real-Time PCR analysis of expression levels of all five *GATL* genes in *Physcomitrella* 6-day-old protonema and 4-week-old leafy gametophores. RNA isolated from triplicate protonema or leafy gametophore cultures were amplified using primers specific for each gene.

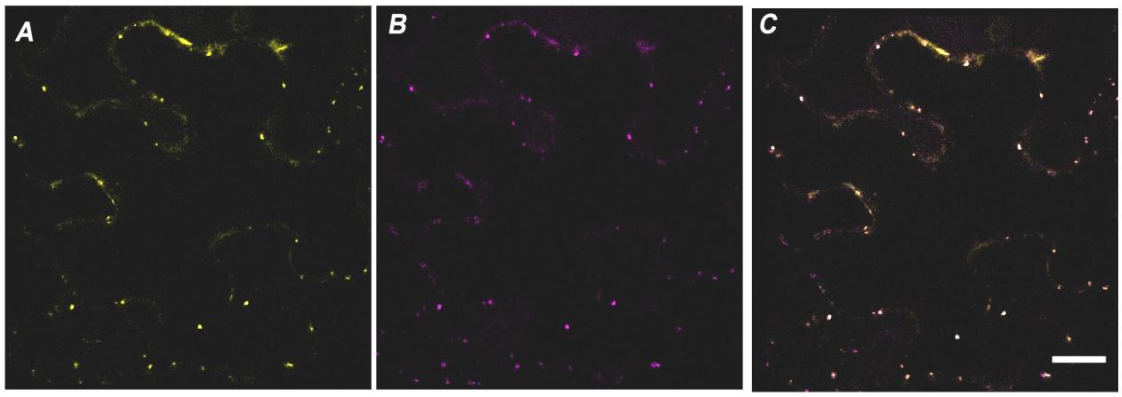


Figure 2.4. Subcellular localization of EYFP-tagged PpGATL-A protein. (A) EYFP-tagged PpGATL-A protein was transiently expressed under the control of 35S promoter in leaf epidermal cells of *Nicotiana.benthamiana* and imaged by confocal laser scanning microscopy. (B) Gmct-ECFP Golgi marker protein was expressed in the same cells as in A. (C) Merged image of A and B, colocalization of PpGATL-A-EYFP and Gmct-ECFP are visible as white dots. Scale bar = 20 μm.

Subcellular localization of the PpGATL proteins

The PARVUS/AtGATL1 protein has been reported to be localized in both endoplasmic reticulum (ER) and Golgi by heterologous expression studies in carrot protoplasts or *Nicotiana benthemiana* leaves (Lee et al., 2007; Kong et al., 2009). Five other AtGATL proteins, AtGATL2, AtGATL3, AtGATL5, AtGATL7 and AtGATL9 are also localized in Golgi (Kong et al. 2011; Kong et al. 2013). To experimentally investigate the subcellular localization of the PpGATL proteins, we fused PpGATL-A, PpGATL-C and PpGATL-E with enhanced yellow fluorescent protein (EYFP) at the C-terminus. The recombinant constructs were then transformed into *Nicotiana.benthamiana* leaves together with Gmct-ECFP, an enhanced cyan

fluorescent protein (ECFP)-tagged Golgi marker (Saint-Jore-Dupas et al. 2006; Nelson et al. 2007) or ECFP-WAK2-HDEL, an endoplasmic reticulum marker (Nelson et al. 2007). Confocal microscopy was used to determine the sub-cellular localization of the recombinant PpGATLs. EYFP-tagged PpGATL-A showed a punctuate localization pattern in tobacco leaf epidermal cells, which overlapped with the pattern of Golgi marker Gmct-ECFP in colocalization experiment (Figure 2.4). These results demonstrate that PpGATL-A is a Golgi-localized protein. Similar subcellular localizations were also observed for PpGATL-C and PpGATL-E proteins (Figure S2.1). The Golgi localization of these PpGATLs is consistent with possible role(s) for these proteins in plant cell wall matrix polysaccharide synthesis (Nebenfuhr and Staehelin 2001) .

*PpGATL-A* Rescues *Arabidopsis parvus/AtGATL1* Mutant Phenotypes

To determine whether the function of PpGATL proteins are conserved between *Arabidopsis* and *Physomitrella*, we performed mutant complementation analysis by overexpression of *PpGATL* genes in the *Arabidopsis* heterozygous *parvus/gatl1* mutant background, since homozygous *parvus/gatl1* mutant plants are semi-sterile (Lao et al., 2003; Shao et al., 2004; Lee et al., 2007). cDNAs corresponding to the three genes (*PpGATL-A, PpGATL-C, PpGATL-E*) with relatively higher expression levels were isolated by RT-PCR from 6-day old protonema tissues and amplified by gene-specific primers and then inserted into pCAMBIA vectors behind the CaMV 35S promoter. Transgenic plants were selected on hygromycin, and homozygous lines were identified by PCR. Homologous *gatl1* mutants show severe dwarfed growth and sterility with smaller leaves, flowers and siliques (Lao *et al*., 2003; Shao *et al*., 2004; Lee *et al*., 2007). Overexpression of *PpGATL-A* in mutant plants rescued the morphological defects

caused by the *parvus* mutation. The morphology of the complemented plants is indistinguishable from that of WT *Arabidopsis* plants (Figure 2.5A). Six independent *Arabidopsis* transgenic lines with a homozygous *parvus* background are shown in Figure 4B. Both T-DNA insertion and absence of endogenous *PARVUS*/*AtGATL1* gene in the transgenic lines were confirmed by PCR detection. RT-PCR was also conducted to confirm *PpGATL-A* mRNA expression in all transgenic lines (Figure 2.5B). Overexpression of *PpGATL-C* or *PpGATL-E* did not complement the growth phenotype of the *parvus* mutant (data not shown).

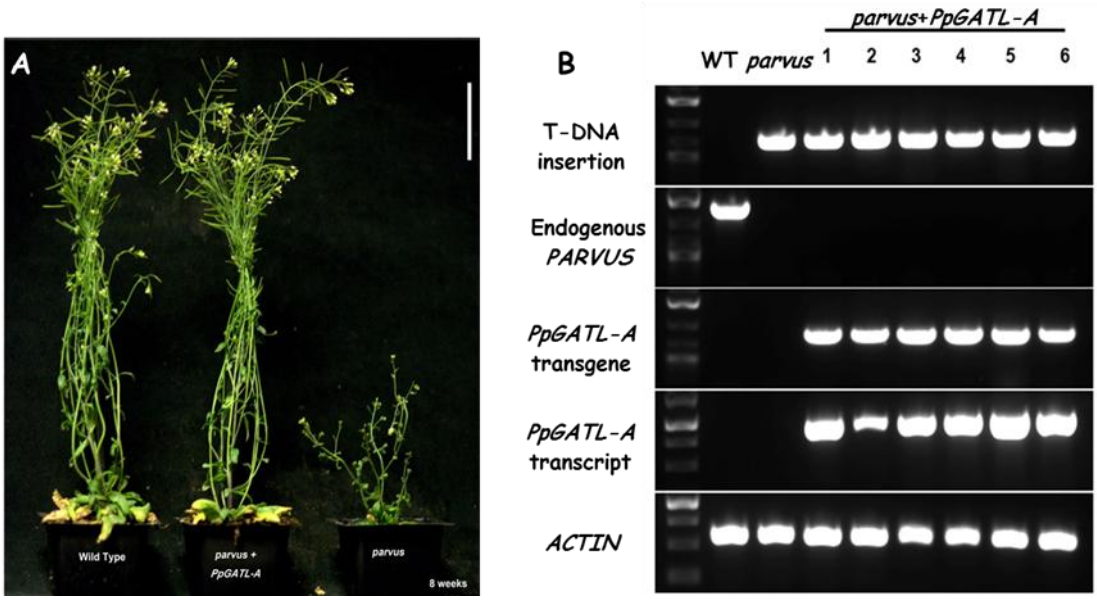


Figure 2.5. (A) The *parvus/gatl1* mutant (right) has a short inflorescence stem and a small rosette size. Overexpression of *PpGATL-A* in the *parvus/gatl1* plant (middle) restored the stem height and rosette size to those of WT (left). Overexpression of *PpGATL-C* or *PpGATL-E* did not complement the growth phenotype of the *parvus* mutant (not shown). (B) PCR detection of the *PpGATL-A* transgene and its transcript in transgenic *parvus/gatl1* plants. The expression of the *ACTIN* gene was used as an internal control. Scale bar in (A) = 5 cm.

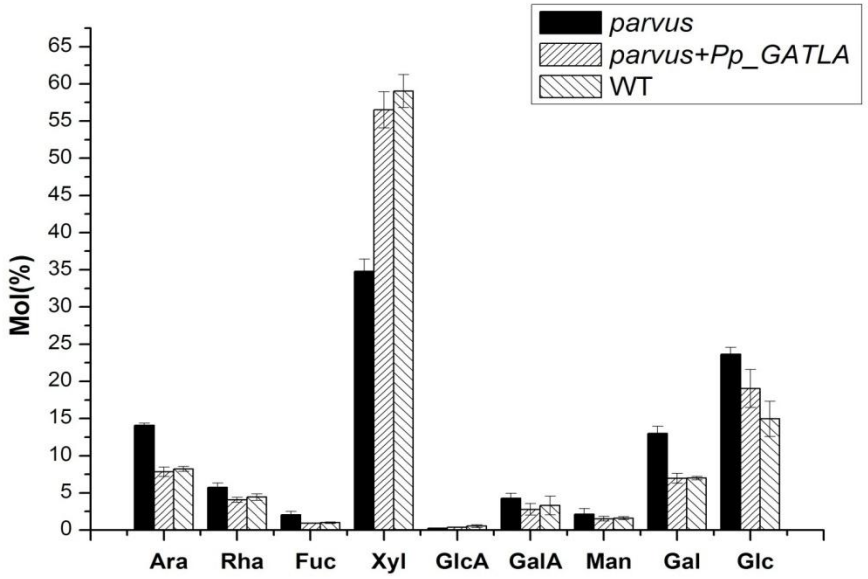


Figure 2.6. Monosaccharide composition of cell walls isolated from the stems of *parvus*, *parvus* complemented with *PpGATL-A*, and wild-type plants. Cell walls were prepared from stems of 8-week-old plants and their glycosyl compositions were determined by gas chromatography-mass spectrometry (GC-MS) of trimethyl silyl derivatives as described in "Materials and Methods". Data are displayed as means (mol %) ± SE of measured sugars from analyses on three biological replicates pooled from multiple plants.

Mutation of the *PARVUS* gene leads to a large reduction in secondary thickening and xylose content in stems (Brown et al. 2007; Lee et al. 2007). Mutant plants also exhibit a collapsed xylem vessel phenotype (Lee et al. 2007). To determine the biochemical basis for the complementation phenotype, monosaccharide analysis was performed on total cell wall material isolated from stems of the transgenic plants (Figure 2.6). In *parvus/gatl1* mutants, the xylose

content is decreased by about 41% compared to w.t., and overexpression of *PpGATL-A* in a *parvus/gatl1* background restored the level of xylose to about 96% of w.t. levels.

To examine cell wall structure changes resulting from the *parvus/gatl1* mutation, glycome profiling (Pattathil et al. 2012) was used to compare extractable cell wall polymers prepared from wild-type, *parvus/gatl1* and *parvus+PpGATL-A* stem cell walls. In this analysis, sequential cell wall extracts are ELISA-screened using a toolkit of approximately 150 plant cell wall glycan-directed monoclonal antibodies (mAb) that recognize diverse epitopes present on most major classes of plant cell wall polysaccharides, including arabinogalactans, pectins, xyloglucans, xylans, and mannans (Pattathil et al. 2010). Glycome profiles of *parvus/gatl1* walls show major differences compared to wild type and complemented plants cell walls (Figure 2.7). The oxalate extracts of *parvus/gatl1* stems contain easily detectable levels of acetylated mannan epitopes, whereas the oxalate extracts of wild-type and *parvus+PpGATL-A* walls showed much less detectable acetylated mannan epitopes as outlined in orange boxes. In contrast to wild type plants, the sodium carbonate extracts prepared from *parvus/gatl1* walls contained less xylan epitopes recongized by the xylan-4 through xylan-7 groups of monoclonal antibodies (white boxes). The 1M KOH extracts of *parvus/gatl1* showed enhanced levels of xylan-4 to xylan-7 epitopes, HG backbone and RG-I backbone epitopes (yellow boxes) and pectic arabinogalactan (RG-I/AG) epitopes (green boxes). However, lower amounts of carbohydrate were recovered in the 1M KOH extracts prepared from *parvus/gatl1* walls. The complemented line, *parvus+PpGATl-A*, exhibits similar cell wall glycome profiles as wild type. These results show that the overall cell wall structure is altered by the *parvus* mutation, leading to the changes in glycan epitope extractability patterns, including xylan, pectin and

arabinogalactan; and overexpression of *PpGATL-A* in the *parvus* mutant restored these changes to wild-type.

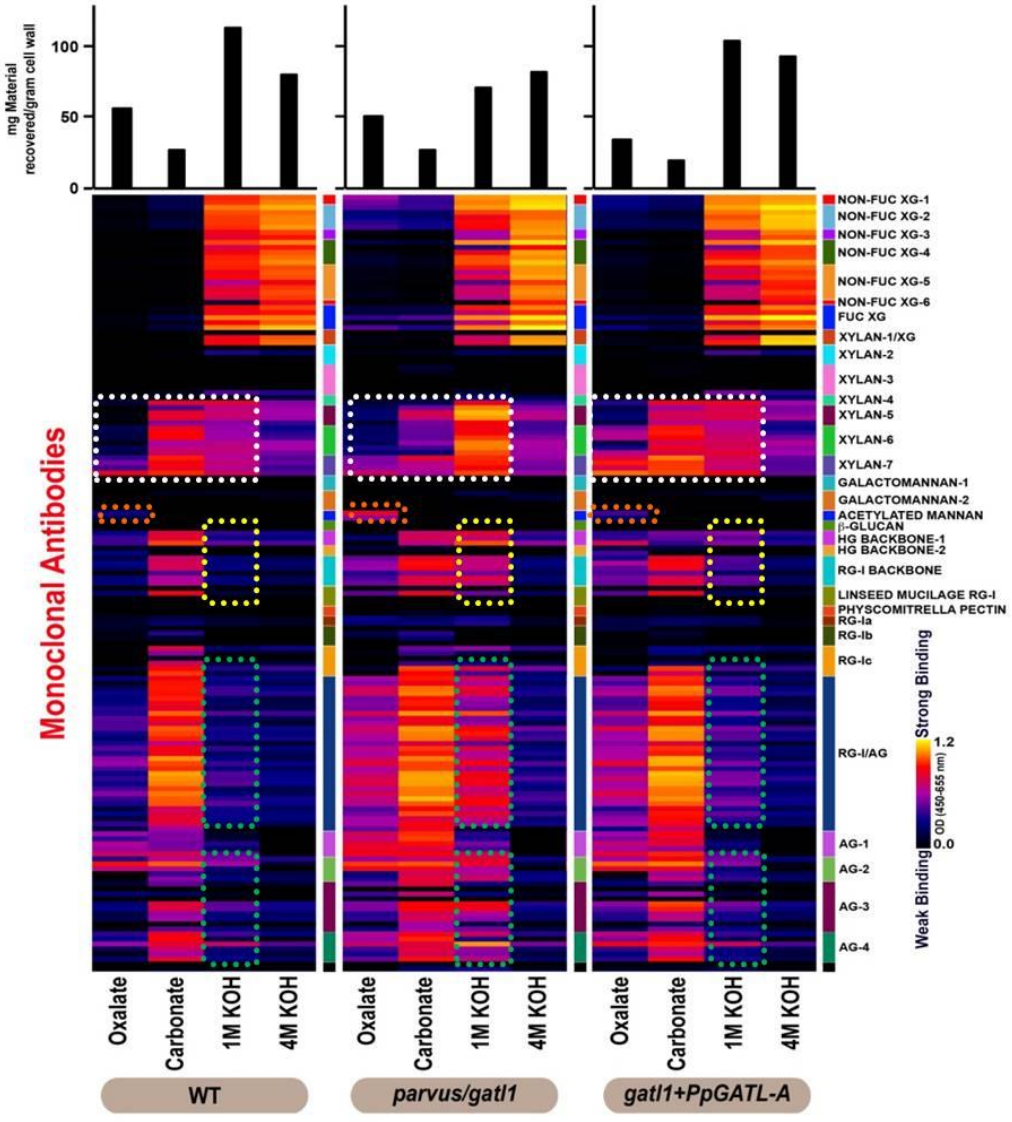


Figure 2.7. Glycome profiling of cell walls prepared from 8-week-old stem tissues of *Arabidopsis* wild-type (WT), *parvus/gatl1* and *parvus+PpGATL-A* plants. Stem cell walls from different plant lines were sequentially extracted using ammonium oxalate (oxalate), sodium carbonate (carbonate) and potassium hydroxide (1 M and 4 M KOH). The wall extracts were screened by ELISA using 155

plant cell wall glycan-directed monoclonal antibodies for presence of cell wall glycan epitopes (Pattathil et al. 2010), and the data are presented as heat maps. The strength of the ELISA signal is indicated by a yellow-red-black scale (depicting strong, medium, and no binding, respectively). The panels at the right-hand side of the figure depict the array of antibodies used, which are grouped according to the principal cell wall glycans recognized by each antibody group, and the list of individual antibodies used in this analysis are as previously described (Pattathil et al. 2012). The amounts of material extracted with each extraction reagent are indicated in the bar graphs above the heat maps. Major changes in glycome profiles among different plant lines extracts are outlined in white (xylan groups 4 to 7), orange (Acetylated mannan), yellow (HG backbone and RG-1 backbone) and green (pectic arabinogalactan and arabinogalactan epitopes) boxes.

Immunolocalization of xylan using four monoclonal antibodies that recognize different epitopes on xylan polymers was also carried out to investigate whether the complementation by *PpGATL-A* could be correlated with the rescue of xylan synthesis. LM10 has been reported to bind to unsubstituted or lower-substituted xylans, while LM11 binds to both linear and substituted xylan (McCartney et al. 2005). CCRC-M138 bind to xylopentaose and CCRC-M149 bind to both xylotriose and xylopentaose in ELISAs (Pattathil et al. 2010). Immunolabeling of transverse sections of WT stems and hypocotyls with all four xylan-directed antibodies showed specific binding to xylem cells and interfascicular fibers (Figure 2.8). Compared to wild type xylem and fiber cells, the labeling intensity was largely reduced in the *parvus/gatl1* mutant (Figure 2.8). In *PpGATL-A* complemented *parvus/gatl1* plants, the labeling intensity were

restored to wild type levels (Figure 2.8). These results indicate that PpGATL-A can functionally replace PARVUS/GATL1 in *Arabidopsis*.

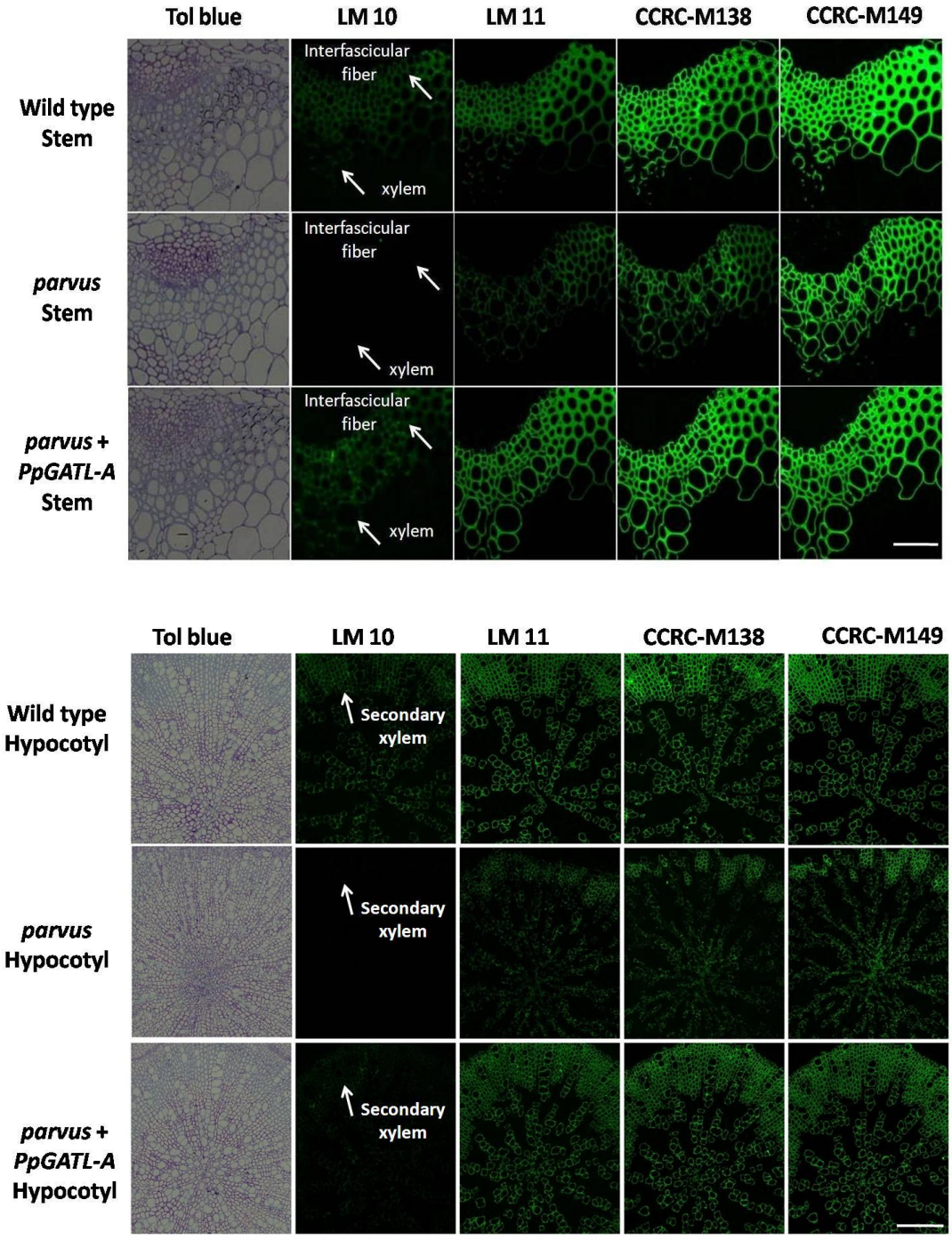

Figure 2.8. Immunofluorescent labeling of transverse sections of wild-type, *parvus*, and *parvus+PpGATL-A* stems and hypocotyls. Stems and hypocotyls of 8-week-old plants were sectioned (250 nm thick) and stained with toluidine blue or labeled with LM10, LM11, CCRC-M138 and CCRC-M149, which recognize different epitopes on xylan polymers. Scale bar= 50 μm.

**Discussion**

Five homologs of the *Arabidopsis GATL* genes, named *PpGATL-A-E*, had been identified previously in *Physcomitrella patens* genome (Rensing et al. 2008). The five PpGATL proteins lie basal to all angiosperm GATLs (Yin et al. 2010) and share 48%-63% sequence identity with PARVUS/ATGATL1. Here, we demonstrate that overexpression of *PpGATL-A* can compensate for the lack of functional PARVUS/AtGALT1 in the *parvus* mutant of *Arabidopsis*, indicating that these two proteins retain functional conservation in at least one basic function. Although PpGATL-C and PpGATL-E share 93% and 89% identity with PpGATL-A in amino acid sequence, neither of them is able to rescue the growth defects of the *parvus* mutant by overexpression studies.

The highly degree of sequence conservation between the three PpGATL proteins suggest that these proteins are paralogs originating from recent gene duplication events. Such duplicated genes can have diverse fates subsequent to the duplication. The duplicated gene copies can retain their original ancestral function during subsequent evolution, or one of the copies may lose its function due to a deleterious mutation and become a pseudogene. More importantly,

duplicated genes may accumulate changes in DNA sequence and undergo functional specialization, resulting in sub-functionalization of the related proteins (Force et al. 1999). In *Populus*, there are two paralogs of AtGATL1 that share high sequence identity with each other (Aspeborg et al. 2005; Kong et al. 2009). Expression of either of these *Populus* genes in the *Arabidopsis parvus* mutant rescues the plant growth defects and structural defects of xylan caused by the *parvus* mutation (Kong et al. 2009; Lee et al. 2009). The two poplar paralogs arose out of a very recent whole genome duplication that occurred about 15 million years ago (Tuskan et al. 2006). Thus, the two poplar GATL1 isoforms appear not to have diverged functionally from each other, though their gene expression patterns are very different in poplar tissues (Kong et al. 2009). Investigations in *Physcomitrella* based on EST sequences inferred that the genome duplication occurred between 30 and 60 million years ago (Rensing et al. 2007). In *Physcomitrella*, *PpGATL-A, -C* and *–E* have different transcription levels as shown in Figure 2.3. More importantly, only *PpGATL–A* is able to rescue the *parvus/gatl1* mutation. These results suggest that sub-functionalization has occurred for these three genes and that at least one function of PpGATL-A has remained conserved between non-vascular and vascular plants. Given the extensive sequence identity between the three *Physcomitrella* GATLs in this clade, it appears that subtle differences in amino acid sequences of the PpGATLs have resulted in altered enzymatic activity or other activities for these proteins, which have yet to be demonstrated experimentally.

*PARVUS/AtGATL1* has been suggested to play a role in xylan synthesis, specifically, to be involved in the synthesis of the GalA-containing tetrasaccharide sequence located at the reducing end of dicot and gymnosperm xylans (Brown et al. 2007; Brown et al. 2009; Pena et al. 2007;

Persson et al. 2007). The *parvus* mutation leads to large reductions in cell wall xylose content and loss of this reducing-end sequence in *Arabidopsis*. However, it is still not clear whether *AtGATL1* is directly involved in xylan synthesis, or indirectly through the synthesis of another polysaccharide to which the xylan reducing end tetrasaccharide sequence is attached (Mohnen 2008). A recent study indicates that this distinctive GalA-containing tetrasaccharide sequence is absent in *Physcomitrella* xylan (Kulkarni et al. 2012b) Furthermore, xylan shows only a very limited presence in *Physcomitrella* as determined by immunological and biochemical analyses (Kulkarni et al. 2012b). Xylan-specific epitopes have only been detected in leaf cells and axillary hairs in *Physcomitrella*. Thus, xylan seems not to be a major component in *Physcomitrella* cell walls since only a limited number of cells make this polysaccharide (Kulkarni et al. 2012b). Moreover, the phenotype of the *parvus/gatl1* mutant in *Arabidopsis* is complex. In addition to defects in secondary cell wall formation, *Arabidopsis* plants carrying the *parvus* mutation show many characteristics consistent with other pectin mutants (Bouton et al. 2002; Orfila et al. 2005; Persson et al. 2007; Hao et al. 2014). Mutants in *AtGATL1* display humidity-sensitive semi-sterile dwarf phenotypes with indehiscent anthers and reduced levels of branching in RG- I (Lao et al. 2003). The hypocotyls of the *parvus* mutant also exhibit defects in the radial organization of the central cell files (Kong et al. 2009). These characters cannot be simply attributable to defects in xylan synthesis, which occurs only of xylem cells in *Arabidopsis*. Expression of *PpGATL-A* in the *parvus* mutant not only complements the decreased xylose content in cell wall monosaccharide composition, but also rescues the changes in plant growth and tissue morphology; the mutant plant has been fully restored to the wild-type phenotype.

Histochemical analysis of *AtGATL1* using a GUS reporter gene construct reveals that *AtGATL1* is strongly expressed in the root apical meristem and elongation zones; these tissues are not associated with xylan synthesis in *Arabidopsis* (Kong et al. 2011). The above evidence supports another possibility that *AtGATL1* is likely to be involved in the synthesis of other polymers, such as pectin, which provide a foundational structure for xylan synthesis and deposition. A similar conclusion was drawn recently for the *GAUT12/IRX8* gene in *Arabidopsis*, whose mutation also leads to defects in both xylan and pectin deposition (Hao et al. 2014).

In conclusion, we have shown that *PpGATL-A* is a functional ortholog of *PARVUS/AtGATL1* in *Arabidopsis.* The ability of genes from *Populus* and *Physcomitrella* to complement the *Arabidopsis parvus* mutant demonstrates that at least one basic function of GATL1 is conserved in highly divergent land plants. The results of this study provide further evidence that *PARVUS*/AtGATL1 may not be directly involved in xylan synthesis by contributing to the GalA-containing reducing end oligosaccharide synthesis as previously hypothesized. Elucidation of the precise function of *PpGATL-A* will require further study to understand this gene's contribution to pectin and xylan biosynthesis.

## Material and Methods

### Bioinformatic Analyses

The *Physcomitrella patens* subsp *patens* v1.1 database was used to search for homologs using the *Arabidopsis* GATL proteins sequences. Sequences were aligned using MUSCLE

(Edgar 2004), and the resulting alignment was used to perform maximum likelihood phylogeny reconstruction using PhyML 3.0 (Guindon et al. 2010).

Plant Material

*Arabidopsis* plants were grown on soil in a controlled-environment chamber under a 14-h light/10-h dark cycle at 19 ℃ during the light period and 15 ℃ during the dark period. The light intensity was 150 μE $m^{-2}s^{-1}$, and the relative humidity was maintained at 60-70%. *Arabidopsis* plants of the Columbia ecotype were used for transformation and isolation of DNA and RNA. TDNA- mutagenized seeds were obtained from the SALK Institute (http://signal.salk.edu/cgibin/tdnaexpress) through the *Arabidopsis* Biological Resource Center. T-DNA insertions were identified using the gene-flanking primers (LP and RP) generated by the SIGnal T-DNA verification primer design website (http://signal.salk.edu/tdnaprimers.html) and primers from the T-DNA left border LBa1 (5'-GCGTGGACCGCTTGCTGCAACT-3') and LBb1 (5'-TCAAACAGGATTTTCGCCTGCT-3').

For *Physcomitrella patens*, the wild type Gransden strain was used in this study. Protonema and leafy gametophores tissues were grown with a 16 h light (50–70 μmol photons $m^{-2}$ $s^{-1}$) and 8 h dark cycle at 23 ℃ on basal medium with ammonium tartrate (BCDAT) medium (Nishiyama et al. 2000) overlaid with cellophane.

Quantitative RT-PCR

RNA was extracted with RNeasy plant mini kit (Qiagen,Valencia, CA) from triplicate protonema and leafy gametophores cultures harvested 6 days and 16 weeks after inoculation,

respectively. Contaminating genomic DNA was removed using RNase-free DNase (Qiagen) and cDNA synthesis was carried out using Superscript III reverse transcriptase (Invitrogen), oligo-dT primers and 1μg of total RNA/20μ L reaction. The resulting cDNA (1μL/reaction) was subjected to quantitative PCR in an iCycler iQ system (Bio-Rad) using IQ™ SYBR® Green Supermix (Bio-Rad) and primers (Supplemental Table S2.1) specific for each of the 5 *PpGATL* genes. EFα1 was used as a reference gene to normalize for variation in the amount of cDNA template (Exposito-Rodriguez et al. 2008).

Mutant Complementation Analysis

The *PpGATL-A, -C, -E* cDNAs were isolated by RT-PCR from 6-day old *Physcomitrella* protonema tissues and amplified by gene-specific primers (Supplemental Table S2.2) and then inserted into the plant transformation vector, pCAMBIA (Hajdukiewicz et al. 1994), after the CaMV 35S promoter as described (Pattathil et al. 2005). The constructs were introduced into *Arabidopsis parvus/gatl1* heterozygous mutant plants using the *Agrobacterium-mediated* floral dip method (Clough and Bent 1998). Transgenic plants were selected on hygromycin, and homozygous lines were identified by PCR.

Sub-Cellular Localization of PpGATLs

The coding regions for *PpGATL-A, -C* and *–E* were cloned in frame with an EYFP gene under the control of the CaMV 35S promoter in a pCAMBIA-based binary vector (Pattathil et al. 2005) to generate the fusion constructs 35S-*PpGATL-EYFP*. Primers used for creating the EYFP fusions are listed in Supplemental Table S2.3. The *PpGATL* constructs were sequenced

and transformed individually into *Agrobacterium tumefaciens* strain GV3101. The constructs were then individually co-transformed into fully expanded leaves of 8-week-old *Nicotiana benthamiana* plants together with the ECFP-tagged Golgi marker Gmct-ECFP (Saint-Jore-Dupas et al. 2006; Nelson et al. 2007). Three or four days after the infiltration, the injected area was cut and analyzed by Leica TCs SP5 confocal microscope (Leica Microsystems, Heidelberg, Germany) equipped with an argon laser (514 nm for EYFP excitation and 458nm for CFP excitation). Images were processed using Adobe Photoshop.

Tissue Fixation and Immunolabeling

Stems and hypocotyls from 8-week-old transgenic Arabidopsis plants were fixed overnight at 4 ℃ in 25 mM sodium phosphate buffer (pH 7.1) containing 1.6% (w/v) paraformaldehyde and 0.2% (w/v) glutaraldehyde. After fixation, the tissues were dehydrated using a graded ethanol series [20, 35, 50, 62, 75, 85, 95 (v/v), 100, 100, 100% EtOH, 30 min each step] and embedded in LR White resin in a gradient (1:1, 3:1 resin:ethanol [v/v]) and finally three times with 100% resin, 24 hours each (Ted Pella Inc., http://www.tedpella.com). The infiltrated tissue was transferred into gelatin capsules filled with 100% resin, and polymerized under 365nm UV light at 4℃ for 48 h. Sections (250 nm thick) were cut using using a Leica EM UC6 microtome (Leica Microsystems, http://www.leicamicrosystems.com) and stained with toluidine blue for light microscopy.

Immunolabelling was carried out at RT as previously described (Avci et al. 2012). Sections (250 nm thick) of stems and hypocotyls prepared as described above were incubated with selected

monoclonal antibodies which recognize glucuronoxylan. The secondary antibody used for the LM series antibodies was Alexa-fluor 488 goat anti-rat IgG (Invitrogen), while the secondary antibody used for the CCRC series antibodies was Alexa-fluor 488 goat anti-mouse IgG (Invitrogen). Negative controls were carried out in the absence of primary antibody.

Light microscopy was carried out using an Eclipse 80i microscope (Nikon, http://www.nikon.com/) equipped with differential interference contrast and epifluorescence optics. Images were captured with Nikon DS-Ri1 camera head (Nikon) using NIS-Elements Basic Research software. Images were assembled using Adobe Photoshop.

Cell Wall Extraction and Sugar Analysis

Cell walls were prepared as alcohol-insoluble residues (AIR) as described previously (Persson et al. 2007). In brief, stems from 8-week-old Arabidopsis plants were harvested on ice, flash frozen in liquid nitrogen, and ground to a fine powder with a mortar and pestle. The ground materials were extracted with 2 vol. of 100 mL of ice-cold 80% (v/v) ethanol, 100% ethanol, chloroform:methanol (1:1; v/v), and 100% acetone. Starch was removed from the walls by treatment with Type-I porcine α-amylase (Sigma-Aldrich; 47 units/100 mg cell wall) in 100 mM ammonium formate for 48 h at room temperature with rotation. De-starched walls were centrifuged, washed twice with sterile water, twice with 100% acetone, and air dried. Sugar composition analyses were carried out on three independently prepared cell wall preparations using trimethyl silyl ethers of methyl glycosides as described (Caffall et al. 2009).

Cell Wall Fractionation for Glycome Profiling

Sequential extraction of cell walls (AIR) was done on 10 mg/mL suspensions with increasingly harsh reagents as described previously (Pattathil et al. 2012). First, the AIR samples were suspended in 50 mM ammonium oxalate (oxalate). The suspension was stirred overnight at room temperature. After the incubation, the suspension was centrifuged at 4000 x g for 15 mins, the supernatant was decanted and saved, and the pellet was washed three times with deionized water before subsequent extraction steps. The washed pellet was then sequentially extracted in the same manner using 50 mM sodium carbonate containing 0.5% (w/v) of sodium borohydride (carbonate), 1 M KOH containing 1% (w/v) of sodium borohydride, and 4 M KOH containing 1% (w/v) of sodium borohydride. In each step, the supernatants were individually decanted and saved. The 1 M and 4 M KOH extracts were neutralized with glacial acetic acid. All cell wall extracts were dialyzed against four changes of de-ionized water (sample:water,1:60) at room temperature for a total of 48 h and then lyophilized.

Total sugar estimation and ELISA

Cell wall extracts were dissolved in deionized water at a concentration of 0.2 mg/mL, and total sugar contents of the extracts were estimated using the phenol sulfuric acid method (Masuko et al. 2005). All extracts were diluted to the same sugar concentration (60 μg sugar/mL). ELISA plates (Costar 3598) were loaded with 50 μL of the diluted cell wall extracts per well and the solutions were allowed to evaporate to dryness overnight at 37 ℃. A BioTek robotic system (Burlington, VT) was used to perform fully automated ELISAs using a series of 150 monoclonal antibodies directed against plant cell wall carbohydrate epitopes (Pattathil et al. 2010).

Monoclonal Antibodies

Monoclonal antibodies were obtained as hybridoma cell culture supernatants either from laboratory stocks at the Complex Carbohydrate Research Center (CCRC, JIM and MAC series; available from CarboSource Services [http://www.carbosource.net]), or from Plant Probes (LM series [http://www.plantprobes.net]).

**Supplemental Data**

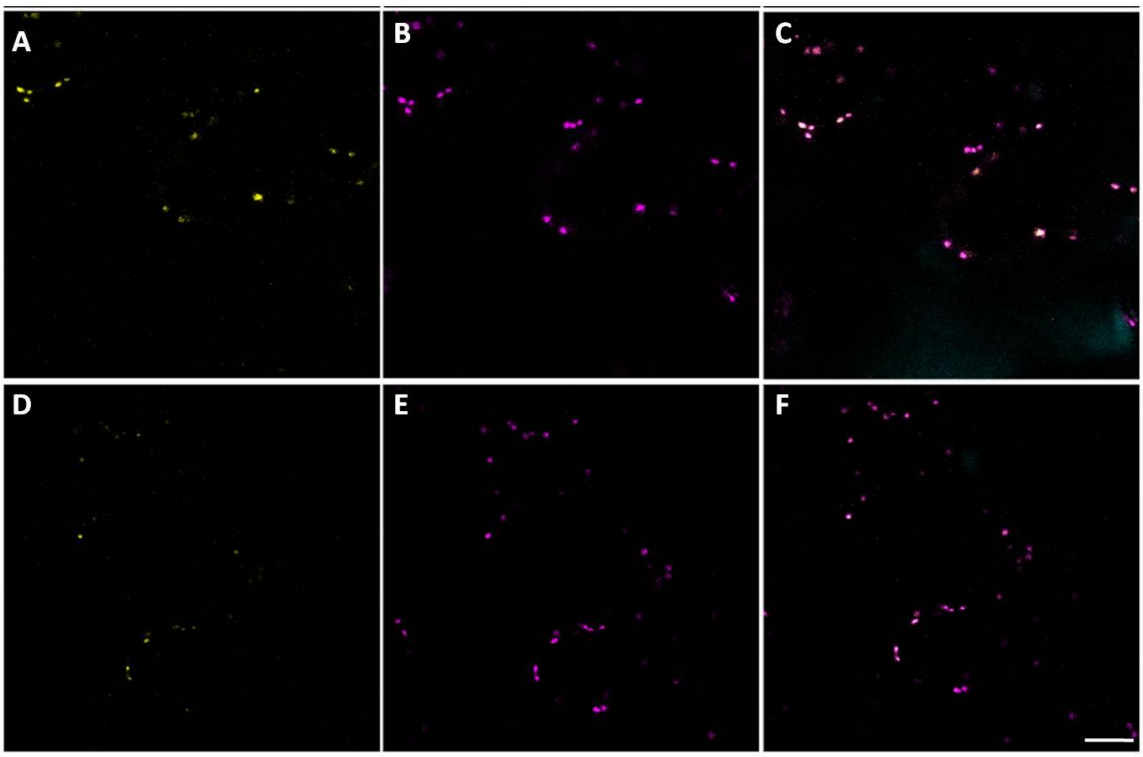


Figure S2.1. Subcellular localization of EYFP-tagged PpGATL-C and PpGATL-E protein. EYFP-tagged PpGATL-C (A) and PpGATL-E (D) gene fusion constructs were transiently expressed under the control of 35S promoter in leaf epidermal cells of *N.benthamiana* and imaged by confocal laser scanning microscopy. (B) and (E) Gmct-ECFP Golgi marker protein was expressed in the same cells as shown in A and D. (C) is the merged image of A and B, and

F is the merged image of D and E. The colocalization of PpGATL-EYFP and Gmct-ECFP are visible as white dots. Scale bar = 20 μm.

Table S2.1. Primers for qRT–PCR analysis of *PpGATLs.*

| **Gene Name** | **Primer Name** | **Primer Sequence (5'-3')** |
|---|---|---|
| | 768q-F | GTGGCTCTATGGCCGCGGTT |
| *PpGATL-A* | 768q-R | GCTCGTCACGGTCTGCAGCAA |
| | 550q-F | ACAATGAGGCGCAGGGGAGC |
| *PpGATL-B* | 550q-R | AGCCGCCATAGAACCACGCA |
| | 454q-F | CCATGGCGGCCGTTTTCTCG |
| *PpGATL-C* | 454q-R | TCGCAGCTGTTCATCTCGGTCC |
| | 568q-F | GGAACCAACATGGCCTGGGG |
| *PpGATL-D* | 568q-R | GCATATCGAGTCGCCGCCA |
| | 911q-F | CGCCGCGAATCGAGATGAGGA |
| *PpGATL-E* | 911q-R | CACCAGCGCCTCGTCGAAGT |
| | EF1aq-F | ATCCAGCGAAGGAGGCTGCG |
| *EF1a* | EF1aq-R | CCAGCACTGGAGCGTACCCG |

Table S2.2. Primers for over-expression constructs of *PpGATLs*.

| **Gene Name** | **Primer Name** | **Primer Sequence (5'-3')** |
|---|---|---|
| | 768KpnI-F | GGTACCAATGACACTCGATGTGAAATATCTGC |
| *PpGATL-A* | 768NheI-R | GCTAGCTTATTGATAAGATAATGTGGAGGGGAG |
| | 454KpnI-F | GGTACCAATGACACTGGATGTGAAGTAC |
| *PpGATL-C* | 454NheI-R | GCTAGCTTATTGGTAAGATAATGCGGAGG |
| | 911KpnI-F | GGTACCAATGACGCTTGATGTAGAATATTTGC |
| *PpGATL-E* | 911NheI-R | GCTAGCTTATTGGTAAGACAACGGGGAAAG |

Table S2.3. Primers for 35S-*PpGATL-EYFP* constructs for sub-cellular localization analysis.

| Gene Name | Primer Name | Primer Sequence (5'-3') |
|---|---|---|
| *PpGATL-A* | 768KpnI-F | GGTACCAATGACACTCGATGTGAAATATCTGC |
| | 768SalI-R | GTCGACATTTGATAAGATAATGTGGAGGGGAG |
| *PpGATL-C* | 454KpnI-F | GGTACCAATGACACTGGATGTGAAGTAC |
| | 454SalI-R | GTCGACATTTGGTAAGATAATGCGGAGG |
| *PpGATL-E* | 911KpnI-F | GGTACCAATGACGCTTGATGTAGAATATTTGC |
| | 911SalI-R | GTCGACATTTGGTAAGACAACGGGGAAAG |

# CHAPTER 3

# A FUNCTIONAL ORTHOLOG OF THE *ARABIDOPSIS PARVUS/ATGATL1* GENE IS REQUIRED FOR LEAFY GAMETOPHORE DEVELOPMENT IN THE MOSS *PHYSCOMITRELLA PATENS*

Yiwen Yang, Utku Avci, Sivakumar Pattathil and Michael G. Hahn. To be submitted to Plant Physiology.

**Abstract**

The *Arabidopsis Galacturonosyl-transferase-Like* (*GATL*) gene family is closely related to 15 *GAUT* (Galacturonosyltransferase) genes, and one of them (*GAUT1*) has been functionally determined to be involved in pectin synthesis as a galacturonosyltransferase. Previous work showed that 10 Arabidopsis *GATL* genes encode proteins involved in cell wall biosynthesis. Analysis of the genome of the moss, *Phycomitrella patens,* revealed the presence of five *GATL* (*PpGATL-A,B,C,D,E*) homologs, which form a sister group that lies basal to all vascular plant GATLs. We investigated the roles of *GATL* genes in *Physcomitrella* using molecular genetic, biochemical and immunological approaches. Transgenic *Physcomitrella* expressing the *β*-glucuronidase reporter gene under individual native *PpGATL* promoters revealed both overlapping and unique expression patterns for these genes in various tissues. Single gene knockouts of *PpGATL-A, -C* and *-E* were generated by homologous recombination and screened for phenotypic changes. While *ppgatl-c* and *ppgatl-e* did not show any obvious growth defects compared to wild type, *ppgatl-a* knockout lines produce significantly fewer numbers of leafy gametophores. Antibody-based glycome profiling of cell wall extracts from *ppgatl-a* mutants revealed a loss of xylan epitopes in the 1M KOH and 4M KOH extracts. Monosaccharide composition analysis revealed largely reduced xylose content in the 1M KOH extracts of the *ppgatl-a* mutant walls. Cell wall extracts prepared from wild type juvenile protonema tissue exhibit similar glycome profiles with the *ppgatl-a* mutants, and showed reduced xylose content in the 1M KOH extracts by glycosyl residue composition analysis. Our data suggest that *PpGATL-A* is required for the transition from juvenile protonema to adult leafy gametphores in *Physcomitrella*.

## Introduction

The plant cell walls are complicated polysaccharide-rich networks, composed of a variety of carbohydrate polymers, including cellulose, hemicelluloses and pectins, along with ~10% glycoproteins (Burton et al. 2010). The synthesis of these complex cell wall polymers requires over 2000 genes in *Arabidopsi*s (~15% of the *Arabidopsi*s genome), many of which encode glycosyltransferases, or methyl- and acetyl transferases that belong to multigene families (Carpita et al. 2001; Henrissat et al. 2001).

The *Arabidopsis GATL* (*Galacturonosyltransferase-Like*) gene family has been bioinformatically identified to be closely related to a group of 15 genes, named *GAUT1* (*Galacturonosyltransferase1*) to *GAUT15*. *GAUT1* is the first identified galacturonosyl-transferase (GalAT) that has been functionally determined to be involved in pectin synthesis. It specifically catalyzes the transfer of GalA from UDP-GalA onto oligosaccharide acceptors of HG (Sterling et al. 2006). The *GATL* gene family consists of 10 genes named *GATL1* to *GATL10* with 23-29% sequence identity and 42-53% similarity to *GAUT1*. All 15 *Arabidopsis GAUT* genes and 10 *GATL* genes were suggested to represent putative GalATs and have been grouped into a *GAUT1*-related gene superfamily (Sterling et al. 2006).

Mutational studies have provided evidence for the involvement of GATL proteins in the synthesis of xylan and/or pectins. The *parvus/atgatl1* mutants grown under low humidity conditions exhibit severely dwarfed growth phenotypes and have reduced anther dehiscence and semi-sterility (Lao et al. 2003). Early glycosyl composition analyses of the *parvus/atgatl1* mutant showed slightly increases in Rha, Ara and Gal residues and decreased xylose content

compared to WT. Linkage analysis showed the ratio of 2- to 2,4-linked Rha residues was 2:1 in mutant leaves while the ratio was 1:1 in wild-type leaves, indicating reduced levels of RG-I branching in the *parvus/gatl1* mutant (Lao et al. 2003). Later studies demonstrated that the *parvus/gatl1* mutant plants have a collapsed xylem phenotype with significant decreases in xylan content of the cell walls and a drastic reduction of the secondary walls thickness in xylem tissues (Brown et al. 2007; Lee et al. 2007; Kong et al. 2009). It was also shown that the tetrasaccharide sequence [4-β-D-Xyl-1,3-α-L-Rha-1,2-α-D-GalA-1,4-D-Xyl] present at the reducing end of xylans in wild-type dicots plants is absent in the *parvus/gatl1* mutant (Pena et al. 2007). These results suggest that GATL1 may participate in xylan and possibly pectin synthesis. Plants carrying T-DNA insertions in three *AtGATL* genes, *atgatl3*, *atgatl6* and *atgatl9*, show 23.7%, 16.4% and 20.5% reduction in GalA content, respectively, suggesting that these *GATLs* may encode putative GalATs involved in pectin synthesis (Kong et al. 2011). Mutations in *AtGATL5* result in defects in seed mucilage synthesis and cell adhesion, and a significant reduction of GalA and Rha content in seed mucilage compared to wild type (Kong et al. 2013). These results suggest a role for *AtGATL5* in pectin, particularly in RG-I biosynthesis. *Arabidopsis* plants carrying single mutations in the other *GATL* genes do not show easily identifiable morphological defects or cell wall abnormalities, indicating that some functional redundancies may exist in the *GATL* gene family.

The absence of functional characterization of most of the GATL proteins leaves open the question of their roles in cell wall synthesis. Recent phylogenetic analyses of the GATL gene family incorporating 95 GATL proteins from 12 plant species including the moss, *Physcomitrella*

*patens,* and the spike moss, *Selaginella moellendorffii,* gives new insight into the evolution of *GATL* gene family (Kong et al. 2011). Five *GATL* orthologs named *PpGATL-A* to *PpGATL-E* have been identified in the *Physcomitrella* genome: they form a sister group to all seed plant GATLs (Yin et al. 2010; Kong et al. 2011). Previous work reported in Chapter 2 showed that *PpGATL-A* is a functional ortholog of *Arabidopsis PARVUS/GATL1*. Therefore, the GATL1 protein from these two highly divergent land plants originated from a common ancestor, whose function is shared and has been conserved.

The moss *Physcomitrella patens* is a representative bryophyte that is used as a model system to study plant evolution, development and physiology. The life cycle of *Physcomitrella* comprises an alternation of two generations that is typical of all mosses and vascular plants: a haploid gametophyte generation followed by a diploid sporophyte (Reski 1998). The predominant gametophyte phase in *Physcomitrella* is further divided into two developmental stages: a two-dimensional filamentous stage, termed the protonema, and a three-dimensional leafy adult stage, termed the gametophore. The gametophores is comprised of stems, leaves, and rhizoids, and can generate sex organs that ultimately give rise to the diploid sporophyte (Schaefer and Zryd 2001). The simple morphology, the basal position in land plant phylogeny, the feasibility of gene targeting and the reduced gene redundancy in multigene families makes *Physcomitrella* an attractive system for physiological studies and comparative studies of the evolution of plant gene function (Schaefer and Zryd 1997; Rensing et al. 2002; Cove 2005). *Physcomitrella* is also an ideal model for investigating cell wall biosynthesis genes with the potential to provide insight into evolutionary aspects of plant cell wall biosynthesis and

physiology, as it contains only primary cell walls, whose composition is comparable with that of primary walls in vascular plants (Moller et al. 2007; Roberts et al. 2012). A few cell-wall-related gene knockout studies have been carried out successfully in *Physcomitrella*, including mutations in three members from the *CESA* gene family, *PpCESA5* (Goss et al. 2012), *PpCESA6* and *PpCESA7* (Wise et al. 2011), and a knockout of the *Physcomitrella IRX-10* holomogous gene *PpGT47a* (Hornblad et al. 2013), which encodes a xylan xylosyltransferase (Jensen et al. 2014). However, no targeted mutagenesis studies have been carried out in pectin-related gene families of *Physcomitrella* so far.

Here, we report a study of three members of the *GATL* gene family (*PpGATl-A*, *PpGATL-C* and *PpGATL-E* ) in *Physcomitrella* to identify their role(s) in plant cell wall biosynthesis. These three *PpGATL* genes showed the highest expression levels in *Physcomitrella* tissues (see Figure 2.3; Chapter 2). The roles of these *PpGATL*s were further investigated by targeted gene mutagenesis studies. Our data show that *PpGATL-A* is required for *Physcomitrella* leafy gametophores development. *ppgatl-a* knockout mutants show defects in the transition from the juvenile protonema to the adult leafy gametophores developmental stage. The cell wall composition and glycome profiles of *ppgatl-a* mutants resemble those of wild type juvenile protonema tissue.

## Results

### Expression pattern of *PpGATL* genes

To investigate whether the expression of the three PpGATLs is associated with specific tissues or developmental growth stages, we generated *PpGATL promoter::GUS* lines for *PpGATL-A*,

*PpGATL-C* and *PpGATL-E* using gene targeting to integrate the *GUS* reporter gene in frame immediately upstream of the stop codons of the *PpGATL* genes (Figure 3.1A). At least two stable independent lines were generated for each of the three *PpGATLs*, all of which were verified by PCR analysis (Figure S3.1 in the Supplementary Material). The expression patterns of the fusion constructs in *Physcomitrella* were analysed in all independent lines by histochemical staining, and for each *PpGATL* examined, all of the independent *PpGATL promoter::GUS* lines showed the same overall staining pattern. The expression of *PpGATL-A* and *PpGATL-C* was detected in young leaflets of bud/juvenile gametophores and at the base of leaves in the apical region of leafy gametophores, but in different intensities for each of the two genes (Figure 3.1 B-E). GUS expression from the *PpGATL-A* promoter was observed after 24 h of incubation at 37 ˚C (Figure 3.1 B-C), whereas for *PpGATL-C*, the gametophores were weakly stained after 48 h with lower intensity (Figure 3.1 D-E). *PpGATL-E* expression was detected in protonema filaments (Figure 3.1 G), rhizoids, the upper side of leaves, as well as in the axillary hairs that differentiate at the base of the leaves (Figure 3.1 F-H), an expression pattern that is distinct from the expression patterns of *PpGATL-A* and *PpGATL-C*.

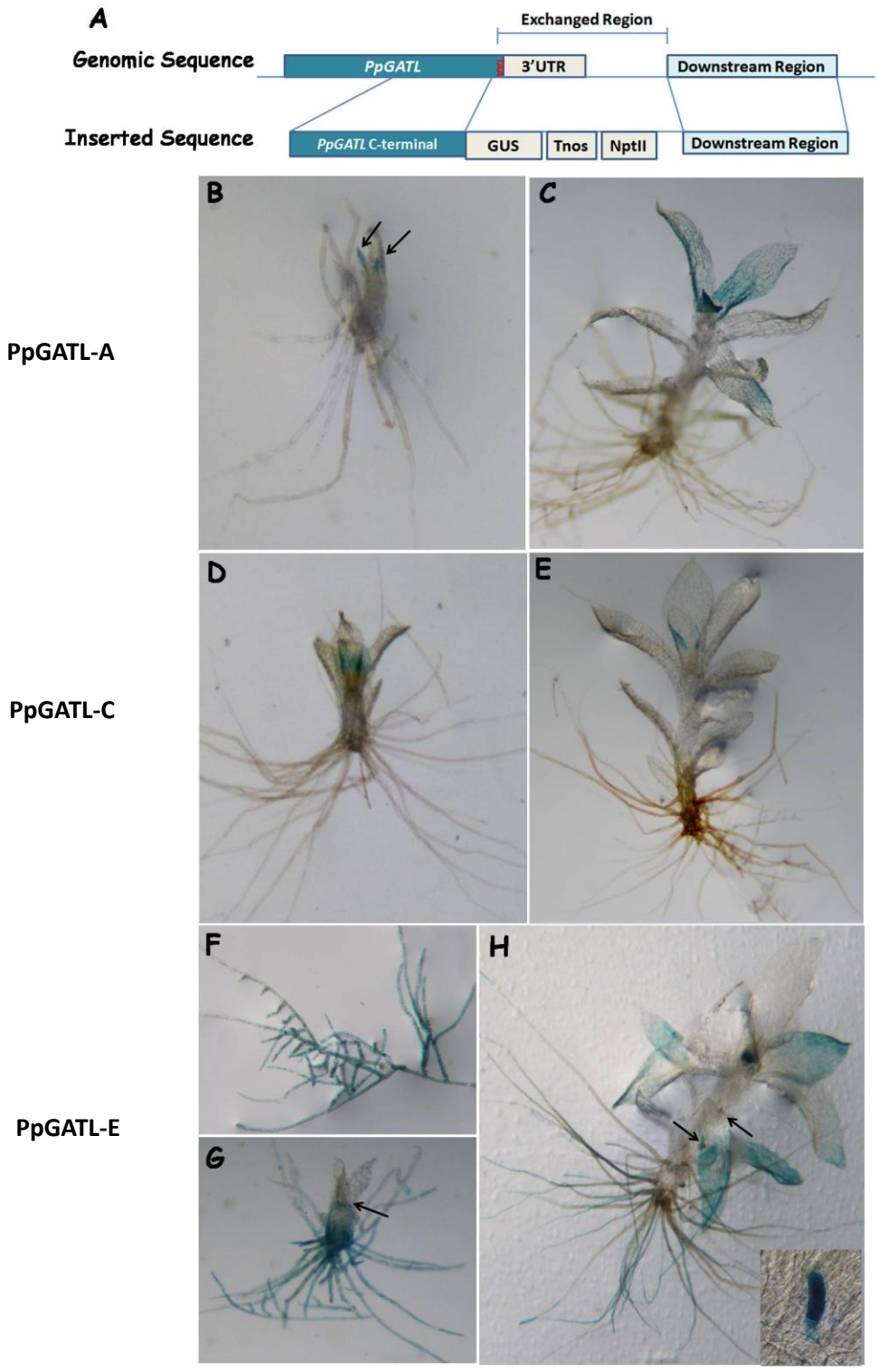


Figure 3.1. Tissue-specific expression pattern of *PpGATL-A* (B-C), *PpGATL–C* （D-E ）and *PpGATL–E* (F-H) analyzed by histochemical staining of stable *PpGATL promoter::GUS* lines. (A)

Schematic drawing describing generation of *PpGATL::GUS* reporter lines. (B) A Bud/juvenile gametophore of *PpGATL-A::GUS* line exhibiting GUS staining in young leaflets (arrows). (C) Adult gametophore of *PpGATL-A::GUS* line showing GUS staining at the base of leaves in the apical region of leafy gametophore. The *PpGATl-C::GUS* line shows similar expression patterns with *PpGATL-A* in bud/ juvenile gametophores (D) and adult gametophores (E), yet the staining in gametophores is weaker compared to *PpGATL-A*. (F) GUS-stained protonema filaments of *PpGATL-E::GUS* line. (G) Bud/juvenile gametophore of *PpGATL-E::GUS* line with GUS-stained young rhizoids and putative axillary hairs differentiating at the adaxial base of the leaf in the shoot apex (arrow). (H) Adult gametophore of *PpGATL-E::GUS* line showing GUS staining of leaves, rhizoids and axillary hairs that differentiate at the adaxial base of the leaf (arrows). Insert shows one magnified axillary hair.

Generation of *PpGATL* knockout lines

Knockout constructs comprising genomic *PpGATL*s fragments separated by a selection cassette that confers resistance to hygromycin were generated for *PpGATL-A*, *PpGATL-C* and *PpGATL-E* (Figure 3.2 A). Knockout vectors were constructed by Gateway Multisite Cloning using the destination vector pBHSNRG (Roberts et al. 2011). The constructs were introduced into protoplasts isolated from 6-day-old *Physcomitrella* protonema tissue employing PEG-mediated transformation(Schaefer et al. 1991). All stable transformants after two rounds of antibiotic selection were screened via PCR-based genotyping for disruption of the wild-type *PpGATL* gene as well as correct 5' and 3' integration of the knockout vector. The absence of

the corresponding *PpGATL* transcripts was also verified by RT-PCR analysis. Two independent lines of *ppgatl-a* single knockout mutants, two independent lines of *ppgatl-c* single knockout mutants and one *ppgatl-e* single knockout mutant were identified (Figure S 3.2). The confirmed knockout mutants and wild type plants were grown from protoplasts on PRMB medium for 5 days and then transferred to BCDAT medium for 5 weeks to synchronize development for phenotype analysis.

The leafy gametophore numbers are significantly reduced (around 9-fold) in colonies of the two *ppgatl-a* knockout lines, *ppgatl-a ko12* and *ppgatl-a ko22*, compared to those of wild-type colonies (Figure 3.2 B-D, G). No defects were identified in the protonema filament development or in the buds/juvenile gametophores that give rise to leafy gametophores in the two *ppgatl-a* knockout lines. *ppgatl-c* and *ppgatl-e* knockout mutant lines were visually similar to wild type with no obvious morphological defects (data not shown). Since *PpGATL-A* is a functional ortholog of *PARVUS/AtGATL1*, which can rescue the defects caused by the *parvus* mutation in *Arabidopsis*, and loss of *PpGATL-A* in *Physcomitrella* affects leafy gametophore development, subsequent studies focused only on the two *ppgatl-a* knockout lines.

In order to verify that the observed growth defects in the two *ppgatl-a* knockout lines were caused by loss of the *PpGATL-A* gene, both *ppgatl-a* knockout lines were complemented by overexpression of *PpGATL-A* driven by a modified 35S (E7113) promoter (Mitsuhara et al. 1996). The expression cassette *p35S:PpGATL-A* together with a zeocin resistance selection cassette were integrated into the *Physcomitrella* BS213 locus, which can be disrupted with no effect on moss growth and development (Schaefer and Zryd 1997). For each of the two knockout lines, one *PpGATL-A* complemented line

was identified, and both of the two complemented lines restored normal leafy gametophore development (Figure 3.2 E-F). The number of leafy gametophores was restored to about 50% of wild type levels (Figure 3.2 G).

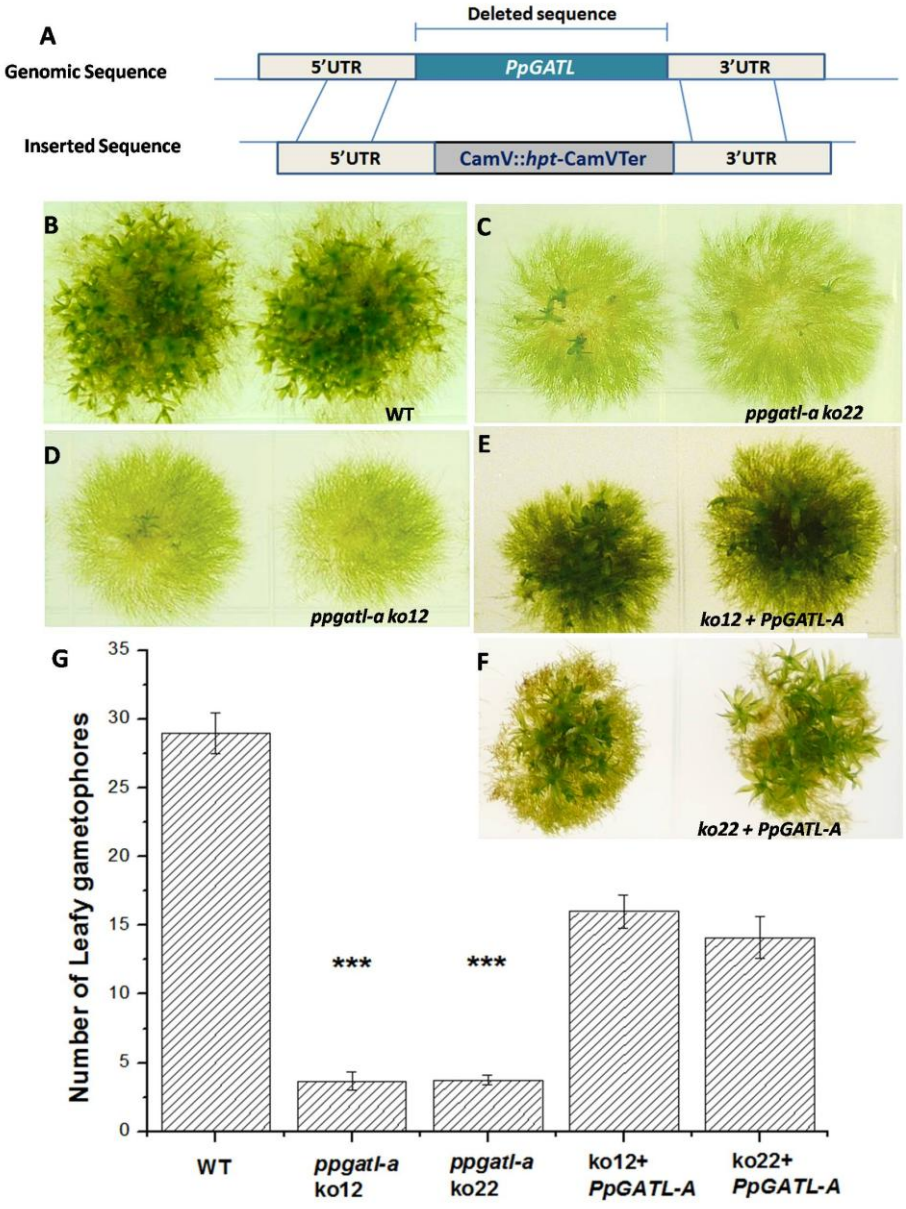


Figure 3.2. *Physcomitrella patens* wild type, *ppgatl-a* knockout lines and complemented *ppgatl-a* knockout lines. Colonies were grown from protoplasts and cultured on BCDAT medium for 5 weeks.

(A) Schematic drawing describing the generation of the *ppgatl* knockout lines. Two *ppgatl-a* knockout lines *ppgatl-a ko12* (D) and *ppgatl-a ko22* (C), have reduced numbers of leafy gametophores compared to wild type colonies (B). Complemented lines (E-F) generated by overexpression of *PpGATL-A* under control of a modified 35S (E7113) promoter in the knockout mutants restores normal gametophores development. (G) Numbers of leafy gametophores (per colony) of 5-week-old WT, two *ppgatl-a* KO lines and complemented lines for the two knockouts. * $P<0.001$ by Student's t-test, as compared with wild type and complemented lines.

The leafy gametophore development is initiated by the formation of buds, which are three-faced apical cells differentiated from protonema tissues (Schaefer and Zryd 2001). However, the defect in leafy gametophore development observed in the two *ppgatl-a* knockout mutants was not due to loss of budding capacity. 9-day-old wild-type and two mutant lines cultured on BCD medium all produced gametophores buds with similar appearance (Figure 3.3).

To determine if the mutation in the *PpGATL-A* gene affected cell wall structure, we analyzed extractable cell wall polymers prepared from wild type, two *ppgatl-a* knockout lines and one complemented line (*ppgatl-a ko22 + PpGATL-A* ) using glycome profiling (Pattathil et al. 2012). In this analysis, sequential cell wall extracts are ELISA-screened using a toolkit of approximately 150 plant cell wall glycan-directed monoclonal antibodies (mAb) that recognize diverse epitopes present on most major classes of plant cell wall polysaccharides, including arabinogalactans, pectins, xyloglucans, xylans, and mannans (Pattathil et al. 2010). Differences in the glycome profile patterns provide information about the detectable epitopes present in the cell walls and the

changes in the extractability of these epitopes from the walls (Zhu et al. 2010). Glycome profiles of the two *ppgatl-a* knockout mutants walls show major differences compared to those of wild type and complemented line cell walls. The two knockout lines exhibited similar changes in their glycome profiles (Figure 3.4).

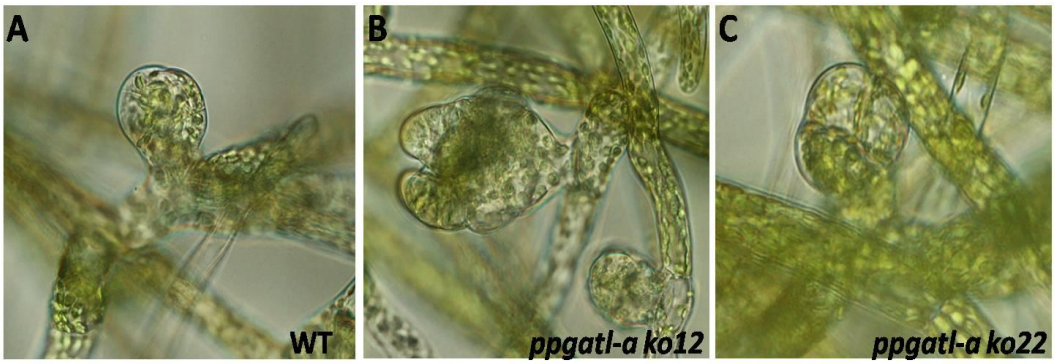


Figure 3.3. Buds produced by 9-day-old *Physcomitrella patens* wild type (A), *ppgatl-a ko12* (B) and *ppgatl-a ko22* (B) knockout lines. Colonies were grown from protoplasts and cultured on BCD medium for 9 days.

The most dramatic differences between knockout mutants and wild type cell wall glycome profiles are the levels of xylan epitopes in the 1M KOH and 4M KOH extracts. In contrast to wild type plants, the 1M KOH extracts prepared from *ppgatl-a ko12* and *ppgatl-a ko22* walls contained significantly less xylan epitopes recognized by the xylan-4 through xylan-7 groups monoclonal antibodies. Furthermore, much less or none of the xylan-4 and xylan-5 epitopes were detected in the 4M KOH extracts of *ppgatl-a ko12* and *ppgatl-a ko22* walls. A reduction in xylan-4 to xylan-7 epitopes was also observed in the 1M KOH and 4M KOH extracts of wild-type protonema cell walls.

The amounts of carbohydrate material recovered in the 1M KOH extracts of walls prepared from wild-type protonema, *ppgatl-a ko12* and *ppgatl-a ko22* are similar to each other; these extracts contain more carbohydrate mass compared to that recovered in the equivalent extract of walls prepared from 5-week old wild-type gametophoric colonies. Thus, there is less xylan in the 1M KOH extracts of wild-type protonema, *ppgatl-a ko12* and *ppgatl-a ko22*.

Other differences in the glycome profiles of the two knockout mutant lines include the enhanced level of pectic arabinogalactan epitopes (RG-I/AG) in all of the extracts, and a reduced presence of fucosylated xyloglucan (Fuc-XG) epitopes in the 4M KOH extracts. For the two knockouts, higher levels of RG-I/AG epitopes were detected in the oxalate, carbonate, 1M KOH and 4M KOH extracts, while drastically reduced levels of Fuc-XG epitopes were detected in the 4M KOH extracts compared to wild type plants. The glycome profiles of wild type protonema walls exhibit similar patterns as the two mutants, except for the presence of Fuc-XG epitopes in protonemal wall extracts. The complemented line *ppgatl-a ko22+PpGATl-A* showed similar cell wall glycome profiles as wild type. The reduced levels of xylan-4 to xylan-7 epitopes in the 1M KOH extracts, and reduced levels of xylan-4 and xylan-5 epitopes and Fuc-XG epitopes in the 4M KOH extracts of the two mutants walls were restored in the glycome profiles of the complemented line.

Monosaccharide composition analysis was performed on total cell wall material isolated from 14-day old and 5-week old *Physcomitrella* wild-type plants and two knockout lines to determine whether the disruption of *PpGATL-A* gene caused any alterations in the sugar composition of the walls. The two knockout lines did not show any significant differences in

the levels of monosaccharides detected compared to 5-week old wild-type colonies rich in leafy gametophores, or compared with the 14-day old wild-type protonema (Figure 3.5).

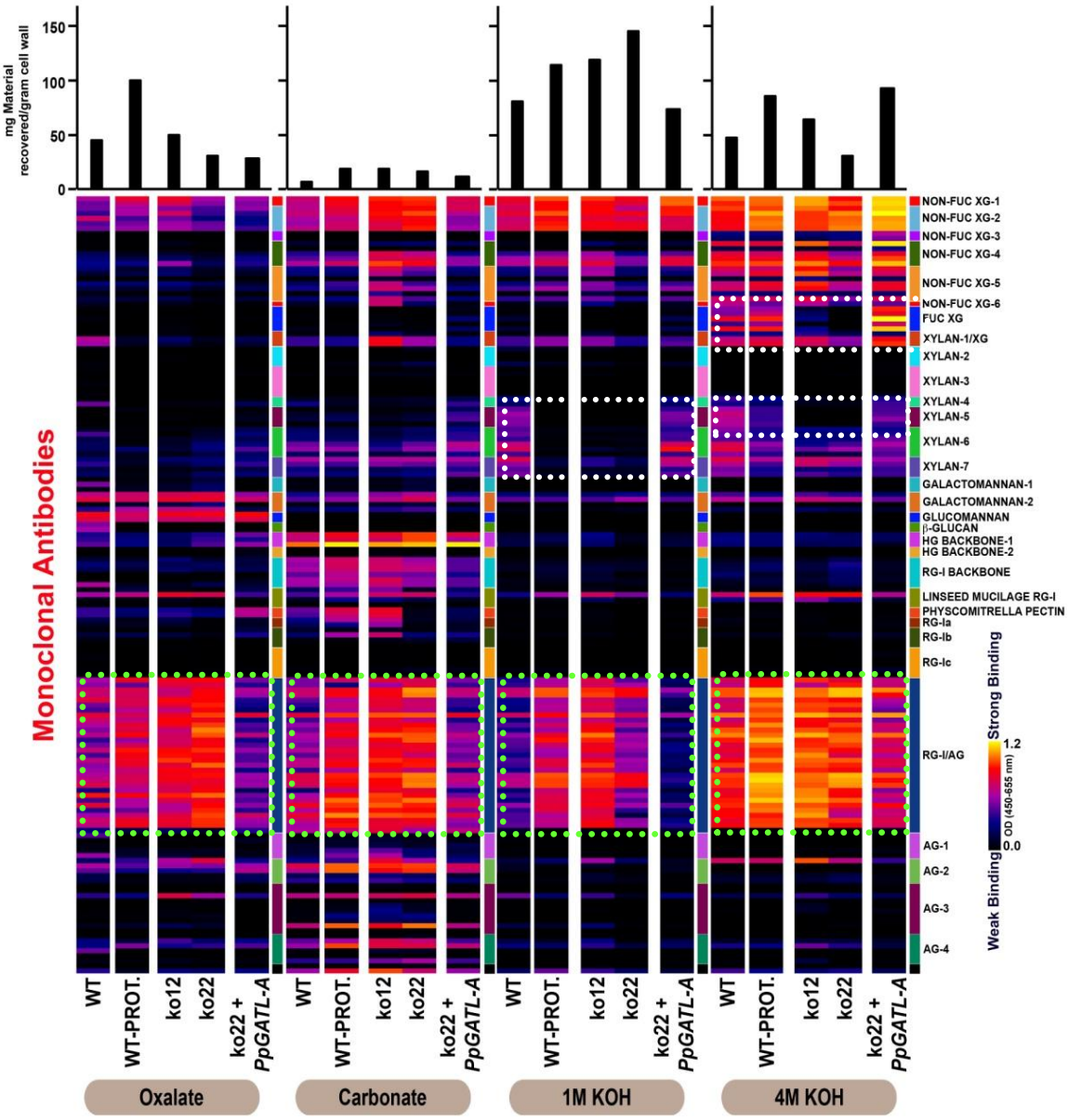


Figure 3.4. Glycome profiling of sequential cell wall extracts prepared from 14-day-old *Physcomitrella* wild-type protonema and 5-week-old wild-type plants, two *ppgatl-a* knockout mutants and a *ppgatl-a ko22+PpGATL-A* complemented line. Reagents used for different extraction steps are indicated in grey labels at the bottom. Extracts were screened by ELISA using 155 plant cell

wall glycan-directed monoclonal antibodies for presence of cell wall glycan epitopes (Pattathil et al. 2010), and the data are presented as heat maps. The strength of the ELISA signal is indicated by a yellow-red-black scale (yellow, red and black depict strong, medium, and no binding, respectively). The panels at the right hand side of the figure depict the array of antibodies used, which are grouped according to the principal cell wall glycans recognized by each antibody group, and the list of individual antibodies used in this analysis are as previously described (Pattathil et al. 2012). The amounts of material extracted with each extraction reagent are indicated in the bar graphs above the heat maps. Major changes in glycome profiles among different plant lines extracts are outlined in white (glycan epitopes with reduced signals for knockout mutants) and green (epitopes with increased signals for knockout mutants) boxes.

However, monosaccharide composition analysis of the sequential cell wall extracts showed a significant reduction of xylose content in the 1M KOH extract from the two knock out mutant lines cell walls compared with the wild type (Table 3.1). In *ppgatl-a ko12* and *ppgatl-a ko22* mutants, the xylose content is decreased by 82.7% and 80.9% compared to wild type, and the complemented line *ppgatl-a ko22+PpGATL-A* restored the xylose content to 53.2% of wild type levels. The mannose content is also significantly reduced in the two knockout mutants, while the level of glucose is significantly increased compared to wild type plants. The results from sugar composition analyses of the sequential cell wall extracts are consistent with the changes in glycome profiles patterns of the corresponding plants, and these two analyses together indicate the altered extractability of specific xylan fractions in walls of the *ppgatl-a* knock out mutants.

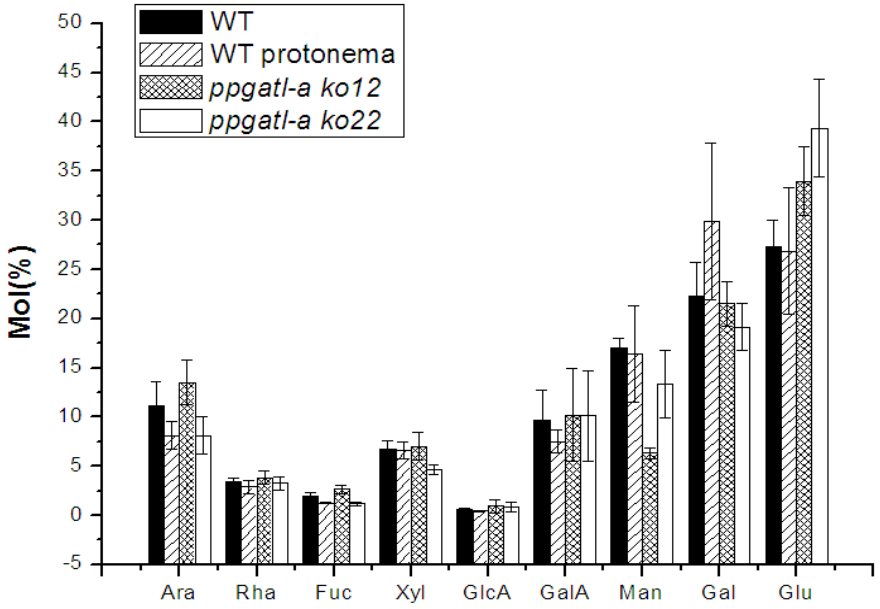


Figure 3.5. Monosaccharide composition of total cell walls isolated from 5-week old *Physcomitrella* wild-type, *ppgatll-a ko12* and *ppgatl-a ko22* plants, and 14-day old wild type protonema. The glycosyl residue composition of total cell wall material isolated from different *Physcomitrella* plants was determined by GC-MS of trimethyl silyl derivatives as described in "Materials and Methods". Data are displayed as mol % ± SE of measured sugars from analyses of three biological replicates pooled from multiple plants.

Table 3.1 Glycosyl residue composition analysis of sequential solvent extracts of AIRs (cell walls) from 5-week old *Physcomitrella* wild-type, *ppgatll-a ko12*, *ppgatl-a ko22*, and *ppgatl-a ko22+ PpGATL-A* plants and 14-day old *Physcomitrella* wild-type protonema.

Data are mol % ± SE of three pooled samples for mutant and two pooled wild type biological samples. * P<0.001 by Student's t-test, as between wild type and mutant lines.

| Extraction | Plant | Ara | Rha | Fuc | Xyl | Man | Gal | Glc | GlcA | GalA |
|---|---|---|---|---|---|---|---|---|---|---|
| Oxalate | Wild type | 12.8 ± 1.0 | 1.4 ± 0.9 | 2.4 ± 0.7 | 5.2 ± 0.2 | 2.5 ± 0.9 | 60.6 ± 2.5 | 9.6 ± 0.7 | 1.7 ± 1.2 | 3.8 ± 0.4 |
| | WT-Protonema | 12.0±0.3 | 5.5±0.7 | 1.8±0.2 | 3.7±0.1 | 1.6±0.1 | 55.9±1.6 | 5.9±0.5 | 0.8±0.1 | 12.9±1.7 |
| | *ppgatl-a ko12* | 13.2 ± 4.4 | 3.0 ± 1.0 | 1.9 ± 0.3 | 3.9 ± 0.3 | 1.6 ± 0.3 | 43.8 ± 7.3 | 20.4 ± 7.0 | 0.5 ± 0.1 | 5.3 ± 1.6 |
| | *ppgatl-a ko22* | 12.7 ± 4.6 | 1.8 ± 0.5 | 1.3 ± 0.4 | 4.0 ± 0.5 | 3.8 ± 0.6 | 54.6 ± 2.8 | 15.6 ± 1.2 | 1.1 ± 0.4 | 5.2 ± 2.9 |
| | *ppgatl-a ko22+PpGATL-A* | 19.1±7.0 | 2.3±0.5 | 3.8±1.2 | 7.1±0.6 | 5.1±1.3 | 44.3±3.7 | 7.9±5.7 | 1.8±1.4 | 8.7±1.4 |
| Carbonate | Wild type | 27.6 ± 2.6 | 2.3 ± 0.4 | 7.3 ± 1.1 | 13.4 ± 0.4 | 6.7 ± 2.6 | 34.9 ± 2.3 | 4.1 ± 1.1 | 1.0 ± 0.1 | 2.8 ± 0.7 |
| | WT-Protonema | 22.2±1.2 | 4.1±0.2 | 4.7±0.4 | 4.3±0.1 | 6.2±0.4 | 51.4±1.2 | 3.3±0.4 | 1.3±0.4 | 2.4±0.6 |
| | *ppgatl-a ko12* | 18.0 ± 3.9 | 2.4 ± 0.9 | 8.9 ± 1.7 | 12.1 ± 1.7 | 4.4 ± 0.9 | 42.6 ± 9.7 | 9.5 ± 0.1 | 1.1 ± 0.5 | 2.5 ± 2.0 |
| | *ppgatl-a ko22* | 16.4 ± 3.9 | 2.8 ± 0.3 | 1.5 ± 0.3 | 5.9 ± 0.5 | 8.2 ± 1.5 | 44.1 ± 6.3 | 17.8 ± 2.6 | 0.4 ± 0.2 | 2.8 ± 1.9 |
| | *ppgatl-a ko22+PpGATL-A* | 28.6±0.5 | 1.8±0.3 | 16.2±0.3 | 19.0±1.1 | 8.0± 1.9 | 18.3±0.1 | 4.9±0.4 | 0.8±0.8 | 2.5±1.2 |
| 1M KOH | Wild type | 7.0 ± 0.8 | 0.8 ± 0.1 | 1.1 ± 0.4 | **17.3 ± 2.5*** | **14.1 ± 4.0*** | 20.2 ± 2.4 | **37.7 ± 3.7*** | 0.5 ± 0.1 | 1.3 ± 0.8 |
| | WT-Protonema | 5.1±0.1 | 1.9±0.1 | 0.9±0.1 | **5.7±0.1*** | 13.3±1.1 | 10.3±0.7 | **60.0±1.5*** | 0.2±0.1 | 2.7±0.1 |
| | *ppgatl-a ko12* | 4.9 ± 2.2 | 0.3 ± 0.1 | 0.4 ± 0.2 | **3.0 ± 0.1*** | **2.3 ± 1.1*** | 10.5 ± 2.3 | **78.1 ± 5.1*** | 0.3 ± 0.2 | 0.3 ± 0.2 |
| | *ppgatl-a ko22* | 2.3 ± 0.5 | 0.3 ± 0.1 | 0.1 ± 0.1 | **3.3 ± 0.7*** | **5.2 ± 0.2*** | 14.5 ± 2.8 | **73.8 ± 4.2*** | 0.2 ± 0.2 | 0.3 ± 0.2 |
| | *ppgatl-a ko22+PpGATL-A* | 11.9 ± 2.3 | 1.5 ± 0.8 | 3.9±1.5 | 9.2 ± 0.9 | 17.6 ± 1.2 | 14.8 ± 0.9 | 37.3±2.0 | 0.6 ± 0.2 | 3.3 ± 1.8 |
| 4M KOH | Wild type | 6.5± 0.5 | 2.0± 0.7 | 0.9± 0.1 | 18.3± 6.3 | 21.9± 2.8 | 22.5 ± 2.9 | 23.6±2.8 | 0.3 ± 0.1 | 4.1± 1.8 |
| | WT-Protonema | 7.1±0.1 | 2.2±0.1 | 0.6±0.3 | 13.6±0.7 | 4.6±0.3 | 49.6±0.6 | 20.4±0.1 | 0.4±0.5 | 1.6±0.1 |
| | *ppgatl-a ko12* | 5.8 ± 0.4 | 2.3 ± 0.1 | 0.9 ± 0.1 | 14.1 ± 1.0 | 6.0 ± 1.9 | 38.6 ± 5.3 | 28.7 ± 5.3 | 0.2 ± 0.1 | 3.5 ± 1.0 |
| | *ppgatl-a ko22* | 8.4 ± 2.7 | 2.1 ± 0.3 | 0.8 ± 0.1 | 12.5 ± 1.1 | 11.7 ± 2.8 | 33.5 ± 1.9 | 27.2 ± 6.1 | 0.4 ± 0.1 | 3.4 ± 0.2 |
| | *ppgatl-a ko22+PpGATL-A* | 9.5±0.8 | 1.7±0.2 | 1.5 ±0.2 | 13.2 ±0.8 | 22.2 ±1.2 | 17.5± 2.9 | 28.7 ± 2.4 | 0.3 ± 0.1 | 5.4± 0.8 |

Immunolabeling studies of leafy gametophores from *Physcomitrella* wild type and *ppgatl-a* knockout mutant plants

The results of glycome profiling and sugar composition analysis obtained from overall cell wall materials prepared from different plants revealed changes in the extractability of certain glycan epitopes including xylan, xyloglucan and pectin. To compare the organ and cell distribution patterns of these epitopes in the knockout mutants and wild type plants, immunolocalization of different glycan epitopes was performed in leafy gametophores of wild type plants and two knockout mutants.

Cross-sections of 5-week old leafy gametophores from different plants were stained with toluidine blue to visualize the overall cellular organization (Figure 3.6 A, H, O), and immunolabeled with several mAbs that recognize distinct xylan epitopes. Similar patterns of labeling were observed for wild type and two knockout mutants leaf sections: CCRC-M137 labeled both leaf cell walls and axillary hair cells (Figure 3.6 B,I,P), CCRC-M150 (Figure 3.6 C,J,Q) labeled leaf cell walls more strongly than axillary hairs, and CCRC-M147 (Figure 3.6 D,K,R) specifically labeled axillary hairs and weakly labeled leaf cell walls. The sections were also labeled with mAbs that recognize other glycan epitopes including pectin and xyloglucan. CCRC-M38, which recognizes deesterified homogalacturonan (Pattathil et al.2010) labeled leafy cell walls and shoot-axis, and weakly labeled axillary hair cell walls (Figure 3.6 E, L, S). CCRC-M88 recognizes a nonfucosylated xyloglucan epitope (Pattathil et al. 2010), and it strongly labeled shoot-axes as well as leafy cell walls and axillary hair (Figure 3.6 F, M, T). CCRC-M7 which binds to a 1,6-β-galactan epitope in RG-I epitope (Steffan et al. 1995) weakly labeled the leafy cell walls and shoot-axis (Figure 3.6 G, N, U). No obvious differences were observed in the labeling of leafy gametophore cross-sections between wild type and the mutants, and the leafy gametophore morphology of the mutants also looked similar to wild type (Figure S3.3). The presence of xylan in *Physcomitrella* protonema tissues is very limited based on mmunological and biochemical analyses, while the alkali extracts prepared from *Physcomitrella* leafy gametophores contain abundant xylan epitopes that are more easily extractable in 4M KOH compared to 1M KOH (Moller et al. 2007; Kulkarni et al. 2012b). Glycome profiling and sugar composition analyses are based on the overall cell wall material and give averages of information about different polysaccharides across different cell and tissue types, while

immunolabeling provides information about the distribution of glycan epitopes in specific cell types. Taken together, these data suggest that although the *ppgatl-a* knockout mutants are able to generate normal leaves which are indistinguishable from wild type leaves, the mutation largely blocks the transition from protonema to leafy gametophores, resulting in a significant reduction in the number of leafy gametophores, thereby giving rise to the altered overall cell wall composition observed in the mutant plants.

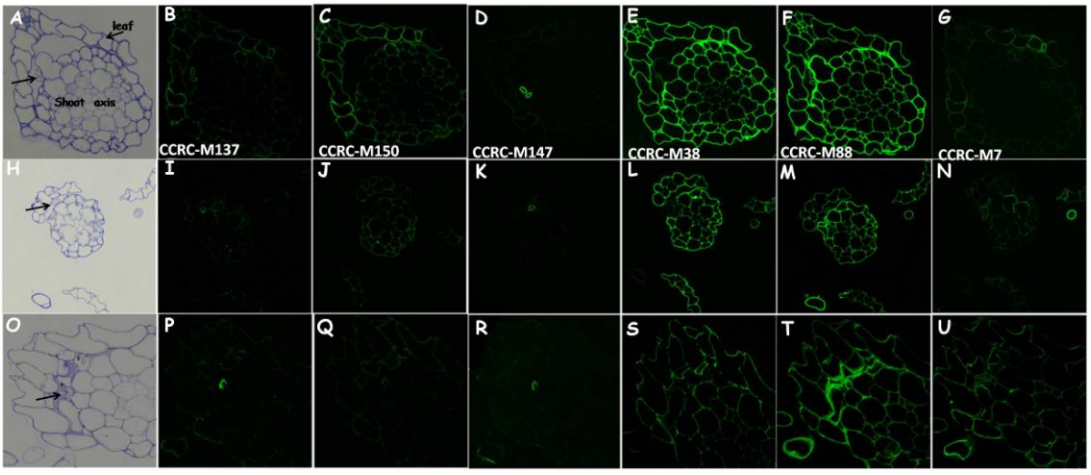


Figure 3.6. Bright-field (A, H and O) and immunofluorescent labeling of cross-sections of *Physcomitrella* leafy gametophores from 5-week old wild type (B-G), *ppgatl-a ko12* (I-N)and *ppgatl-a ko22* mutant plants (P-U). Section size differences among different plants are due to variations in leafy gametophores morphologies. Antibodies used for labeling are indicated in the figure: CCRC-M137 (B,I,P), CCRC-M150 (C,J Q) and CCRC-M147 (D,K,R) recognize structurally distinct xylan epitopes; CCRC-M38 (E,L,S) recognizes deesterified homogalacturonan, CCRC-M88 (F,M,T) binds to a nonfucosylated xylogluncan epitope, and CCRC-M7 recognizes a

RG-I/arabinogalactan epitope. Arrows in (A), (H) and (O) indicated axillary hair cells that differentiate at the base of the leaves.

**Discussion**

*Physcomitrella patens* is a non-vascular, multicellular land plant belonging to the bryophyte family. Although structurally simple, moss gametophytes exist in two morphologically distinct forms containing different cell types. The juvenile filamentous protonema tissue consists of chloronemal cells with many fully developed chloroplasts, and the fast-growing caulonemal cells that contain fewer less-developed plastids and have oblique cell walls (Prigge and Bezanilla 2010). As the plant grows and becomes mature, protonema cells can differentiate into buds, which ultimately give rise to the thick-walled adult leafy gametophores, consisting of stems, leaves, axillary hairs and rhizoids. However, the molecular mechanism for the transition from two-dimensional (protonema) to three dimensional (gametophore) growth is not clear.

Using gene targeting, we generated two knockout lines of *PpGATL-A* in *Physcomitrella*. The deletion of the *PpGATL-A* ORF resulted in a significant reduction in the number of leafy gametophores in both mutant lines (Figure 3.2 B-D). However, the two *ppgatl-a* knockout mutants can produce buds that are morphologically indistinguishable from wild-type (Figure 3.3). Therefore, targeted knockout of *PpGATL-A* appears to block the transition from juvenile protonema to the adult leafy gametophore developmental stage. *PpGATL-A* is a functional ortholog of *Arabidopsis PARVUS/GATL1* (see Chapter 2 of this thesis), which has been suggested to participate in the synthesis of a specific subfraction of pectin or the synthesis of the

GalA-containing xylan reducing end sequence (Brown et al. 2007; Brown et al. 2009; Pena et al. 2007; Persson et al. 2007). Molecular analysis of the *Arabidopsis GATL* gene family suggested that *AtGATL* genes encode proteins involved in cell wall biosynthesis (Kong et al. 2011).

Glycome profiling and glycosyl composition analyses were used to characterize the changes in the cell wall polysaccharide extractability and cell wall composition of the *ppgatl-a* mutants. The semi-quantitative glycome profiling approach revealed a reduced presence of detectable xylan epitopes and higher level of RG-I/AG epitopes in the 1M KOH and 4M KOH extracts in the mutant walls compared to wild type. Although there is no obvious change in the total overall cell wall glycosyl residue composition between wild type and *ppgatl-a* mutants, sugar composition analyses of the sequential cell wall extracts revealed a significant reduction of xylose and mannose content in the 1M KOH extract from the walls of the two mutants cell walls.

The cell wall glycome profiles and sugar composition of *ppgatl-a* mutants resembled those of wild type juvenile protenema tissue. Complementation experiments using the full-length *PpGATL-A* cDNA successfully rescued the morphological defects of the mutants (Figure 3.2 E-G) as well as the changes in glycome profiles and sugar composition in cell wall fractions. These data demonstrate that the composition of xylan and pectin varies in different developmental stages of *Physcomitrella*, and *PpGATL-A* is required for the transition from protonema to leafy gamephores.

Immunolabeling of wild type and *ppgatl-a* mutants leafy gametophore cross-sections was also performed to examine the distribution of specific epitopes in different cells (Figure 3.6). Xylan-directed monoclonal antibodies from xylan-4 through xylan-7 groups that recognize

diverse and distinct xylan epitopes were selected. Antibodies in the xylan-4 group bind to both unsubstituted and substituted xylans, antibodies in the xylan-5 group recognize methylated GlcA side chains of xylan, and antibodies in the xylan-6 and xylan-7 groups recognize unsubstituted homoxylan epitopes of different degrees of polymerization (unpublished results, Hahn lab). CCRC-M150 (xylan-4 group), CCRC-M147 (xylan-6 group) and CCRC-M137 (xylan-7 group) labeled leaf cell walls, axillary hairs cells and shoot-axis with different levels of intensity. CCRC-M150 labeled leaf cell walls more strongly than axillary hairs, while CCRC-M147 specifically labeled axillary hairs and weakly labeled leaf cell walls. Labeling of leafy gametophores sections by mAbs from xylan-5 group is very weak (data not shown), which is consistent with the reported absence of 4-*O*-methyl-α-D-glucosyluronic acid side chains in *Physcomitrella* xylan (Kulkarni et al. 2012b). Other mAbs that recognize pectin and xyloglucan epitopes were also used for immunolabeling studies. However, no obvious differences were observed in the distribution pattern of these epitopes between wild type and the mutants. Individual leafy gametophores produced by *ppgatl-a* mutant plants are indistinguishable from wild type either by morphology (Figure S3.3) or by immunolabeling results.

Single knockouts of two other *Physcomitrella GATL*s (*PpGATL-C* and *PpGATL-E*) did not show any obvious morphological differences compared to wild type plants. The three PpGATL proteins show high identity/similarity with each other; PpGATL-A shares 93% amino acid identity to PpGATL-C and 87% identity to PpGATL-E. The phylogenetic tree of the GATL protein family (Kong et al. 2011) (see Figure 1.4 in Chapter 1 of this thesis) suggests that these three proteins may have arisen by recent genome duplication events. Promoter::*β*-glucuronidase expression studies show that *PpGATL-A* is expressed at the base of leaves in the apical region of the *Physcomitrella* leafy

gametophores; *PpGATL-C* exhibits similar but weaker expression to *PpGATL-A*. However, a different expression pattern was observed in *PpGATL-E*. *PpGATL-E* is expressed in protonema filaments, rhizoids, the upper side of leaves, as well as in the axillary hairs. The divergence in the tissue-specific expression patterns between the *PpGATL*s suggests functional specialization and neofunctionalization of the duplicated genes. *ppgatl-c* and *ppgatl-e* single knockout mutants did not show obvious morphological changes. Further experiments will need to be carried out to test if there are any changes in their cell wall compositions.

In summary, we demonstrate that *PpGATL-A* is required for leafy gametophore development in *Physcomitrella*. Although *ppgatl-a* knockout mutants are able to generate normal leaves, their numbers are dramatically reduced. Thus, the mutation affects the developmental switch from protenema to leafy gametophores, resulting in a protonema-rich mutant phenotype with a different cell wall composition compared to leafy gametophore-rich wild type colonies. The molecular mechanism of the developmental switch remains unknown. *ppgatl-a* knockout mutants can produce buds with similar appearance to wild-type, and systematic counting of bud numbers in the two mutants lines will be required to investigate whether the number of buds is also reduced in these two mutants. Functional enzymatic assay for PpGATL-A will be required to identify its enzymatic activity. More extensive gene knockout analyses will also be required to explore the biological functions of the other *Physcomitrella* GATL genes, either by gene knock-down by RNA interference or by generating double or triple *ppgatl* knockout mutants.

## Materials and Methods

### Growth Conditions

*Physcomitrella patens* wild type (ecotype Gransden 2004) and transformed lines were grown under a 16 h light (50–70 μmol photons $m^{-2}$ $s^{-1}$/8 h dark cycle at 23 ℃ on basal medium with ammonium tartrate (BCDAT) medium or ammonium-free basal medium (BCD) (Nishiyama et al. 2000) overlaid with cellophane.

### Knockout Constructs and Transformation

Single gene knockout constructs were prepared for *PpGATL-A, PpGATL-C,*and *PpGATL-E*. Vectors were constructed using Gateway Multisite Cloning (Invitrogen). Genomic DNA was isolated from 6-day-old *Physcomitrella* protonema tissues. About 1 Kb of 5' and 3' homologous sequence upstream and downstream of each *PpGATL* genes was amplified and cloned into pDONR P1-P4 and pDONR P3-P2 vectors using the BP Clonase II recombination reaction as described in the Gateway Multisite instruction manual (Invitrogen, Carlsbad, CA, USA). The two entry clones containing the amplified 5' and 3' homologous regions were cloned into the destination vector pBHSNRG (Roberts et al. 2011) using the LR Clonase II Plus recombination reaction and separated by a hygromycin resistance selection cassette (the *hpt* gene was driven by a double 35S promoter).

The resulting knockout constructs were linearized with SpeI and AvrII, and transformed into *Physcomitrella* using polyethylene glycol (PEG)-mediated transformation of protoplasts as described previously (Schaefer et al. 1991). Protoplasts were prepared from 6-day-old protonema tissues as described (Roberts et al. 2011). Transformants were selected on plates

containing 15 μg/ml hygromycin and analyzed for stable integration of the transgene by PCR. The primers used for plasmid construction are provided in Supplemental Table S3.1 and primers used for PCR-based genotyping of putative knockout mutants are listed in Supplemental Table S3.2.

Mutant Complementation Analysis

*PpGATL-A* was amplified from cDNA using primers 5'-CCGCTCGAGATGACACTGGATGTGAAGTAC-3' and 5'-TCCGGGCCCTTATTGGTAAGATAATGCGGAGG-3', and inserted into the *Xho*I and *Apa*I site of pCMAK1 (http://moss.nibb.ac.jp/) to construct the complementation vector *PpGATL-A* ox. *PpGATL-A* ox was linearized using *Kpn*I before transformation, and transformants were selected on plates containing 50 μg/ml zeocin.

RNA Extraction and RT–PCR

To determine *PpGATL* transcript levels in knockout mutant lines, total RNA was extracted from 6-day-old triplicate protonema cultures with an RNeasy plant mini kit (Qiagen,Valencia, CA). Contaminating genomic DNA was removed using RNA-free DNase (Qiagen) and cDNA synthesis was carried out using Superscript III reverse transcriptase (Invitrogen), oligo-dT primers and 1μg of total RNA/20μL reaction. RT-PCR was performed to show the absence of the *PpGATL* transcript in the knockout plant lines. EFα1 was used as a reference gene to normalize for variation in the amount of cDNA template (Exposito-Rodriguez et al. 2008). Primers used for the analysis are listed in Table S3.3.

GUS Reporter Gene Constructs

The cell-specific expression patterns of three *PpGATL* genes (*PpGATL-A*, *PpGATL-C* and *PpGATL-E*) were studied using the *GUS* reporter gene (Jefferson 1987). For each *PpGATL* promoter::GUS reporter gene construct, approximately 1.5 kb genomic fragments terminating immediately prior to the stop codon of each *PpGATL*s were PCR amplified and inserted in-frame, 5′ to the coding region of the GUS gene in the pTN85 vector (AB267707) (Sakakibara et al. 2008). About 1 kb 3′ downstream genomic homologues sequences containing the 3' flanking region of each *PpGATL* gener were amplified and inserted into the 3′ region of the pTN85 vector directly after the NPTII expression cassette of pTN85. Sequences of the individual gene specific primers containing appropriate restriction sites used are listed in Supplemental Table S3.4. The resulting targeting constructs were sequenced and linearized by KpnI digestion prior to PEG-mediated transformation into *Physcomitrella* protoplasts (Schaefer et al. 1991). Transformants were selected on plates containing 50 μg/ml G418 (G9516, Sigma, Stockholm, Sweden) and stable transformants were screened for 5′- and 3′-end integration by PCR genotyping.

GUS Staining

Expression of *PpGATL::GUS* transgenes was visualized by staining for GUS activity as described (Jefferson 1987). Briefly, transgenic moss tissues were incubated in GUS staining solution (100 mM sodium phosphate, pH7.0, 10 mM EDTA, 1 mM ferricyanide, 1 mM ferrocyanide, 0.1% [v/v] TritonX-100, and 1 mM 5-bromo-4-chloro-3-indolyl β-D-GlcA) at 37 ℃ for 2-24 hours. The staining buffer was removed, and the samples were cleared in 70%

(v/v) ethanol until the blue color became visible. For each construct, at least two transgenic lines were generated and examined. Patterns of gene expression for each construct were consistent across multiple transgenic lines, and representative plants were photographed with a stereoscopic microscope (OlympusSZH-ILLD) equipped with a Nikon DS-Ril camera head using NIS Elements Basic Research software.

Cell wall Extraction and Sugar Analysis

5-week old *Physcomitrella* tissue grown on BCD media was collected from each plant line, and grounded immediately with a mortar and pestle to a fine powder in liquid nitrogen. The ground materials were consecutively washed with 80% (v/v) ethanol, 100% ethanol, chloroform: methanol (1:1, v/v), and 100% acetone with agitation. The alcohol insoluble residues (AIRs) were air-dried in a hood and starch was removed from the walls by treatment with α-amylase (Type IIA from *Bacillus species*, Sigma-Aldrich; 100 units per 100-mg cell wall) in 100 mM sodium acetate buffer (pH 5.0) for 24 h at 37 ℃ on a shaker. Destarched walls were centrifuged, washed three times with sterile water and twice with 100% acetone, and air dried. Sugar composition analyses were carried out on three independently prepared cell wall preparations using trimethyl silyl ethers of methyl glycosides as described (Caffall et al. 2009).

Cell Wall Fractionation for Glycome Profiling

Sequential extraction of cell walls (AIR) was done on 10 mg/ mL suspensions using increasingly harsh reagents as described previously (Pattathil et al. 2012). First, the AIR samples were suspended in 50 mM ammonium oxalate (oxalate). The suspension was stirred overnight at room temperature. After the incubation, the suspension was centrifuged at 4000 x g

for 15 mins, the supernatant was decanted and saved, and the pellet was washed three times with deionized water before subsequent extraction steps. The washed pellet was then sequentially extracted in the same manner using 50 mM sodium carbonate containing 0.5% (w/v) of sodium borohydride (carbonate), 1 M KOH containing 1% (w/v) of sodium borohydride, and 4 M KOH containing 1% (w/v) of sodium borohydride. In each step, the supernatants were individually decanted and saved. The 1 M and 4 M KOH extracts were neutralized with glacial acetic acid. All cell wall extracts were dialyzed against four changes of de-ionized water (sample:water,1:60) at room temperature for a total of 48 h and then lyophilized.

Total Sugar Estimation and ELISA

Cell wall extracts were dissolved in deionized water at a concentration of 0.2 mg /mL, and the total sugar content of the extracts was estimated using the phenolsulfuricacid method (Masuko et al. 2005). All extracts were diluted to the same sugar concentration (60 μg sugar/mL). ELISA plates (Costar 3598) were loaded with 50 μL of the diluted cell wall extracts per well and the solutions were allowed to evaporate to dryness overnight at 37 ℃. A BioTek robotic system (Burlington, VT) was used to perform fully automated ELISAs using a series of 150 monoclonal antibodies directed against plant cell wall carbohydrate epitopes (Pattathil et al. 2010).

Tissue fixation and Immunolabeling

Five week old *Physcomitrella* leafy gametophores were fixed overnight at 4 ℃ in 2.5% (w/v) glutaraldehyde buffered with 0.05 M phosphate buffer (pH 6.8). After fixation, the tissues were dehydrated using a graded ethanol series [20, 35, 50, 62, 75, 85, 95 (v/v), 100, 100, 100% EtOH,

30 min each step] and embedded in LR White resin in a graded series [1:1, 3:1 resin:ethanol (v/v)] and finally three times with 100% resin, 24 hours each (Ted Pella Inc.,http://www.tedpella.com). The infiltrated tissues were transferred into gelatin capsules filled with 100% resin and polymerized under 365 nm UV light at 4 ℃ for 48h. Sections (250 nm thick) were cut using using a Leica EM UC6 microtome (Leica Microsystems, http://www.leicamicrosystems. com) and stained with toluidine blue for light microscopy.

Immunolabelling was carried out at RT. Sections (250 nm thick) of stems and hypocotyls prepared as described above were incubated with selected glycan-directed monoclonal antibodies. Immunolabelling was carried out at RT as described previously (Avci et al. 2012). The secondary antibody used for the LM series antibodies was Alexa-fluor 488 goat anti-rat IgG (Invitrogen), while the secondary antibody used for the CCRC series antibodies was Alexa-fluor 488 goat anti-mouse IgG (Invitrogen). Negative controls were carried out in the absence of primary antibody.

Light microscopy was carried out using an Eclipse 80i microscope (Nikon, http://www.nikon.com/) equipped with differential interference contrast and epifluorescence optics. Images were captured with Nikon DS-Ri1 camera head (Nikon,) using NIS-Elements Basic Research software. Images were assembled using Adobe Photoshop.

Monoclonal Antibodies

Monoclonal antibodies were obtained as hybridoma cell culture supernatants either from laboratory stocks at the Complex Carbohydrate Research Center (CCRC, JIM and MAC series;

available from CarboSource Services [http://www.carbosource.net]), or from Plant Probes (LM series [http://www.plantprobes.net]).

**Supplemental Data**

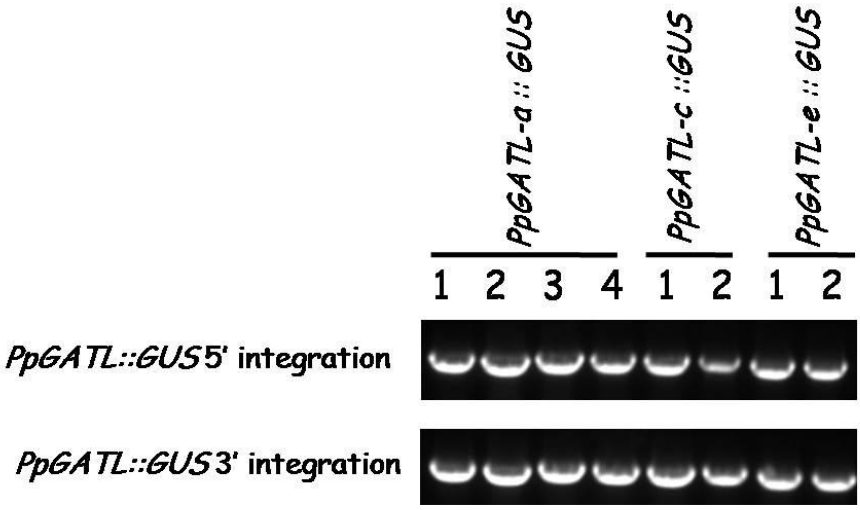


Figure S3.1. PCR verification of the *PpGATL promoter::GUS* lines. Genomic DNA from stable transformants was used as a template for PCR with primers flanking the 5' and 3' integration regions for each *PpGATL*.

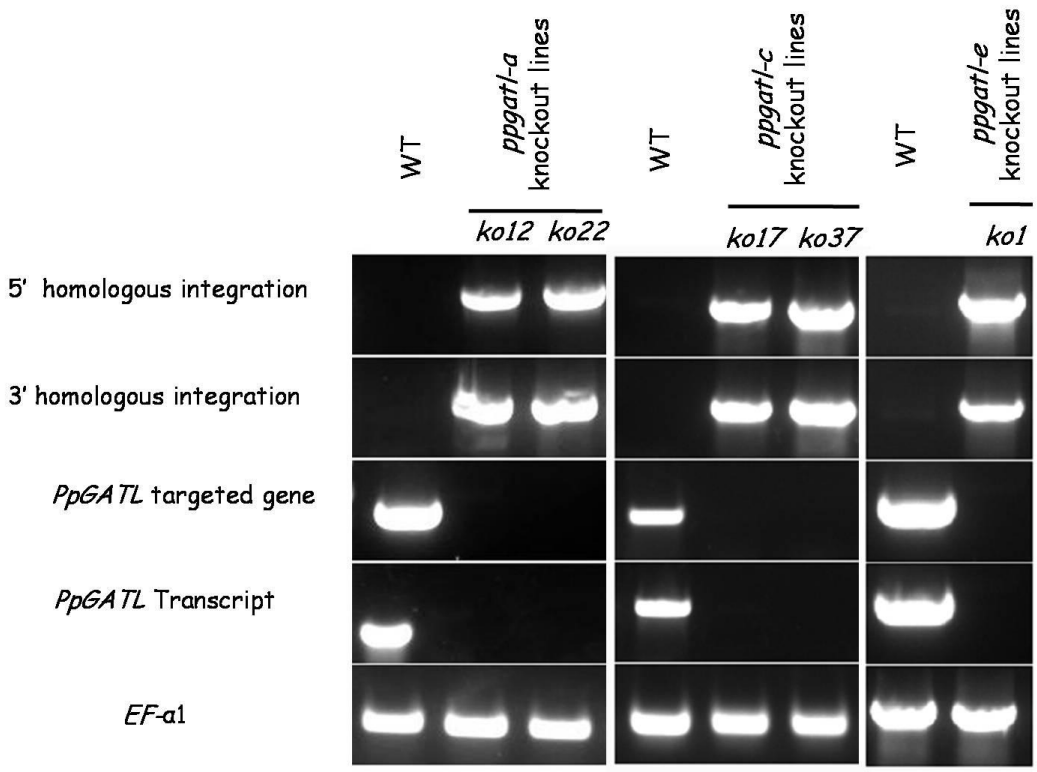


Figure S3.2. PCR and RT-PCR verification of *ppgatl-a*, *ppgatl-c* and *ppgatl-e* knockout lines; the expression of the *EFα1*gene was used as an internal control. For each knockout line, 5' integration of the vector, 3' integration of the vector, disruption of the targeted *PpGATL*gene and absence of the *PpGATL* transcript were confirmed.

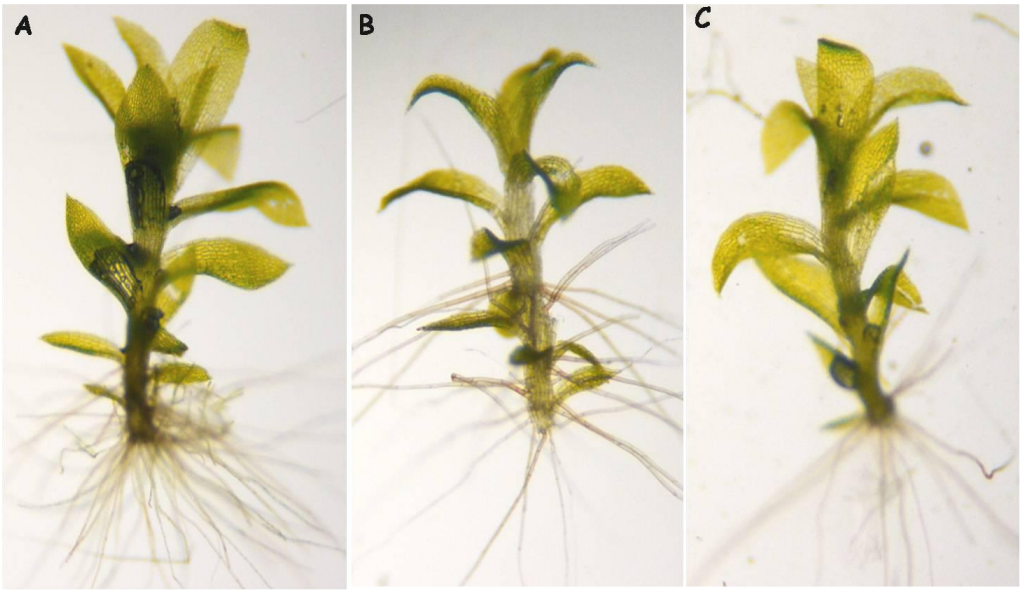


Figure S3.3. Six-week-old wild type (A), *ppgatl-a ko12* (B) and *ppgatl-a ko22* (C) leafy gametophores grown on BCD medium.

Table S 3.1: Primers used for construction of *ppgatl* knockout lines.

PCR products are flanked by different *att*B sites (underlined bps) to generate entry clones by BP recombination reaction.

| **Gene name** | **Primer name** | **Primer sequence （5’- 3’）** |
|---|---|---|
| *PpGATL-A* | 768-5attB1 | GGGGACAAGTTTGTACAAAAAAGCAGGCTGAACTTCACTCTTCTTCGTTTTGC |
| | 768-5attB4 | GGGGACAACTTTGTATAGAAAAGTTGGGTGTTCCGGTCACATATGTGGTC |
| | 768-3attB3 | GGGGACAACTTTGTATAATAAAGTTGGTTCTGTGGGCATCGAGAAG |
| | 768-3attB2 | GGGGACCACTTTGTACAAGAAAGCTGGGTGCATGACAACCTTCTAATCAACG |
| *PpGATL-C* | 454-5attB1 | GGGGACAAGTTTGTACAAAAAAGCAGGCTCACGAGCATTGACCTAGTCAC |
| | 454-5attB4 | GGGGACAACTTTGTATAGAAAAGTTGGGTAGAAATGTGCACCGAGTTCC |
| | 454-3attB3 | GGGGACAACTTTGTATAATAAAGTTGAAGAAGCGAAGGTTAAGAACTG |
| | 454-3attB2 | GGGGACCACTTTGTACAAGAAAGCTGGGTCACATACCTGCTGAACAAACC |
| *PpGATL-E* | 911-5attB1 | GGGGACAAGTTTGTACAAAAAAGCAGGCTGTTGTTTCTGCAAACTGACTTGG |
| | 911-5attB4 | GGGGACAACTTTGTATAGAAAAGTTGGGTTGCACCGAGTTTGGATCG |
| | 911-3attB3 | GGGGACAACTTTGTATAATAAAGTTGAGTGAAGGAAACGCTAACACC |
| | 911-3attB2 | GGGGACCACTTTGTACAAGAAAGCTGGGTCCACCTTCTTGACCTAAGTTCC |

Table S3.2. Primers for PCR Screens of Putative*ppgatl*knockout mutants

| **Gene name** | **Primer name** | **Primer sequence （5’- 3’）** | **Amplified region** |
|---|---|---|---|
| *PpGATL-A* | 768-5F | GAACTTCACTCTTCTTCGTTTTGC | 5' integration site *PpGATL-A* |
| | Vector-R | TCCGAGGGCAAAGAAATAGA | |
| | Vector-F | TGACAGATAGCTGGGCAATG | 3' integration site *PpGATL-A* |
| | 768-3R | GCATGACAACCTTCTAATCAACG | |
| | 768-F | ATGACACTGGATGTGAAGTAC | Target sequence *PpGATL-A* |
| | 768-R | TTATTGGTAAGATAATGCGGAGG | |
| *PpGATL-C* | 454-5F | CACGAGCATTGACCTAGTCAC | 5' integration site *PpGATL-C* |
| | Vector-R | see above | |
| | Vector-F | see above | 3' integration site *PpGATL-C* |
| | 454-3R | CACATACCTGCTGAACAAACC | |
| | 454-F | ATGACACTCGATGTGAAATATCTGC | Target sequence *PpGATL-C* |
| | 454-R | TTATTGATAAGATAATGTGGAGGGGAG | |
| *PpGATL-E* | 911-5F | GTTGTTTCTGCAAACTGACTTGG | 5' integration site *PpGATL-E* |
| | Vector-R | see above | |
| | Vector-F | see above | 3' integration site *PpGATL-E* |
| | 911-3R | CCACCTTCTTGACCTAAGTTTCC | |
| | 911-F | ATGACGCTTGATGTAGAATATTTGC | Target sequence *PpGATL-E* |
| | 911-R | TTATTGGTAAGACAACGGGGAAAG | |

Table S3.3 Primers for RT–PCR Analysis of Putative *ppgatl* knockout mutants.

| | | |
|---|---|---|
| *PpGATL-A* | 768RT-F | GCACCTTTGATGGGAAGAAGC |
| | 768RT-R | TTATTGGTAAGATAATGCGGAGG |
| *PpGATL-C* | 454RT-F | GCGTTCTGGAACAACAGAATC |
| | 454RT-R | TTATTGATAAGATAATGTGGAGGGGAG |
| *PpGATL-E* | 911RT-F | ATTCTGGGCAAACAGAACCTTATC |
| | 911RT-R | TTATTGGTAAGACAACGGGGAAAG |
| *EF-1α* | EF-1α-F | AGCGTGGTATCACAATTGAC |
| | EF-1α-R | GATCGCTCGATCATGTTATC |

Table S3.4: Primers used for construction of *PpGATLpro::GUS* fusions

| **Gene name** | **Primer name** | **Primer sequence （5’- 3’）** |
|---|---|---|
| *PpGATL-A* | 768GUS-5F | GGTACCGGTGATGCTTCGTTGAAGTG |
| | 768GUS-5R | CTCGAGTTGGTAAGATAATGCGGAGG |
| | 768GUS-3R | ACTAGTGTTCTGTGGGCATCGAGAAG |
| | 768GUS-3F | GCGGCCGCGCATGACAACCTTCTAATCAACG |
| *PpGATL-C* | 454GUS-5F | GGTACCATGTTGCTGCTCTGATTGAAG |
| | 454GUS-5R | GTCGACTTGATAAGATAATGTGGAGGGGAG |
| | 454GUS-3F | ACTAGTAAGAAGCGAAGGTTAAGAACTG |
| | 454GUS-3R | GAGCTCCACATACCTGCTGAACAAACC |
| *PpGATL-E* | 911GUS-5F | GGTACCTGGCACGACACTCATTGG |
| | 911GUS-5R | GTCGACTTGGTAAGACAACGGGGAAAG |
| | 911GUS-3F | ACTAGTAGTGAAGGAAACGCTAACACC |
| | 911GUS-3R | GCGGCCGCCCACCTTCTTGACCTAAGTTTCC |

# CHAPTER 4

# CONCLUSIONS

In this dissertation, the moss *Physcomitrella patens* has been used as a model to investigate the origin and functional role(s) of *GATL* gene family members in plant cell wall biosynthesis. It is the first study in which the isolation and characterization of galacturonosyltransferase-related gene knockout mutants in *Physcomitrella* has been carried out using a targeted mutagenesis approach.

Mutational and biochemical studies of the *Arabidopsis GATL* genes revealed that they play a role in cell wall biosynthesis. However, the function(s) for most of the GATL proteins remain unknown. Phylogenetic analyses of glycosyltransferase sequences from the moss *Physcomitrella patens* genome identified five orthologs to *AtGATLs*, providing a basis for investigating the evolution of the *GATL* gene family and identifying their role(s) in plant cell wall biosynthesis using a structurally simple system.

To investigate the biological function of the five *PpGATL*s in *Physcomitrella*, my PhD research was first focused on complementation studies of the *Arabidopsis parvus/gatl1* mutant with homologous *Physcomitrella* genes (Chapter 2). The reason to choose *PARVUS*/*ATGATL1* is because homozygous *parvus/atgatl1* mutants exhibit growth defects that are easily distinguishable from WT plants, including dwarfism, dark-green leaves, reduced size of all organs (i.e. leaves, floral organs, fruits), and reduced fertility (Lao et al. 2003). The *Arabidopsis* mutant

plants also display a collapsed xylem phenotype with a drastic reduction of secondary wall thickness in xylem tissues (Brown et al. 2007; Lee et al. 2007; Kong et al. 2009). I examined the gene expression profiles of the five *PpGATL* genes by quantitative real-time PCR using gene-specific primers and isolated three genes (*PpGATL-A, PpGATL-C*and *PpGATL-E*) with relatively higher expression levels. Subsequent studies focused on these three genes. To determine whether the PpGATL proteins have the same function as PARVUS/AtGATL1, the cDNAs of the three *PpGATL* genes were isolated and fused with CaMV 35S promoter and introduced individually into heterozygous *Arabidopsis parvus/gatl1* mutant lines. Transgenic plants with a homozygous *parvus/gatl1* background were identified by PCR. Overexpression of *PpGATL-A* in the *parvus* mutant rescues plant growth defects as well as the altered cell wall monosaccharide composition and cell wall glycome profiles. Thus, I showed that PpGATL-A is functionally conserved with PARVUS/AtGATL1 and can perform at least one similar biochemical function as the PARVUS/GATL1 protein in *Arabidopsis*.

To further investigate the role of *PpGATL* genes in cell wall biosynthesis, I performed targeted mutagenesis studies of *PpGATL-A, PpGATL-C* and *PpGATl-E* in *Physcomitrella* (Chapter 3). *ppgatl-a* knockout lines produce fewer leafy gametophores. Glycome profiling of cell wall fractions from *ppgatl-a* mutants revealed a loss of xylan epitopes in the 1M KOH and 4M KOH extracts, and cell wall composition analysis revealed a significantly reduced xylose content in 1M KOH extracts. Cell wall fractions prepared from wild type juvenile protonema tissue exhibit similar glycome profiles with the *ppgatl-a* mutants, and showed reduced xylose content in 1M KOH extracts as detected by glycosyl residue composition analysis. These data suggest *PpGATL-A* is required for

the transition from juvenile protonema to adult leafy gametphores in *Physcomitrella*. *ppgatl-c* and *ppgatl-e* knockout plants did not show any obvious growth defects compared to wild type. Promoter::*β*-glucuronidase expression studies showed that *PpGATL-A* and *PpGATL-C* have overlapping expression patterns, though with different expression intensities, while *PpGATL-E* exhibits a distinct expression pattern. The tissue-specific expression divergence between the *PpGATL*s suggests functional specialization and diversification of the PpGATL proteins; the genes encoding these proteins appear to have arisen by recent genome duplication events based on their high degree of sequence identity. More extensive gene knockout analyses will be required to explore the biological functions of the *Physcomitrella GATL* genes, either by gene knock-down by RNA interference or by generating double or triple *ppgatl* knockout mutants.

In conclusion, we have shown that *PpGATL-A* is a functional ortholog of *PARVUS*/AtGATL1 in *Arabidopsis*, and *PpGATL-A* is required for leafy gametophores development in *Physcomitrella*. The phenotype of the *Arabidopsis parvus/gatl1* mutant is complex, exhibiting characteristics consistent with defects in pectin or xylan synthesis ( Lao et al. 2003; Lee et al. 2007; Persson et al. 2007; Lee et al. 2009; Kong et al. 2009). The results of this study provide evidence that PpGATL-A may not be directly involved in xylan synthesis by contributing to the GalA-containing reducing end oligosaccharide synthesis as has been suggested in previous literature, since this xylan reducing end sequence has not been detected in *Physcomitrella* (Kulkarni et al. 2012b). Furthermore, xylan shows only a very limited presence in *Physcomitrella* as by chemical and immnolabeling analyses (Kulkarni et al. 2012b). Axillary hairs are specifically labelled by xylan-directed monoclonal antibodies including LM11,

CCRC-M137, CCRC-M147, CCRC-M154 and CCRC-M160 (Kulkarni et al. 2012b and Figure 3.6 in Chapter 3). Interestingly, *PpGATL-E* is highly expressed in axillary hairs (Figure 3.1 in Chapter 3), suggesting that this gene is possibly involved in xylan synthsis. However, overexpression of *PpGATL-E* in *Arabidopsis parvus/atgatl1* mutant plants does not rescue the defects caused by the *parvus* mutation. The above evidence supports another possibility that PpGATL-A functions in the synthesis of other GalA-containing polymers that provide a substructure for xylan deposition. A similar conclusion was drawn recently for the *Arabidopsis* GAUT12/IRX8 protein; mutation of the gene encoding this protein leads to defects in both xylan and pectin deposition (Hao et al. 2014). The exact biochemical function (s) of PpGATL proteins is not clear, and functional enzymatic assay such as HG:GalAT, RG-I:GalAT and/or RG-II:GalAT enzyme activity assay will be required to elucidate their precise roles in cell wall biosynthesis.

# REFERENCES

Anders N, Wilkinson MD, Lovegrove A, Freeman J, Tryfona T, Pellny TK, Weimar T, Mortimer JC, Stott K, Baker JM, Defoin-Platel M, Shewry PR, Dupree P, Mitchell RA (2012) Glycosyl transferases in family 61 mediate arabinofuranosyl transfer onto xylan in grasses. Proc Natl Acad Sci U S A 109 (3):989-993. doi:10.1073/pnas.1115858109

Andersson S-I, Samuelson O, Ishihara M, Shimizu K (1983) Structure of the reducing end-groups in spruce xylan. Carbohydrate research 111 (2):283-288. doi:http://dx.doi.org/10.1016/0008-6215(83)88312-8

Aspeborg H, Schrader J, Coutinho PM, Stam M, Kallas A, Djerbi S, Nilsson P, Denman S, Amini B, Sterky F, Master E, Sandberg G, Mellerowicz E, Sundberg B, Henrissat B, Teeri TT (2005) Carbohydrate-active enzymes involved in the secondary cell wall biogenesis in hybrid aspen. Plant Physiol 137 (3):983-997. doi:10.1104/pp.104.055087

Atmodjo MA, Hao Z, Mohnen D (2013) Evolving views of pectin biosynthesis. Annu Rev Plant Biol 64:747-779. doi:10.1146/annurev-arplant-042811-105534

Atmodjo MA, Sakuragi Y, Zhu X, Burrell AJ, Mohanty SS, Atwood JA, 3rd, Orlando R, Scheller HV, Mohnen D (2011) Galacturonosyltransferase (GAUT)1 and GAUT7 are the core of a plant cell wall pectin biosynthetic homogalacturonan:galacturonosyltransferase complex. Proc Natl Acad Sci U S A 108 (50):20225-20230. doi:10.1073/pnas.1112816108

Avci U, Pattathil S, Hahn MG (2012) Immunological approaches to plant cell wall and biomass characterization: immunolocalization of glycan epitopes. Methods in molecular biology

(Clifton, NJ) 908:73-82. doi:10.1007/978-1-61779-956-3_7

Becker B, Marin B (2009) Streptophyte algae and the origin of embryophytes. Annals of botany 103 (7):999-1004. doi:10.1093/aob/mcp044

Bezanilla M, Pan A, Quatrano RS (2003) RNA interference in the moss Physcomitrella patens. Plant Physiol 133 (2):470-474. doi:10.1104/pp.103.024901

Bezanilla M, Perroud PF, Pan A, Klueh P, Quatrano RS (2005) An RNAi system in Physcomitrella patens with an internal marker for silencing allows for rapid identification of loss of function phenotypes. Plant biology (Stuttgart, Germany) 7 (3):251-257. doi:10.1055/s-2005-837597

Bouton S, Leboeuf E, Mouille G, Leydecker MT, Talbotec J, Granier F, Lahaye M, Hofte H, Truong HN (2002) Quasimodo1 encodes a putative membrane-bound glycosyltransferase required for normal pectin synthesis and cell adhesion in Arabidopsis. Plant Cell 14 (10):2577-2590. doi:10.1105/tpc.004259

Britt AB, May GD (2003) Re-engineering plant gene targeting. Trends Plant Sci 8 (2):90-95. doi:10.1016/s1360-1385(03)00002-5

Bromley JR, Busse-Wicher M, Tryfona T, Mortimer JC, Zhang Z, Brown DM, Dupree P (2013) GUX1 and GUX2 glucuronyltransferases decorate distinct domains of glucuronoxylan with different substitution patterns. The Plant journal : for cell and molecular biology 74 (3):423-434. doi:10.1111/tpj.12135

Brown D, Wightman R, Zhang Z, Gomez LD, Atanassov I, Bukowski JP, Tryfona T, McQueen-Mason SJ, Dupree P, Turner S (2011) Arabidopsis genes IRREGULAR

XYLEM (IRX15) and IRX15L encode DUF579-containing proteins that are essential for normal xylan deposition in the secondary cell wall. The Plant journal : for cell and molecular biology 66 (3):401-413. doi:10.1111/j.1365-313X.2011.04501.x

Brown DM, Goubet F, Vicky WWA, Goodacre R, Stephens E, Dupree P, Turner SR (2007) Comparison of five xylan synthesis mutants reveals new insight into the mechanisms of xylan synthesis. Plant Journal 52 (6):1154-1168. doi:10.1111/j.1365-313X.2007.03307.x

Brown DM, Zeef LA, Ellis J, Goodacre R, Turner SR (2005) Identification of novel genes in Arabidopsis involved in secondary cell wall formation using expression profiling and reverse genetics. Plant Cell 17 (8):2281-2295. doi:10.1105/tpc.105.031542

Brown DM, Zhang ZN, Stephens E, Dupree P, Turner SR (2009) Characterization of IRX10 and IRX10-like reveals an essential role in glucuronoxylan biosynthesis in Arabidopsis. Plant Journal 57 (4):732-746. doi:10.1111/j.1365-313X.2008.03729.x

Buda GJ, Barnes WJ, Fich EA, Park S, Yeats TH, Zhao L, Domozych DS, Rose JK (2013) An ATP binding cassette transporter is required for cuticular wax deposition and desiccation tolerance in the moss Physcomitrella patens. Plant Cell 25 (10):4000-4013. doi:10.1105/tpc.113.117648

Burton RA, Fincher GB (2014) Plant cell wall engineering: applications in biofuel production and improved human health. Current Opinion in Biotechnology 26 (0):79-84. doi:http://dx.doi.org/10.1016/j.copbio.2013.10.007

Burton RA, Gidley MJ, Fincher GB (2010) Heterogeneity in the chemistry, structure and function of plant cell walls. Nature chemical biology 6 (10):724-732. doi:10.1038/nchembio.439

Caffall KH, Mohnen D (2009) The structure, function, and biosynthesis of plant cell wall pectic polysaccharides. Carbohydrate research 344 (14):1879-1900. doi:10.1016/j.carres.2009.05.021

Caffall KH, Pattathil S, Phillips SE, Hahn MG, Mohnen D (2009) Arabidopsis thaliana T-DNA Mutants Implicate GAUT Genes in the Biosynthesis of Pectin and Xylan in Cell Walls and Seed Testa. Molecular Plant 2 (5):1000-1014. doi:10.1093/mp/ssp062

Cantarel BL, Coutinho PM, Rancurel C, Bernard T, Lombard V, Henrissat B (2009) The Carbohydrate-Active EnZymes database (CAZy): an expert resource for Glycogenomics. Nucleic Acids Research 37:D233-D238. doi:10.1093/nar/gkn663

Carafa A, Duckett JG, Knox JP, Ligrone R (2005) Distribution of cell-wall xylans in bryophytes and tracheophytes: new insights into basal interrelationships of land plants. The New phytologist 168 (1):231-240. doi:10.1111/j.1469-8137.2005.01483.x

Carpita N, Tierney M, Campbell M (2001) Molecular biology of the plant cell wall: searching for the genes that define structure, architecture and dynamics. Plant Molecular Biology 47 (1-2):1-5. doi:10.1023/a:1010603527077

Cavalier DM, Keegstra K (2006) Two xyloglucan xylosyltransferases catalyze the addition of multiple xylosyl residues to cellohexaose. The Journal of biological chemistry 281 (45):34197-34207. doi:10.1074/jbc.M606379200

Cho SH, Chung YS, Cho SK, Rim YW, Shin JS (1999) Particle bombardment mediated transformation and GFP expression in the moss Physcomitrella patens. Molecules and cells 9 (1):14-19

Clough SJ, Bent AF (1998) Floral dip: a simplified method for Agrobacterium-mediated transformation of Arabidopsis thaliana. Plant Journal 16 (6):735-743. doi:10.1046/j.1365-313x.1998.00343.x

Coenen GJ, Bakx EJ, Verhoef RP, Schols HA, Voragen AGJ (2007) Identification of the connecting linkage between homo- or xylogalacturonan and rhamnogalacturonan type I. Carbohydrate Polymers 70 (2):224-235. doi:http://dx.doi.org/10.1016/j.carbpol.2007.04.007

Cosgrove DJ (2005) Growth of the plant cell wall. Nature reviews Molecular cell biology 6 (11):850-861. doi:10.1038/nrm1746

Cove D (2005) The moss Physcomitrella patens. Annual review of genetics 39:339-358. doi:10.1146/annurev.genet.39.073003.110214

Cove DJ, Perroud PF, Charron AJ, McDaniel SF, Khandelwal A, Quatrano RS (2009) Isolation and regeneration of protoplasts of the moss Physcomitrella patens. Cold Spring Harbor protocols 2009 (2):pdb.prot5140. doi:10.1101/pdb.prot5140

Deblaere R, Bytebier B, De Greve H, Deboeck F, Schell J, Van Montagu M, Leemans J (1985) Efficient octopine Ti plasmid-derived vectors for Agrobacterium-mediated gene transfer to plants. Nucleic Acids Res 13 (13):4777-4788

Dhugga KS, Barreiro R, Whitten B, Stecca K, Hazebroek J, Randhawa GS, Dolan M, Kinney AJ, Tomes D, Nichols S, Anderson P (2004) Guar Seed β-Mannan Synthase Is a Member of the Cellulose Synthase Super Gene Family. Science 303 (5656):363-366. doi:10.1126/science.1090908

Ebringerová A, Heinze T (2000) Xylan and xylan derivatives – biopolymers with valuable properties, 1. Naturally occurring xylans structures, isolation procedures and properties. Macromolecular Rapid Communications 21 (9):542-556. doi:10.1002/1521-3927(20000601)21:9<542::AID-MARC542>3.0.CO;2-7

Edgar RC (2004) MUSCLE: multiple sequence alignment with high accuracy and high throughput. Nucleic Acids Research 32 (5):1792-1797. doi:10.1093/nar/gkh340

Egelund J, Damager I, Faber K, Olsen CE, Ulvskov P, Petersen BL (2008) Functional characterisation of a putative rhamnogalacturonan II specific xylosyltransferase. Febs Letters 582 (21-22):3217-3222. doi:10.1016/j.febslet.2008.08.015

Egelund J, Petersen BL, Motawia MS, Damager I, Faik A, Olsen CE, Ishii T, Clausen H, Ulvskov P, Geshi N (2006) Arabidopsis thaliana RGXT1 and RGXT2 encode Golgi-localized (1,3)-alpha-D-xylosyltransferases involved in the synthesis of pectic rhamnogalacturonan-II. Plant Cell 18 (10):2593-2607. doi:10.1105/tpc.105.036566

Exposito-Rodriguez M, Borges AA, Borges-Perez A, Perez JA (2008) Selection of internal control genes for quantitative real-time RT-PCR studies during tomato development process. BMC Plant Biol 8:131. doi:10.1186/1471-2229-8-131

Faik A, Jiang N, Held M (2014) Xylan Biosynthesis in Plants, Simply Complex. In: McCann MC, Buckeridge MS, Carpita NC (eds) Plants and BioEnergy, vol 4. Advances in Plant Biology. Springer New York, pp 153-181. doi:10.1007/978-1-4614-9329-7_10

Force A, Lynch M, Pickett FB, Amores A, Yan YL, Postlethwait J (1999) Preservation of duplicate genes by complementary, degenerative mutations. Genetics 151 (4):1531-1545

Freshour G, Clay RP, Fuller MS, Albersheim P, Darvill AG, Hahn MG (1996) Developmental and Tissue-Specific Structural Alterations of the Cell-Wall Polysaccharides of Arabidopsis thaliana Roots. Plant Physiol 110 (4):1413-1429

Fu H, Yadav MP, Nothnagel EA (2007) Physcomitrella patens arabinogalactan proteins contain abundant terminal 3-O-methyl-L-rhamnosyl residues not found in angiosperms. Planta 226 (6):1511-1524. doi:10.1007/s00425-007-0587-y

Gille S, Pauly M (2012) O-acetylation of plant cell wall polysaccharides. Frontiers in plant science 3:12. doi:10.3389/fpls.2012.00012

Girod PA, Fu H, Zryd JP, Vierstra RD (1999) Multiubiquitin chain binding subunit MCB1 (RPN10) of the 26S proteasome is essential for developmental progression in Physcomitrella patens. Plant Cell 11 (8):1457-1472

Goss CA, Brockmann DJ, Bushoven JT, Roberts AW (2012) A CELLULOSE SYNTHASE (CESA) gene essential for gametophore morphogenesis in the moss Physcomitrella patens. Planta 235 (6):1355-1367. doi:10.1007/s00425-011-1579-5

Grabber JH (2005) How Do Lignin Composition, Structure, and Cross-Linking Affect Degradability? A Review of Cell Wall Model Studies This paper was originally presented at the Lignin and Forage Digestibility Symposium, 2003 CSSA Annual Meeting, Denver, CO. Crop Sci 45 (3):820-831. doi:10.2135/cropsci2004.0191

Grimsley NH, Ashton NW, Cove DJ (1977) The production of somatic hybrids by protoplast fusion in the moss, Physcomitrella patens. Molec Gen Genet 154 (1):97-100. doi:10.1007/BF00265582

Guillemin F, Guillon F, Bonnin E, Devaux MF, Chevalier T, Knox JP, Liners F, Thibault JF (2005) Distribution of pectic epitopes in cell walls of the sugar beet root. Planta 222 (2):355-371. doi:10.1007/s00425-005-1535-3

Guindon S, Dufayard J-F, Lefort V, Anisimova M, Hordijk W, Gascuel O (2010) New Algorithms and Methods to Estimate Maximum-Likelihood Phylogenies: Assessing the Performance of PhyML 3.0. Systematic Biology 59 (3):307-321. doi:10.1093/sysbio/syq010

Hajdukiewicz P, Svab Z, Maliga P (1994) The small, versatile pPZP family of Agrobacterium binary vectors for plant transformation. Plant Mol Biol 25 (6):989-994

Hao Z, Avci U, Tan L, Zhu X, Glushka J, Pattathil S, Eberhard S, Scholes T, Rothstein GE, Lukowitz W, Orlando R, Hahn MG, Mohnen D (2014) Loss of Arabidopsis GAUT12/IRX8 causes anther indehiscence and leads to reduced G lignin associated with altered matrix polysaccharide deposition. Frontiers in plant science 5. doi:10.3389/fpls.2014.00357

Harholt J, Jensen JK, Sorensen SO, Orfila C, Pauly M, Scheller HV (2006) ARABINAN DEFICIENT 1 is a putative arabinosyltransferase involved in biosynthesis of pectic arabinan in Arabidopsis. Plant Physiol 140 (1):49-58. doi:10.1104/pp.105.072744

Harholt J, Sorensen I, Fangel J, Roberts A, Willats WGT, Scheller HV, Petersen BL, Banks A, Ulvskov P (2012) The Glycosyltransferase Repertoire of the Spikemoss Selaginella moellendorffii and a Comparative Study of Its Cell Wall. PloS one 7 (5). doi:10.1371/journal.pone.0035846

Held MA, Be E, Zemelis S, Withers S, Wilkerson C, Brandizzi F (2011) CGR3: a Golgi-localized

protein influencing homogalacturonan methylesterification. Mol Plant 4 (5):832-844. doi:10.1093/mp/ssr012

Henrissat B, Coutinho PM, Davies GJ (2001) A census of carbohydrate-active enzymes in the genome of Arabidopsis thaliana. Plant Molecular Biology 47 (1-2):55-72. doi:10.1023/a:1010667012056

Hiei Y, Ohta S, Komari T, Kumashiro T (1994) Efficient transformation of rice (Oryza sativa L.) mediated by Agrobacterium and sequence analysis of the boundaries of the T-DNA. The Plant journal : for cell and molecular biology 6 (2):271-282

Hongo S, Sato K, Yokoyama R, Nishitani K (2012) Demethylesterification of the primary wall by PECTIN METHYLESTERASE35 provides mechanical support to the Arabidopsis stem. Plant Cell 24 (6):2624-2634. doi:10.1105/tpc.112.099325

Hornblad E, Ulfstedt M, Ronne H, Marchant A (2013) Partial functional conservation of IRX10 homologs in physcomitrella patens and Arabidopsis thaliana indicates an evolutionary step contributing to vascular formation in land plants. Bmc Plant Biology 13. doi:10.1186/1471-2229-13-3

Imaizumi T, Kadota A, Hasebe M, Wada M (2002) Cryptochrome light signals control development to suppress auxin sensitivity in the moss Physcomitrella patens. Plant Cell 14 (2):373-386

Ishii T, Matsunaga T (2001) Pectic polysaccharide rhamnogalacturonan II is covalently linked to homogalacturonan. Phytochemistry 57 (6):969-974. doi:http://dx.doi.org/10.1016/S0031-9422(01)00047-4

Ishii T, Matsunaga T, Hayashi N (2001) Formation of rhamnogalacturonan II-borate dimer in pectin determines cell wall thickness of pumpkin tissue. Plant Physiol 126 (4):1698-1705

Iwai H, Masaoka N, Ishii T, Satoh S (2002) A pectin glucuronyltransferase gene is essential for intercellular attachment in the plant meristem. Proceedings of the National Academy of Sciences of the United States of America 99 (25):16319-16324. doi:10.1073/pnas.252530499

Jefferson R (1987) Assaying chimeric genes in plants: The GUS gene fusion system. Plant Mol Biol Rep 5 (4):387-405. doi:10.1007/BF02667740

Jensen JK, Johnson NR, Wilkerson CG (2014) Arabidopsis thaliana IRX10 and two related proteins from psyllium and Physcomitrella patens are xylan xylosyltransferases. The Plant journal : for cell and molecular biology. doi:10.1111/tpj.12641

Jensen JK, Kim H, Cocuron JC, Orler R, Ralph J, Wilkerson CG (2011) The DUF579 domain containing proteins IRX15 and IRX15-L affect xylan synthesis in Arabidopsis. The Plant journal : for cell and molecular biology 66 (3):387-400. doi:10.1111/j.1365-313X.2010.04475.x

Jensen JK, Sorensen SO, Harholt J, Geshi N, Sakuragi Y, Moller I, Zandleven J, Bernal AJ, Jensen NB, Sorensen C, Pauly M, Beldman G, Willats WGT, Scheller HV (2008) Identification of a xylogalacturonan xylosyltransferase involved in pectin biosynthesis in Arabidopsis. Plant Cell 20 (5):1289-1302. doi:10.1105/tpc.107.050906

Johansson MH, Samuelson O (1977) Reducing end groups in brich xylan and their alkaline degradation. Wood Sci Technol 11 (4):251-263. doi:10.1007/BF00356924

Kamisugi Y, Cuming AC, Cove DJ (2005) Parameters determining the efficiency of gene targeting in the moss Physcomitrella patens. Nucleic Acids Res 33 (19):e173. doi:10.1093/nar/gni172

Khraiwesh B, Ossowski S, Weigel D, Reski R, Frank W (2008) Specific gene silencing by artificial MicroRNAs in Physcomitrella patens: an alternative to targeted gene knockouts. Plant Physiol 148 (2):684-693. doi:10.1104/pp.108.128025

Klein TM, Fromm M, Weissinger A, Tomes D, Schaaf S, Sletten M, Sanford JC (1988) Transfer of foreign genes into intact maize cells with high-velocity microprojectiles. Proc Natl Acad Sci U S A 85 (12):4305-4309

Kong Y, Zhou G, Abdeen AA, Schafhauser J, Richardson B, Atmodjo MA, Jung J, Wicker L, Mohnen D, Western T, Hahn MG (2013) GALACTURONOSYLTRANSFERASE-LIKE5 is involved in the production of Arabidopsis seed coat mucilage. Plant Physiol 163 (3):1203-1217. doi:10.1104/pp.113.227041

Kong Y, Zhou G, Yin Y, Xu Y, Pattathil S, Hahn MG (2011) Molecular Analysis of a Family of Arabidopsis Genes Related to Galacturonosyltransferases. Plant Physiology 155 (4):1791-1805. doi:10.1104/pp.110.163220

Kong YZ, Zhou GK, Avci U, Gu XG, Jones C, Yin YB, Xu Y, Hahn MG (2009) Two Poplar Glycosyltransferase Genes, PdGATL1.1 and PdGATL1.2, Are Functional Orthologs to PARVUS/AtGATL1 in Arabidopsis. Molecular Plant 2 (5):1040-1050. doi:10.1093/mp/ssp068

Krupkova E, Immerzeel P, Pauly M, Schmulling T (2007) The TUMOROUS SHOOT DEVELOPMENT2 gene of Arabidopsis encoding a putative methyltransferase is required for cell adhesion and co-ordinated plant development. The Plant journal : for cell and molecular biology 50 (4):735-750. doi:10.1111/j.1365-313X.2007.03123.x

Kulkarni AR, Pattathil S, Hahn MG, York WS, O'Neill MA (2012a) Comparison of arabinoxylan structure in bioenergy and model grasses. Industrial Biotechnology 8 (4):222-229

Kulkarni AR, Pena MJ, Avci U, Mazumder K, Urbanowicz BR, Pattathil S, Yin Y, O'Neill MA, Roberts AW, Hahn MG, Xu Y, Darvill AG, York WS (2012b) The ability of land plants to synthesize glucuronoxylans predates the evolution of tracheophytes. Glycobiology 22 (3):439-451. doi:10.1093/glycob/cwr117

Laine C, Tamminen T, Hortling B (2004) Carbohydrate structures in residual lignin-carbohydrate complexes of spruce and pine pulp. Holzforschung 58 (6):611-621. doi:10.1515/hf.2004.115

Lao NT, Long D, Kiang S, Coupland G, Shoue DA, Carpita NC, Kavanagh TA (2003) Mutation of a family 8 glycosyltransferase gene alters cell wall carbohydrate composition and causes a humidity-sensitive semi-sterile dwarf phenotype in Arabidopsis. Plant Molecular Biology 53 (5):687-701. doi:10.1023/B:PLAN.0000019074.60542.6c

Lee C, Teng Q, Huang WL, Zhong RQ, Ye ZH (2009) The Poplar GT8E and GT8F Glycosyltransferases are Functional Orthologs of Arabidopsis PARVUS Involved in Glucuronoxylan Biosynthesis. Plant and Cell Physiology 50 (11):1982-1987. doi:10.1093/pcp/pcp131

Lee C, Teng Q, Zhong R, Ye ZH (2011) The four Arabidopsis reduced wall acetylation genes are expressed in secondary wall-containing cells and required for the acetylation of xylan. Plant & cell physiology 52 (8):1289-1301. doi:10.1093/pcp/pcr075

Lee C, Teng Q, Zhong R, Ye ZH (2012a) Arabidopsis GUX proteins are glucuronyltransferases responsible for the addition of glucuronic acid side chains onto xylan. Plant & cell physiology 53 (7):1204-1216. doi:10.1093/pcp/pcs064

Lee C, Zhong R, Richardson EA, Himmelsbach DS, McPhail BT, Ye Z-H (2007) The PARVUS gene is expressed in cells undergoing secondary wall thickening and is essential for glucuronoxylan biosynthesis. Plant and Cell Physiology 48 (12):1659-1672. doi:10.1093/pcp/pcm155

Lee C, Zhong R, Ye ZH (2012b) Arabidopsis family GT43 members are xylan xylosyltransferases required for the elongation of the xylan backbone. Plant & cell physiology 53 (1):135-143. doi:10.1093/pcp/pcr158

Lee KJ, Sakata Y, Mau SL, Pettolino F, Bacic A, Quatrano RS, Knight CD, Knox JP (2005a) Arabinogalactan proteins are required for apical cell extension in the moss Physcomitrella patens. Plant Cell 17 (11):3051-3065. doi:10.1105/tpc.105.034413

Lee KJD, Knight CD, Knox JP (2005b) Physcomitrella patens: A moss system for the study of plant cell walls. Plant Biosystems 139 (1):16-19. doi:10.1080/11263500500055213

Liepman AH, Nairn CJ, Willats WG, Sorensen I, Roberts AW, Keegstra K (2007) Functional genomic analysis supports conservation of function among cellulose synthase-like a gene family members and suggests diverse roles of mannans in plants. Plant Physiol 143

(4):1881-1893. doi:10.1104/pp.106.093989

Liepman AH, Wightman R, Geshi N, Turner SR, Scheller HV (2010) Arabidopsis - a powerful model system for plant cell wall research. Plant Journal 61 (6):1107-1121. doi:10.1111/j.1365-313X.2010.04161.x

Liepman AH, Wilkerson CG, Keegstra K (2005) Expression of cellulose synthase-like (Csl) genes in insect cells reveals that CslA family members encode mannan synthases. Proc Natl Acad Sci U S A 102 (6):2221-2226. doi:10.1073/pnas.0409179102

Liu XL, Liu LF, Niu QK, Xia CA, Yang KZ, Li R, Chen LQ, Zhang XQ, Zhou YH, Ye D (2011) MALE GAMETOPHYTE DEFECTIVE 4 encodes a rhamnogalacturonan II xylosyltransferase and is important for growth of pollen tubes and roots in Arabidopsis. Plant Journal 65 (4):647-660. doi:10.1111/j.1365-313X.2010.04452.x

Liu YC, Vidali L (2011) Efficient polyethylene glycol (PEG) mediated transformation of the moss Physcomitrella patens. Journal of visualized experiments : JoVE (50). doi:10.3791/2560

Liwanag AJM, Ebert B, Verhertbruggen Y, Rennie EA, Rautengarten C, Oikawa A, Andersen MCF, Clausen MH, Scheller HV (2012) Pectin Biosynthesis: GALS1 in Arabidopsis thaliana Is a beta-1,4-Galactan beta-1,4-Galactosyltransferase. Plant Cell 24 (12):5024-5036. doi:10.1105/tpc.112.106625

Manabe Y, Nafisi M, Verhertbruggen Y, Orfila C, Gille S, Rautengarten C, Cherk C, Marcus SE, Somerville S, Pauly M, Knox JP, Sakuragi Y, Scheller HV (2011) Loss-of-function mutation of REDUCED WALL ACETYLATION2 in Arabidopsis leads to reduced cell wall acetylation and increased resistance to Botrytis cinerea. Plant Physiol 155

(3):1068-1078. doi:10.1104/pp.110.168989

Manabe Y, Verhertbruggen Y, Gille S, Harholt J, Chong SL, Pawar PM, Mellerowicz EJ, Tenkanen M, Cheng K, Pauly M, Scheller HV (2013) Reduced Wall Acetylation proteins play vital and distinct roles in cell wall O-acetylation in Arabidopsis. Plant Physiol 163 (3):1107-1117. doi:10.1104/pp.113.225193

Martin A, Lang D, Hanke ST, Mueller SJ, Sarnighausen E, Vervliet-Scheebaum M, Reski R (2009) Targeted gene knockouts reveal overlapping functions of the five Physcomitrella patens FtsZ isoforms in chloroplast division, chloroplast shaping, cell patterning, plant development, and gravity sensing. Mol Plant 2 (6):1359-1372. doi:10.1093/mp/ssp076

Masuko T, Minami A, Iwasaki N, Majima T, Nishimura S, Lee YC (2005) Carbohydrate analysis by a phenol-sulfuric acid method in microplate format. Analytical biochemistry 339 (1):69-72. doi:10.1016/j.ab.2004.12.001

Matsunaga T, Ishii T, Matsumoto S, Higuchi M, Darvill A, Albersheim P, O'Neill MA (2004) Occurrence of the primary cell wall polysaccharide rhamnogalacturonan II in pteridophytes, lycophytes, and bryophytes. Implications for the evolution of vascular plants. Plant Physiol 134 (1):339-351. doi:10.1104/pp.103.030072

McCarthy TW, Der JP, Honaas LA, dePamphilis CW, Anderson CT (2014) Phylogenetic analysis of pectin-related gene families in Physcomitrella patens and nine other plant species yields evolutionary insights into cell walls. Bmc Plant Biology 14. doi:10.1186/1471-2229-14-79

McCartney L, Marcus SE, Knox JP (2005) Monoclonal antibodies to plant cell wall xylans and

arabinoxylans. Journal of Histochemistry & Cytochemistry 53 (4):543-546. doi:10.1369/jhc.4B6578.2005

McNeil M, Darvill AG, Fry SC, Albersheim P (1984) STRUCTURE AND FUNCTION OF THE PRIMARY-CELL WALLS OF PLANTS. Annual Review of Biochemistry 53:625-663. doi:10.1146/annurev.bi.53.070184.003205

Menand B, Calder G, Dolan L (2007) Both chloronemal and caulonemal cells expand by tip growth in the moss Physcomitrella patens. Journal of experimental botany 58 (7):1843-1849. doi:10.1093/jxb/erm047

Mengiste T, Paszkowski J (1999) Prospects for the precise engineering of plant genomes by homologous recombination. Biological chemistry 380 (7-8):749-758. doi:10.1515/bc.1999.095

Miao Y, Li HY, Shen J, Wang J, Jiang L (2011) QUASIMODO 3 (QUA3) is a putative homogalacturonan methyltransferase regulating cell wall biosynthesis in Arabidopsis suspension-cultured cells. Journal of experimental botany 62 (14):5063-5078. doi:10.1093/jxb/err211

Mitsuhara I, Ugaki M, Hirochika H, Ohshima M, Murakami T, Gotoh Y, Katayose Y, Nakamura S, Honkura R, Nishimiya S, Ueno K, Mochizuki A, Tanimoto H, Tsugawa H, Otsuki Y, Ohashi Y (1996) Efficient promoter cassettes for enhanced expression of foreign genes in dicotyledonous and monocotyledonous plants. Plant & cell physiology 37 (1):49-59

Mittmann F, Brucker G, Zeidler M, Repp A, Abts T, Hartmann E, Hughes J (2004) Targeted knockout in Physcomitrella reveals direct actions of phytochrome in the cytoplasm. Proc

Natl Acad Sci U S A 101 (38):13939-13944. doi:10.1073/pnas.0403140101

Mohnen D (2008) Pectin structure and biosynthesis. Current Opinion in Plant Biology 11 (3):266-277. doi:10.1016/j.pbi.2008.03.006

Moller I, Sorensen I, Bernal AJ, Blaukopf C, Lee K, Obro J, Pettolino F, Roberts A, Mikkelsen JD, Knox JP, Bacic A, Willats WGT (2007) High-throughput mapping of cell-wall polymers within and between plants using novel microarrays. Plant Journal 50 (6):1118-1128. doi:DOI 10.1111/j.1365-313X.2007.03114.x

Mortimer JC, Miles GP, Brown DM, Zhang Z, Segura MP, Weimar T, Yu X, Seffen KA, Stephens E, Turner SR, Dupree P (2010) Absence of branches from xylan in Arabidopsis gux mutants reveals potential for simplification of lignocellulosic biomass. Proc Natl Acad Sci U S A 107 (40):17409-17414. doi:10.1073/pnas.1005456107

Mouille G, Ralet MC, Cavelier C, Eland C, Effroy D, Hematy K, McCartney L, Truong HN, Gaudon V, Thibault JF, Marchant A, Hofte H (2007) Homogalacturonan synthesis in Arabidopsis thaliana requires a Golgi-localized protein with a putative methyltransferase domain. The Plant journal : for cell and molecular biology 50 (4):605-614. doi:10.1111/j.1365-313X.2007.03086.x

Nakamura A, Furuta H, Maeda H, Takao T, Nagamatsu Y (2002) Structural studies by stepwise enzymatic degradation of the main backbone of soybean soluble polysaccharides consisting of galacturonan and rhamnogalacturonan. Bioscience, biotechnology, and biochemistry 66 (6):1301-1313

Nebenfuhr A, Staehelin LA (2001) Mobile factories: Golgi dynamics in plant cells. Trends in

Plant Science 6 (4):160-167. doi:10.1016/s1360-1385(01)01891-x

Nelson BK, Cai X, Nebenfuhr A (2007) A multicolored set of in vivo organelle markers for co-localization studies in Arabidopsis and other plants. Plant Journal 51 (6):1126-1136. doi:10.1111/j.1365-313X.2007.03212.x

Nishiyama T, Hiwatashi Y, Sakakibara I, Kato M, Hasebe M (2000) Tagged mutagenesis and gene-trap in the moss, Physcomitrella patens by shuttle mutagenesis. DNA research : an international journal for rapid publication of reports on genes and genomes 7 (1):9-17

O'Neill MA, Eberhard S, Albersheim P, Darvill AG (2001) Requirement of borate cross-linking of cell wall rhamnogalacturonan II for Arabidopsis growth. Science 294 (5543):846-849. doi:10.1126/science.1062319

O'Neill MA, Ishii T, Albersheim P, Darvill AG (2004) Rhamnogalacturonan II: Structure and function of a borate cross-linked cell wall pectic polysaccharide. Annual Review of Plant Biology 55:109-139. doi:10.1146/annurev.arplant.55.031903.141750

Ogawa M, Kay P, Wilson S, Swain SM (2009) ARABIDOPSIS DEHISCENCE ZONE POLYGALACTURONASE1 (ADPG1), ADPG2, and QUARTET2 are Polygalacturonases required for cell separation during reproductive development in Arabidopsis. Plant Cell 21 (1):216-233. doi:10.1105/tpc.108.063768

Olsson T, Thelander M, Ronne H (2003) A novel type of chloroplast stromal hexokinase is the major glucose-phosphorylating enzyme in the moss Physcomitrella patens. The Journal of biological chemistry 278 (45):44439-44447. doi:10.1074/jbc.M306265200

Orfila C, Sorensen SO, Harholt J, Geshi N, Crombie H, Truong HN, Reid JSG, Knox JP, Scheller

HV (2005) QUASIMODO1 is expressed in vascular tissue of Arabidopsis thaliana inflorescence stems, and affects homogalacturonan and xylan biosynthesis. Planta 222 (4):613-622. doi:10.1007/s00425-005-0008-z

Pattathil S, Avci U, Baldwin D, Swennes AG, McGill JA, Popper Z, Bootten T, Albert A, Davis RH, Chennareddy C, Dong R, O'Shea B, Rossi R, Leoff C, Freshour G, Narra R, O'Neil M, York WS, Hahn MG (2010) A Comprehensive Toolkit of Plant Cell Wall Glycan-Directed Monoclonal Antibodies. Plant Physiology 153 (2):514-525. doi:10.1104/pp.109.151985

Pattathil S, Avci U, Miller JS, Hahn MG (2012) Immunological approaches to plant cell wall and biomass characterization: Glycome Profiling. Methods in molecular biology (Clifton, NJ) 908:61-72. doi:10.1007/978-1-61779-956-3_6

Pattathil S, Harper AD, Bar-Peled M (2005) Biosynthesis of UDP-xylose: characterization of membrane-bound AtUxs2. Planta 221 (4):538-548. doi:10.1007/s00425-004-1471-7

Pauly M, Keegstra K (2010) Plant cell wall polymers as precursors for biofuels. Curr Opin Plant Biol 13 (3):305-312. doi:10.1016/j.pbi.2009.12.009

Pena MJ, Darvill AG, Eberhard S, York WS, O'Neill MA (2008) Moss and liverwort xyloglucans contain galacturonic acid and are structurally distinct from the xyloglucans synthesized by hornworts and vascular plants. Glycobiology 18 (11):891-904. doi:10.1093/glycob/cwn078

Pena MJ, Zhong R, Zhou G-K, Richardson EA, O'Neill MA, Darvill AG, York WS, Ye Z-H (2007) Arabidopsis irregular xylem8 and irregular xylem9: Implications for the complexity of

glucuronoxylan biosynthesis. Plant Cell 19 (2):549-563. doi:10.1105/tpc.106.049320

Persson S, Caffall KH, Freshour G, Hilley MT, Bauer S, Poindexter P, Hahn MG, Mohnen D, Somerville C (2007) The Arabidopsis irregular xylem8 mutant is deficient in glucuronoxylan and homogalacturonan, which are essential for secondary cell wall integrity. Plant Cell 19 (1):237-255. doi:10.1105/tpc.106.047720

Popper ZA, Fry SC (2003) Primary cell wall composition of bryophytes and charophytes. Annals of botany 91 (1):1-12

Popper ZA, Fry SC (2005) Widespread occurrence of a covalent linkage between xyloglucan and acidic polysaccharides in suspension-cultured angiosperm cells. Annals of botany 96 (1):91-99. doi:10.1093/aob/mci153

Popper ZA, Michel G, Herve C, Domozych DS, Willats WG, Tuohy MG, Kloareg B, Stengel DB (2011) Evolution and diversity of plant cell walls: from algae to flowering plants. Annu Rev Plant Biol 62:567-590. doi:10.1146/annurev-arplant-042110-103809

Popper ZA, Tuohy MG (2010) Beyond the green: understanding the evolutionary puzzle of plant and algal cell walls. Plant Physiol 153 (2):373-383. doi:10.1104/pp.110.158055

Prigge MJ, Bezanilla M (2010) Evolutionary crossroads in developmental biology: Physcomitrella patens. Development 137 (21):3535-3543. doi:Doi 10.1242/Dev.049023

Rennie EA, Hansen SF, Baidoo EE, Hadi MZ, Keasling JD, Scheller HV (2012) Three members of the Arabidopsis glycosyltransferase family 8 are xylan glucuronosyltransferases. Plant Physiol 159 (4):1408-1417. doi:10.1104/pp.112.200964

Rensing SA, Ick J, Fawcett JA, Lang D, Zimmer A, De Peer YV, Reski R (2007) An ancient

genome duplication contributed to the abundance of metabolic genes in the moss Physcomitrella patens. Bmc Evolutionary Biology 7. doi:10.1186/1471-2148-7-130

Rensing SA, Lang D, Zimmer AD, Terry A, Salamov A, Shapiro H, Nishiyama T, Perroud PF, Lindquist EA, Kamisugi Y, Tanahashi T, Sakakibara K, Fujita T, Oishi K, Shin IT, Kuroki Y, Toyoda A, Suzuki Y, Hashimoto S, Yamaguchi K, Sugano S, Kohara Y, Fujiyama A, Anterola A, Aoki S, Ashton N, Barbazuk WB, Barker E, Bennetzen JL, Blankenship R, Cho SH, Dutcher SK, Estelle M, Fawcett JA, Gundlach H, Hanada K, Heyl A, Hicks KA, Hughes J, Lohr M, Mayer K, Melkozernov A, Murata T, Nelson DR, Pils B, Prigge M, Reiss B, Renner T, Rombauts S, Rushton PJ, Sanderfoot A, Schween G, Shiu SH, Stueber K, Theodoulou FL, Tu H, Van de Peer Y, Verrier PJ, Waters E, Wood A, Yang L, Cove D, Cuming AC, Hasebe M, Lucas S, Mishler BD, Reski R, Grigoriev IV, Quatrano RS, Boore JL (2008) The Physcomitrella genome reveals evolutionary insights into the conquest of land by plants. Science 319 (5859):64-69. doi:10.1126/science.1150646

Rensing SA, Rombauts S, Van de Peer Y, Reski R (2002) Moss transcriptome and beyond. Trends Plant Sci 7 (12):535-538

Reski R (1998) Development, Genetics and Molecular Biology of Mosses. Botanica Acta 111 (1):1-15. doi:10.1111/j.1438-8677.1998.tb00670.x

Ridley BL, O'Neill MA, Mohnen DA (2001) Pectins: structure, biosynthesis, and oligogalacturonide-related signaling. Phytochemistry 57 (6):929-967. doi:10.1016/s0031-9422(01)00113-3

Roach MJ, Mokshina NY, Badhan A, Snegireva AV, Hobson N, Deyholos MK, Gorshkova TA

(2011) Development of cellulosic secondary walls in flax fibers requires beta-galactosidase. Plant Physiol 156 (3):1351-1363. doi:10.1104/pp.111.172676

Roberts AW, Bushoven JT (2007) The cellulose synthase (CESA) gene superfamily of the moss Physcomitrella patens. Plant Mol Biol 63 (2):207-219. doi:10.1007/s11103-006-9083-1

Roberts AW, Dimos CS, Budziszek MJ, Goss CA, Jr., Lai V (2011) Knocking Out the Wall: Protocols for Gene Targeting in Physcomitrella patens. In: Popper ZA (ed) Plant Cell Wall: Methods and Protocols, vol 715. Methods in Molecular Biology. pp 273-290. doi:10.1007/978-1-61779-008-9_19

Roberts AW, Roberts EM, Haigler CH (2012) Moss cell walls: structure and biosynthesis. Frontiers in plant science 3:166. doi:10.3389/fpls.2012.00166

Saint-Jore-Dupas C, Nebenfuhr A, Boulaflous A, Follet-Gueye ML, Plasson C, Hawes C, Driouich A, Faye L, Gomord V (2006) Plant N-glycan processing enzymes employ different targeting mechanisms for their spatial arrangement along the secretory pathway. Plant Cell 18 (11):3182-3200. doi:10.1105/tpc.105.036400

Sakakibara K, Nishiyama T, Deguchi H, Hasebe M (2008) Class 1 KNOX genes are not involved in shoot development in the moss Physcomitrella patens but do function in sporophyte development. Evolution & development 10 (5):555-566. doi:10.1111/j.1525-142X.2008.00271.x

Sawahel W, Onde S, Knight C, Cove D (1992) Transfer of foreign DNA intoPhyscomitrella patens protonemal tissue by using the gene gun. Plant Mol Biol Rep 10 (4):314-315. doi:10.1007/BF02668906

Schaefer D, Zryd JP, Knight CD, Cove DJ (1991) STABLE TRANSFORMATION OF THE MOSS PHYSCOMITRELLA-PATENS. Molecular & General Genetics 226 (3):418-424

Schaefer DG (2001) Gene targeting in Physcomitrella patens. Curr Opin Plant Biol 4 (2):143-150

Schaefer DG, Zryd JP (1997) Efficient gene targeting in the moss Physcomitrella patens. Plant Journal 11 (6):1195-1206. doi:10.1046/j.1365-313X.1997.11061195.x

Schaefer DG, Zryd JP (2001) The moss Physcomitrella patens, now and then. Plant Physiol 127 (4):1430-1438

Scheller HV, Ulvskov P (2010) Hemicelluloses. Annu Rev Plant Biol 61:263-289. doi:10.1146/annurev-arplant-042809-112315

Shimizu K, Ishihara M, Ishihara T (1976) Hemicellulases of brown rotting fungus, Tyromyces palustris, 2: The oligosaccharides from the hydrolysate of a hardwood xylan by the intracellular xylanase. Journal of the Japan Wood Research Society

Siedlecka A, Wiklund S, Peronne MA, Micheli F, Lesniewska J, Sethson I, Edlund U, Richard L, Sundberg B, Mellerowicz EJ (2008) Pectin methyl esterase inhibits intrusive and symplastic cell growth in developing wood cells of Populus. Plant Physiol 146 (2):554-565. doi:10.1104/pp.107.111963

Šmídková M, Holá M, Angelis KJ (2010) Efficient biolistic transformation of the moss Physcomitrella patens. Biol Plant 54 (4):777-780. doi:10.1007/s10535-010-0141-9

Sorensen I, Pettolino FA, Bacic A, Ralph J, Lu F, O'Neill MA, Fei Z, Rose JK, Domozych DS, Willats WG (2011) The charophycean green algae provide insights into the early origins of plant cell walls. The Plant journal : for cell and molecular biology 68 (2):201-211.

doi:10.1111/j.1365-313X.2011.04686.x

Steffan W, Kovac P, Albersheim P, Darvill AG, Hahn MG (1995) Characterization of a monoclonal antibody that recognizes an arabinosylated (1-->6)-beta-D-galactan epitope in plant complex carbohydrates. Carbohydrate research 275 (2):295-307

Sterling JD, Atmodjo MA, Inwood SE, Kolli VSK, Quigley HF, Hahn MG, Mohnen D (2006) Functional identification of an Arabidopsis pectin biosynthetic homogalacturonan galacturonosyltransferase. Proceedings of the National Academy of Sciences of the United States of America 103 (13):5236-5241. doi:10.1073/pnas.0600120103

Strepp R, Scholz S, Kruse S, Speth V, Reski R (1998) Plant nuclear gene knockout reveals a role in plastid division for the homolog of the bacterial cell division protein FtsZ, an ancestral tubulin. Proc Natl Acad Sci U S A 95 (8):4368-4373

Suzuki S, Li L, Sun YH, Chiang VL (2006) The cellulose synthase gene superfamily and biochemical functions of xylem-specific cellulose synthase-like genes in Populus trichocarpa. Plant Physiol 142 (3):1233-1245. doi:10.1104/pp.106.086678

Tan L, Eberhard S, Pattathil S, Warder C, Glushka J, Yuan C, Hao Z, Zhu X, Avci U, Miller JS, Baldwin D, Pham C, Orlando R, Darvill A, Hahn MG, Kieliszewski MJ, Mohnen D (2013) An Arabidopsis cell wall proteoglycan consists of pectin and arabinoxylan covalently linked to an arabinogalactan protein. Plant Cell 25 (1):270-287. doi:10.1105/tpc.112.107334

Thelander M, Nilsson A, Olsson T, Johansson M, Girod PA, Schaefer DG, Zryd JP, Ronne H (2007) The moss genes PpSKI1 and PpSKI2 encode nuclear SnRK1 interacting proteins

with homologues in vascular plants. Plant Mol Biol 64 (5):559-573. doi:10.1007/s11103-007-9176-5

Tsai CJ, Podila GK, Chiang VL (1994) Agrobacterium-mediated transformation of quaking aspen (Populus tremuloides) and regeneration of transgenic plants. Plant cell reports 14 (2-3):94-97. doi:10.1007/bf00233768

Tuskan GA, DiFazio S, Jansson S, Bohlmann J, Grigoriev I, Hellsten U, Putnam N, Ralph S, Rombauts S, Salamov A, Schein J, Sterck L, Aerts A, Bhalerao RR, Bhalerao RP, Blaudez D, Boerjan W, Brun A, Brunner A, Busov V, Campbell M, Carlson J, Chalot M, Chapman J, Chen GL, Cooper D, Coutinho PM, Couturier J, Covert S, Cronk Q, Cunningham R, Davis J, Degroeve S, Dejardin A, dePamphilis C, Detter J, Dirks B, Dubchak I, Duplessis S, Ehlting J, Ellis B, Gendler K, Goodstein D, Gribskov M, Grimwood J, Groover A, Gunter L, Hamberger B, Heinze B, Helariutta Y, Henrissat B, Holligan D, Holt R, Huang W, Islam-Faridi N, Jones S, Jones-Rhoades M, Jorgensen R, Joshi C, Kangasjarvi J, Karlsson J, Kelleher C, Kirkpatrick R, Kirst M, Kohler A, Kalluri U, Larimer F, Leebens-Mack J, Leple JC, Locascio P, Lou Y, Lucas S, Martin F, Montanini B, Napoli C, Nelson DR, Nelson C, Nieminen K, Nilsson O, Pereda V, Peter G, Philippe R, Pilate G, Poliakov A, Razumovskaya J, Richardson P, Rinaldi C, Ritland K, Rouze P, Ryaboy D, Schmutz J, Schrader J, Segerman B, Shin H, Siddiqui A, Sterky F, Terry A, Tsai CJ, Uberbacher E, Unneberg P, Vahala J, Wall K, Wessler S, Yang G, Yin T, Douglas C, Marra M, Sandberg G, Van de Peer Y, Rokhsar D (2006) The genome of black cottonwood, Populus trichocarpa (Torr. & Gray). Science 313 (5793):1596-1604.

doi:10.1126/science.1128691

Underwood W (2012) The plant cell wall: a dynamic barrier against pathogen invasion. Frontiers in plant science 3:85. doi:10.3389/fpls.2012.00085

Urbanowicz BR, Peña MJ, Moniz HA, Moremen KW, York WS (2014) Two Arabidopsis proteins synthesize acetylated xylan in vitro. The Plant Journal 80 (2):197-206. doi:10.1111/tpj.12643

Urbanowicz BR, Pena MJ, Ratnaparkhe S, Avci U, Backe J, Steet HF, Foston M, Li H, O'Neill MA, Ragauskas AJ, Darvill AG, Wyman C, Gilbert HJ, York WS (2012) 4-O-methylation of glucuronic acid in Arabidopsis glucuronoxylan is catalyzed by a domain of unknown function family 579 protein. Proc Natl Acad Sci U S A 109 (35):14253-14258. doi:10.1073/pnas.1208097109

Valvekens D, Montagu MV, Van Lijsebettens M (1988) Agrobacterium tumefaciens-mediated transformation of Arabidopsis thaliana root explants by using kanamycin selection. Proc Natl Acad Sci U S A 85 (15):5536-5540

Van Sandt VS, Guisez Y, Verbelen JP, Vissenberg K (2006) Analysis of a xyloglucan endotransglycosylase/hydrolase (XTH) from the lycopodiophyte Selaginella kraussiana suggests that XTH sequence characteristics and function are highly conserved during the evolution of vascular plants. Journal of experimental botany 57 (12):2909-2922. doi:10.1093/jxb/erl064

Van Sandt VS, Stieperaere H, Guisez Y, Verbelen JP, Vissenberg K (2007) XET activity is found near sites of growth and cell elongation in bryophytes and some green algae: new insights

into the evolution of primary cell wall elongation. Annals of botany 99 (1):39-51. doi:10.1093/aob/mcl232

Vidali L, Augustine RC, Kleinman KP, Bezanilla M (2007) Profilin is essential for tip growth in the moss Physcomitrella patens. Plant Cell 19 (11):3705-3722. doi:10.1105/tpc.107.053413

Vidali L, van Gisbergen PA, Guerin C, Franco P, Li M, Burkart GM, Augustine RC, Blanchoin L, Bezanilla M (2009) Rapid formin-mediated actin-filament elongation is essential for polarized plant cell growth. Proc Natl Acad Sci U S A 106 (32):13341-13346. doi:10.1073/pnas.0901170106

Whetten R, Sederoff R (1995) LIGNIN BIOSYNTHESIS. Plant Cell 7 (7):1001-1013

Willats WGT, McCartney L, Mackie W, Knox JP (2001) Pectin: cell biology and prospects for functional analysis. Plant Molecular Biology 47 (1-2):9-27. doi:10.1023/a:1010662911148

Wise H, Saxena I, Brown RM, Jr. (2011) Isolation and characterization of the cellulose synthase genes PpCesA6 and PpCesA7 in Physcomitrella patens. Cellulose 18 (2):371-384. doi:10.1007/s10570-010-9479-6

Wu AM, Hornblad E, Voxeur A, Gerber L, Rihouey C, Lerouge P, Marchant A (2010) Analysis of the Arabidopsis IRX9/IRX9-L and IRX14/IRX14-L pairs of glycosyltransferase genes reveals critical contributions to biosynthesis of the hemicellulose glucuronoxylan. Plant Physiol 153 (2):542-554. doi:10.1104/pp.110.154971

Wu AM, Rihouey C, Seveno M, Hornblad E, Singh SK, Matsunaga T, Ishii T, Lerouge P,

Marchant A (2009) The Arabidopsis IRX10 and IRX10-LIKE glycosyltransferases are critical for glucuronoxylan biosynthesis during secondary cell wall formation. Plant Journal 57 (4):718-731. doi:10.1111/j.1365-313X.2008.03724.x

Wu SZ, Ritchie JA, Pan AH, Quatrano RS, Bezanilla M (2011) Myosin VIII regulates protonemal patterning and developmental timing in the moss Physcomitrella patens. Mol Plant 4 (5):909-921. doi:10.1093/mp/ssr068

Xiong G, Cheng K, Pauly M (2013) Xylan O-acetylation impacts xylem development and enzymatic recalcitrance as indicated by the Arabidopsis mutant tbl29. Mol Plant 6 (4):1373-1375. doi:10.1093/mp/sst014

Yin Y, Huang J, Xu Y (2009) The cellulose synthase superfamily in fully sequenced plants and algae. BMC Plant Biol 9:99. doi:10.1186/1471-2229-9-99

Yin YB, Chen HL, Hahn MG, Mohnen D, Xu Y (2010) Evolution and Function of the Plant Cell Wall Synthesis-Related Glycosyltransferase Family 8. Plant Physiology 153 (4):1729-1746. doi:10.1104/pp.110.154229

York WS, O'Neill MA (2008) Biochemical control of xylan biosynthesis - which end is up? Curr Opin Plant Biol 11 (3):258-265. doi:10.1016/j.pbi.2008.02.007

Zhu X, Pattathil S, Mazumder K, Brehm A, Hahn MG, Dinesh-Kumar SP, Joshi CP (2010) Virus-Induced Gene Silencing Offers a Functional Genomics Platform for Studying Plant Cell Wall Formation. Molecular Plant 3 (5):818-833. doi:10.1093/mp/ssq023